# 3D Spatial Modeling of Stacked Containers based on Wireless Sensor Network : application to the physical internet

Hoa Tran-Dang

UNIVERSITÉ DE LORRAINE

École doctorale IAEM Lorraine

# 3D Spatial Modeling of Stacked Containers based on Wireless Sensor Network:

∴ ∵ ∴

# Application to the Physical Internet

## THÈSE

présentée et soutenue publiquement le date

pour l'obtention du

**Doctorat de l'Université de Lorraine**

**(mention Automatique)**

par

Hoa TRAN-DANG

**Composition du jury**

| | | |
|---|---|---|
| *Rapporteurs :* | M. Yves Sallez | Maître de Conférences - HDR, Université de Valenciennes et du Hainaut-Cambresis |
| | M. Thierry Val | Professeur, Université de Toulouse |
| *Examinateurs :* | M. Thierry Divoux | Professeur, Université de Lorraine |
| | M. Shenle Pan | Maître de Conférences, CGS, MINES ParisTech |
| *Directeurs de thèse :* | M. Patrick Charpentier | Professeur, Université de Lorraine |
| | M. Nicolas Krommenacker | Maître de Conférences, Université de Lorraine |

**Centre National de la Recherche Scientific (CNRS)**

**Centre de Recherche en Automatique de Nancy (CRAN)— UMR 7039**

Mis en page avec la classe thesul.

# Acknowledgements

First of all, I would like to express my deepest gratefulness and sincerest thanks to my supervisors, Patrick Chapentier and Nicolas Krommenacker, for their constant guidance, precious counseling, encouragement, inspiration and invaluable suggestions throughout the period of my PhD study at CRAN and University of Lorraine. Patrick is a brilliant supervisor who proposed and gave me some interesting topics to work on. Since the first working days at CRAN, he has provided me everything, which I would need to succeed, with his enthusiasm tremendous patience and huge efforts. My work could not be achieved without his great guidance and breakthrough proposition. Nicolas spent his valuable time for discussing insightfully and helped me in writing clearly my problems and solutions. My work and publication could not be achieved without his white nights, particularly the days reaching to be submission deadlines. That really has been my wonderful opportunity and great honor to be their student as well as to work with them during last three years.

Moreover, it is my honor to express indispensable gratitude to all members in CRAN, especially member of ISET and CO2 teams including current and former people that I have had chance to interact with, Houssem Fathallah, Hoang Anh, Si-Hung Ho, Manh-Tuyen Trinh, for their kind assistance, supporting and providing fun environment during my study. I also present sincere thanks to all my Vietnamese friends who work and study in Nancy, Van-Trung Vu, Huu-Hiep Nguyen, Van-Duy Tran, Mai-Huong Vu, Nhu-Thang Le, Xuan-Tung Vu, Dinh-Hoan Trinh, Dinh-Lam Dang and many others for sharing with me the living experiences that could not learn at school.

Additionally, and much importantly, I am greatly thankful the funding source that helped my PhD work possible: CNRS/University of Lorraine grant.

Finally, but definitely not the least, I wish to contribute my thankfulness to my beloved parents and my entire family for their valuable loves, supports and inspirations through my work and life.

*To my beloved parents, Thuoc and Nhung.*

# Abstract

The recent years have witnessed the huge contribution of the logistics activities. For example, the logistics costs of the largest economies account for a large percentage of their GDPs. In another example, to meed the increasing demand of customers, the logistics system should be innovated to provide the high quality of services such as home delivery or same-day delivery. Besides upgrading the infrastructure of transportation system, application of the advanced technologies (e.g., IoT, sensor network, etc.) is the core way to obtain the target of the logistics operations. unsustainability of current logistics operations in all three perspectives: economy, environment, and society. To overcome these problems, many paradigms of logistics systems are proposed and realized such as intelligent logistics, green logistics, reverse logistics and physical internet.

The Physical Internet is expected to replace the current logistics to be a global sustainable logistics network. The goal of the PI is to move, handle, store, realize, supply and use physical objects throughout the world in a manner that improves efficiency, effectiveness and sustainability simultaneously. Inspired by the effective operation of the Digital Internet in storing, handling and transporting data packet universally, the Physical Internet is built based on encapsulation of products in modular containers termed as $\pi$-containers. One of the most important components of the PI is $\pi$-containers that are characterized by modularity, being smart, being green and world standardization.

In this thesis, we are interested in encapsulation of $\pi$-containers. Particularly, at the first level of encapsulation, the P-containers are encapsulated such that the composite $\pi$-container fits in the H-container. Therefore, our contribution is twofold.

As the first contribution, we propose two simple algorithms for the WSN to collect data about the unitary $\pi$-containers arranged inside the H-container. We examine our approach with performance evaluation on simulation implementation, which shows that our algorithms can obtain an accurate number of unitary $\pi$-containers as well as accurate neighbor relations of unitary $\pi$-containers with low delay and acceptable cost.

As the second contribution, we propose a system that can generate 3D layouts automatically or in on-demand manner. To evaluate the effectiveness of our CSP, we carry out extensive experiments in three scenarios distinguished by three different predefined layouts. Heterogeneous and homogeneous $\pi$–containers, rotation allowance are taken into account in these scenarios in order to examine the our methodology in dealing with the generality.

Finally, the results obtained in this thesis can encourage further researches evolving the 3D layouts. For example, we can extend our model to the second level of encapsulation. Thus, the retrieved 3D layout reflects the arrangement of a set of H-containers inside a T-container. The extension is enabled by the capability of wireless sensor nodes.

Accordingly, long communication range of sensor nodes allows the proposed counting algorithm to be deployed effectively. For another example, the feasible 3D layouts can be used as loading patterns which describe effective way to place a set of $\pi$-containers on the H-container. In the PI, this task is usually performed by the $\pi$-composers that run the optimization algorithm to find out the optimal layouts. Thus, given a set of $\pi$-containers and H-container, the feasible layout can reduce the cost of the PI activities.

**Key Words**: Physical Internet, Modular Container, Encapsulation, 3D Layout, Wireless Sensor Network, Proximity, Constraint Satisfaction Problem.

# Résumé

Ce travail de thèse vise à démontrer la faisabilité de la générationautomatique d'un modèle spatial 3D représentant la distribution d'un ensemble deconteneurs élémentaires dans un volume donné. Pour ce faire, chaque conteneur est doté d'un nœud apte à mémoriser, traiter et communiquer dans un certain rayon de couverture. L'ensemble des nœuds forme ainsi un réseau ad-hoc apte à fournir à un nœud puits, via différentes méthodes présentées et développées dans le cadre de cette thèse, une information relative à la proximité des nœuds entre eux. Ce type d'information génère alors des contraintes de proximité, qui ajoutées aux contraintes géométriques (non chevauchement des conteneurs par exemple), nous permet de modéliser un problème de satisfaction de contraintes (CSP) dont les solutions correspondent aux arrangements possibles des conteneurs élémentaires dans un volume donné. Ces solutions peuvent alors être représentées sous la forme d'un modèle spatial 3D.

La problématique abordée dans cette thèse trouve un domaine d'application particulier dans le contexte del'Internet Physique (PI ou $\pi$). Ce nouveau paradigme a été introduit pour transformer globalement la manière dont les objets physiques seront manipulés, entreposés et transportés dans le cadre d'une logistique durable. Dans [Ballot et al., 2014], un constat sans ambiguité est réalisé sur la non efficience de la logistique actuelle. L'Internet Physique cherche à concilier les objectifs économiques, environnementaux et sociétaux des chaines logistiques, en s'inspirant du modèle d'infrastructure distribué et ouvert de l'Internet. Les initiateurs de ce paradigme proposent ainsi un écosystème logistique différent, à savoir : " *Un système logistique mondial ouvert exploitant des réseaux d'approvisionnement interconnectés qui utilisent un ensemble de protocoles collaboratifs, de conteneurs modulaires et d'interfaces intelligentes standards pour accroître l'efficience et la durabilité* " [Ballot, 2012].

L'une des caractéristiques importante de l'Internet Physique est liée à l'encapsulation des marchandises dans des conteneurs modulaires standardisés (à l'image des paquets de données sur l'Internet). Ces conteneurs, dénommés $\pi$-conteneurs, sont ensuite manipulés, entreposés, routés, expédiés, ... par des infrastructures logistiques ($\pi$-hubs) organisées à la manière de l'Internet avec ses routeurs. Pour ce faire, il est nécessaire que les conteneurs, outre leur standardisation, puissent être des éléments actifs de l'automatisation de la chaîne ainsi créée. L' « intelligence » introduite au niveau des conteneurs peut prendre différentes formes, et être supportée par différentes technologies. Dans le contexte de l'Internet Physique, et plus globalement de la logistique, on peut citer entre autre l'identification des conteneurs, la localisation des conteneurs, la surveillance de paramètres à l'intérieur de ces conteneurs, en utilisant des technologies telles que les étiquettes électroniques (RFID) ou encore les réseaux de capteurs (WSN).

Le modèle de fonctionnement de l'Internet Physique, s'il rationnalise les transports,

engendre des manutentions plus nombreuses [Ballot, 2012]. Dans les $\pi$-hubs, les opérations de routage, de déchargement et (re)chargement des conteneurs, nécessitent une organisation et une gestion rationnelle. La multiplicité et la diversité des opérations (automatisées ou non) à mettre en œuvre simultanément ne peut être conduite de manière efficiente qu'en cas de parfaite synchronisation entre la réalité du système physique et de celle du système informationnel. L'obtention, en temps réel, d'une image ou d'un modèle spatial des $\pi$-conteneurs constitue donc une solution potentielle à ce problème de synchronisation. Nos propositions adressent cette problématique applicative et constituent à ce titre une contribution au concept de l'Internet Physique. Nous considérons que chaque conteneur dispose d'un nœud WSN. L'assemblage de ces différents conteneurs au sein d'un conteneur de plus haut niveau (que nous dénommerons ici conteneur composite) permet de constituer alors un réseau de capteurs ad-hoc. Les différents nœuds de ce réseau peuvent alors communiquer dans un certain rayon de couverture Rc (paramètre réglable de chaque nœud) et sont capables de générer une liste de leurs voisins (nœuds présents à l'intérieur du rayon de couverture). A partir de ces informations de voisinage et des informations contenues dans chaque nœud (telles que les dimensions du conteneur ou encore son identifiant), nous proposons de construire un modèle 3D (ou layout) du conteneur composite et de ses composants. Ce modèle est obtenu en résolvant un problème de satisfaction de contraintes où les informations de voisinage sont exprimées sous la forme de contraintes de proximité. La figure 1 suivante illustre le processus complet proposé permettant la construction du modèle spatial des $\pi$-conteneurs.

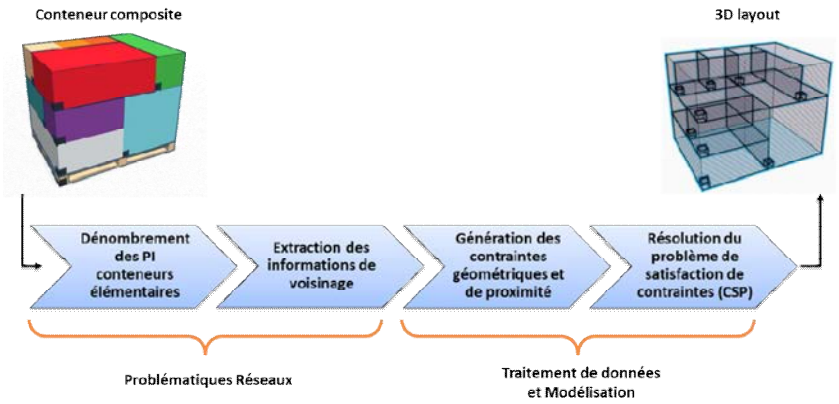


Figure 1: Le processus complet proposé permettant la construction du modèle spatial des $\pi$-conteneurs

Deux types de problématiques de nature différentes apparaissent sur cette figure. La première est relative à des problèmes types dans les réseaux de capteurs sans fils. Des

méthodes et algorithmes seront présentés comme solutions à ces problématiques dans ce contexte. La seconde est relative à des problématiques d'optimisation au sens large par le biais de la proposition d'un nouveau modèle de satisfaction de contraintes. A notre sens, l'originalité de ces travaux de thèse réside pour l'essentiel dans l'usage d'information de proximité pour localiser les $\pi$-conteneurs au sein d'un arrangement 3D. Les techniques de localisation utilisant des technologies sans fil sont généralement basées sur la mesure de caractéristiques du signal (puissance, temps de vol, angle d'arrivée, ...). Dans cette thèse nous préconisons une technique basée sur l'extraction d'informations de proximité moins dépendante de la qualité du signal, et par conséquent des perturbations potentielles dans ce contexte. Nous montrerons que cette approche est suffisante à la construction du modèle spatial 3D. D'autres technologies (caméra ou lidar) pourraient apporter des réponses à ce type de problématique. Néanmoins, le principal avantage de notre approche est de tirer profit de l'instrumentation de chaque $\pi$-conteneur. Ainsi, en tout lieu et à tout moment, le modèle 3D peut être disponible et refléter l'état du composite conteneur. Ce modèle est ainsi utilisable tout au long du cycle de vie du composite conteneur dans l'Internet Physique.

Ces travaux de thèse ont été réalisés au CRAN (Centre de Recherche en Automatique de Nancy) dans le département ISET (Ingénierie des Systèmes Eco-Techniques). Il a été rendu possible grâce à une codirection de ces travaux émanent de l'équipe projet CO2 (Systèmes de Communication Contrainte) et de SIA (Systèmes à Intelligence Ambiante) en lien avec les problématiques énoncées précédemment. Cette thèse est présentée sous la forme de 5 chapitres qui sont maintenant présentés.

Après un rappel des tenants et aboutissants de la logistique et de son importance dans le monde actuel, le premier chapitre présente un état de l'art des paradigmes logistiques apparus ces dernières années, et sensés apporter des réponses plus ou moins complètes au caractère insoutenable de celle-ci. Parmi ces paradigmes, l'Internet Physique semble fédérer les propositions émanant des autres paradigmes, en apportant des éléments de réponse pragmatiques sur les 3 volets classiques de durabilité : l'environnemental, l'économique et le social. Trois composants particuliers apparaissent comme éléments clés de ce paradigme : les $\pi$-conteneurs, les protocoles et le $\pi$-hubs. Ces trois éléments permettraient à tous les acteurs de la chaîne logistique de profiter d'une infrastructure globale, ouverte et standardisée. Le $\pi$-conteneur, outre son rôle de protection des marchandises, permet une délimitation d'un espace privé dans un système ouvert et assure l'interface avec les systèmes logistiques pour son transport, sa manipulation et son stockage, mais également comme support d'information potentiel (identification, routage, ...). Ses caractéristiques idéales (fonctionnalité, dimensions, possibilités d'empilement, ...) sont présentées au travers différentes études menées dans le cadre de projets internationaux et en par-

ticulier le projet MODULUSHCA. Le rôle des protocoles au sein de l'Internet Physique est de définir, à chaque étape logistique, les types d'opération à mener et les conditions nécessaires à leur réalisation. Ils représentent en fait l'ensemble des procédures à appliquer pour la conteneurisation des marchandises, leur expédition sur le réseau logistique, et leur livraison au destinataire en temps voulu. Dans le cadre de l'Internet Digital, les protocoles TCP/IP remplissent cette mission. Les $\pi$-hubs permettent le regroupement, le tri, l'organisation, la composition, le pilotage et la réexpédition des $\pi$-conteneurs vers leur prochaine destination à temps, afin d'assurer un service efficient. Pour remplir ces fonctions, le $\pi$-hub doit avoir accès à de nombreuses données, non seulement sur les $\pi$-conteneurs qu'il reçoit, mais également sur les autres composants du réseau pour être en mesure de diriger correctement les flux. La normalisation des conteneurs et des processus associés, notamment la structuration de l'information et l'automatisation des équipements, sont des éléments clés pour la performance des hubs. Le modèle de fonctionnement de l'Internet Physique, s'il rationnalise les transports engendre des manutentions plus nombreuses sur l'ensemble du réseau logistique. Dans les $\pi$-hubs, les opérations de routage, de déchargement et (re)chargement des conteneurs, nécessitent une organisation et une gestion rationnelle. La multiplicité et la diversité des opérations (automatisées ou non) à mettre en œuvre simultanément ne peut être conduite de manière efficiente qu'en cas de parfaite synchronisation entre la réalité du système physique et de celle du système informationnel. L'obtention, en temps réel, d'une image ou d'un modèle spatial des $\pi$-conteneurs constitue une solution potentielle à ce problème de synchronisation.

Un état de l'art sur les principes et algorithmes de localisation est présenté au **chapitre 2**. De manière complémentaire, les technologies sans fil disponibles pour de la localisation indoor sont exposées avec leurs avantages et inconvénients. Quelques applications de localisation en logistique viennent compléter ce chapitre.Les techniques de mesure pour la localisation peuvent être classées en deux catégories : *range-based* et *range-free*. La première utilise généralement une mesure de distance déduite à partir des propriétés du signal radio (puissance en réception d'un signal reçu,temps de vol, angle d'arrivée, ...). Les méthodes dites *range-free* utilisent quant à elles des informations de connectivité liée à la portée radio. Sur la base des informations issues des différentes techniques de mesure, il est alors possible, par le biais d'algorithmes de positionnement, d'obtenir une position de la cible. Ces algorithmes, plus ou moins complexes, permettent de déduire la position avec une certaine précision. Couplés à des méthodes de mesure *range-based*, ces algorithmes permettent la plupart du temps de localiser de manière précise un objet. Cependant ces techniques, dites fine-grained, sont généralement plus complexes à mettre en œuvre. A l'inverse, les techniques utilisant une approche *range-free* procurent une précision de localisation plus faible (coarsegrained localisation), mais néanmoins généralement suffisante

au regard des besoins de certaines applications. Des solutions de positionnement (basés sur différentes technologies sans fil) sont passées en revue dans ce chapitre, ainsi que leurs performances et leurs limites. Pour finir, un état de l'art des travaux sur le développement de techniques de localisation utilisées à des fins de logistique est présenté.

Dans le **chapitre 3** le problème abordé dans cette thèse, ses hypothèses et nospropositions,sont présentées. L'objectif visé est de garantir, en temps réel, en tout lieu et à tout moment, la possibilité d'obtenir l'image ou le modèle spatial 3D conforme des $\pi$-conteneurs dans le contexte de l'Internet Physique. Ce modèle, constitue une solution potentielle au problème de synchronisation des flux physiques et informationnels durant toute la vie du conteneur. Un ensemble d'hypothèses, liées aux caractéristiques physiques du conteneur et à son instrumentation sont dans un premier temps posées. Sous ces hypothèses,une composition de différents $\pi$-conteneurs instrumentés génère un réseau ad-hoc dans lequel un nœud embarqué sur la $\pi$-palette joue le rôle de nœud puits. L'ensemble de ces nœuds exécute des tâches spécifiques incluant des collaborations avec le voisinage local. Le nœud puits joue le rôle de coordinateur du réseau. Nous proposons ensuite un processus globaldéployé sur ce réseau et permettant au final une visualisation du modèle 3D de l'arrangement. Il peut être résumé en différentes étapes. La première d'entre elles consiste à dénombrer et identifier les caractéristiques (identifiant, dimensions, ...) des $\pi$-conteneurs attachés à un composite conteneur particulier. Cette étape est importante afin de générer un modèle spatial conforme au système réel. Nous proposons ici un algorithme centralisé pour dénombrer le nombre de nœuds présents dans le réseau ad-hoc. Le nombre et la distance entre les nœuds du réseau étant limités par les caractéristiques physiques du composite conteneur, une approche à un saut permet d'estimer de manière fiable le nombre de $\pi$-conteneurs. La seconde étape consiste, pour chacun des nœuds du réseau, à découvrir ses voisins dans un rayon de couverture donné, puis de transmettre ces informations au nœud puits. Un protocole de découverte de voisinage, de type token based, est proposé permettant de limiter les problèmes liés aux collisions lors de transmissions simultanées. A partir des données récoltées sur le nœud puits, celui-ci peut établir une table de voisinage globale, représentant la connectivité de l'ensemble des nœuds du réseau pour un rayon de couverture donné. La dernière étape consiste à traduire cette table de voisinage global en contraintes de proximité. Ces contraintes sont alors insérées dans le modèle de satisfaction de contraintes présenté de manière détaillée dans ce chapitre. La résolution de ce modèle, amène à l'obtention du (ou des) arrangements possibles respectant l'ensemble des contraintes dimensionnelles, de non recouvrement et de proximité. Ce processus global peut être exécuté à tout moment par un opérateur humain ou une ressource matérielle ayant besoin de ce modèle (e.g. robot de déchargement).

Le **quatrième chapitre** de ce manuscrit a pour objectif de valider la faisabilité de la

démarche globale proposée. L'obtention d'un modèle 3D conforme à la réalité est la cible à atteindre pour cette validation globale. Pour autant, sur la base de différents scenarii décrits et se voulant représentatifs de problèmes réels, des résultats de différents tests sont présentés avec pour objectif de valider et mesurer les performances des différents protocoles et algorithmes présentés au chapitre précédent. Les résultats, en termes de temps de calcul et de nombre de solutions du CSP, sont présentés sur différents scenarii. Le nombre d'arrangements possibles respectant toutes les contraintes, et en particulier celles de proximité, dépend naturellement du graphe de connectivité du réseau (et donc du rayon de couverture). Un rayon de couverture trop faible (pas de connectivité) ou trop fort (connectivité totale) n'apporte naturellement aucune information complémentaire permettant de limiter la combinatoire des arrangements potentiels. Une valeur de rayon de couverture médian permet d'obtenir la (ou quelques) solution(s). Afin de réduire le nombre de solutions possibles à l'unique solution conforme, nous proposons dans ce chapitre et de manière complémentaire une procédure spécifique. Celle-ci est basée sur des variations du rayon de couverture et donc des contraintes de proximité engendrées afin d'éliminer les solutions ne les satisfaisant pas. Cette procédure a été testée. Elle permet au final de n'obtenir qu'une et une seule solution conforme à la réalité sur les cas testés, et valide donc la faisabilité de la méthodologie proposée.

Enfin, le **cinquième chapitre** résume les principaux apports de cette thèse et en indique les limites. Sur ces bases, des perspectives sont proposées ouvrant potentiellement de nouvelles pistes de recherche.

# Contents

# List of Tables

# List of Figures

# Chapter 1

# Introduction

## Contents



In this Chapter, a general concept of the logistics including its definitions and its performance is introduced. Although defined by several organizations working in the logistics or logistics-related areas, in our point of view the logistics is encompassed by three significant flows of products: physical, information and financial flow that must be maintained

to be synchronized as tightest as possible to maximize the efficiency of the logistics operations. On the performance perspective, despite the huge positive contribution to the development of nations in almost areas (employment, infrastructure development, etc.), negative impacts caused by inefficient operations of logistics activities are considerable in all three perspectives: economy, environment and society. In order to eliminate the negative influences, novel concepts of logistics paradigms are proposed and developed such as intelligent logistics, green logistics, reverse logistics or Physical Internet. This chapter presents these paradigms and investigates their responses to the three unsustainable perspectives. One of the results derived from the investigation indicates that the Physical Internet is considered the most promising vision toward a sustainable logistics at the global scale. The Physical Internet shorted as PI or $\pi$ relies on a common open global logistic system which is composed of PI hubs interconnected and operated by different services providers, and modular PI containers. The physical goods are encapsulated in smart modular $\pi$-containers which are routed through PI hubs in the global logistic network. Logistic processes such as partial loading/unloading or splitting/merging of PI-containers play an important role for a successful Physical Internet. However, the large variety of transformation processes can introduce desynchronization between the physical and informational flows. At the end of this chapter, we introduce our propositions to build an efficient information system which enable to support, monitor and manage effectively the physical flows of $\pi$-containers.

## 1.1 The Current Logistics

### 1.1.1 The Concept of Logistics

Before the 1950s, the term, *'logistics'*, and its action is originated from the military. Simply, the function of logistics was to supply equipments and vital supplies to troops. Today, with the increase of the globalization, the logistics is developed and expanded broadly and becomes a complicated system combining many relative organizations and a lot of corresponding operations. Accordingly, the missions of logistics are not only to transport people but also to deliver goods from one place to another, from one city to another city, or more distant from one country to other country at global scale.

Th Council of Supply Chain Management Professionals (CSCMP) [1] stated that "*logistics is that part of supply chain that plans, implements, and controls the efficient, effective forward and reverses flow and storage of goods, services and related information between the point of origin and the point of consumption in order to meet various requirements of*

[1] https://cscmp.org/iMIS0/CSCMP/

*customers*". Fig.1.1 illustrates an example of a supply chain.

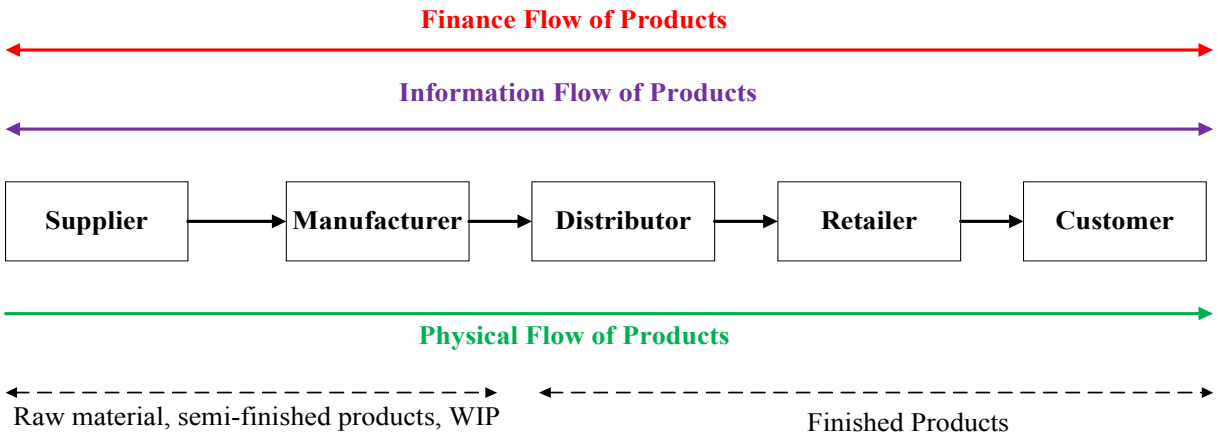


Figure 1.1: A typical model of a supply chain encompassing the three main flows of products and five key players

There are five significant parties participating in all the logistics activities for the flow of delivering the finished products to the end customers: suppliers, manufacturers, distributors, retailers and customers [1]. Fig.1.1 illustrates the relation of the parties participating in the physical flow of products and the associated information and finance flows. The physical flow comprises of two parts. The first part is a movement of raw material or Work-In-Progress products (WIP) from the suppliers to the manufacturer referred as inbound logistics. Meanwhile, the other physical flow called as outbound logistics evolves from the distributing of the final products to the end customers by the distributors and retailers [2]. Obviously, the customers are the main focus of the chain, since the primary purpose of the existence of any supply chain is to satisfy customer needs, in the process generating profit for itself.

On the physical flow of product to move it from its source to the intended destination (i.e., end customers), the product are passed through a set of complicated activities (e.g., handling, storing and transporting) involved in six main components of the logistics system: (1) customer service, (2) transportation, (3) material handling, (4) inventory control, (5) warehousing and (6) information systems [3]. Each component is responsible for specific functions with corresponding activities.

- Customer service is responsible for supporting the orders and requirements from customers. This component is considered as a gateway to connect the customers with logistics services providers or suppliers. Typically, essential tasks of this components include order processing, receiving and responding to demands and feedback of the customers and so on.

- Transportation being the most fundamental component of logistics systems functions to provide means to transport the ordered products to the customers. In order to meet the customer service demands, more important issues should be taken into account such as transport mode selecting, loading planning and route scheduling.

- Material handling involves in utilizing handling equipments to perform a set of activities involved in the placement and movement of products in storage or in-transit areas (e.g., warehouse, cross-docking hubs, etc.). The efficiency and effectiveness of the tasks can be obtained by optimized solutions such as minimizing the movement distance of product, minimizing the cost of usage of handling equipments, optimizing the orders of picking products, etc.

- Inventory control refers to the counting and tracking of goods. The process can be supported effectively by identification technology such as barcodes and radio-frequency identification (RFID). Accordingly,to record an inventory transaction, the inventory control system uses a barcode scanner or RFID reader to automatically identify the inventory product equipped physically with a barcode label or a RFID tag. The data collected from the reading process then is reported to the server or central management system for further processing.

- Warehousing is responsible for storing the products in optimal ways (e.g., optimal orders of storage) while maintaining the quality of products by monitoring and conditioning processes.

- Finally, the information systems allow all components of the logistics system as well as all the players of the physical flow of products to connect and exchange information. The systems include hardware such as computer systems, Internet devices and softwares (Enterprise resource planning (ERP), Warehousing Management System (WMS)) to provide information to manage the logistics effectively.

This sharing of information enables all parties to plan appropriately to meet current and future needs. For an efficient logistic chains, these informational flows must be synchronized throughout the pathway of the physical products in the supply chain.

### 1.1.2 The Positive Impact of Logistic Activities

The logistics simply is just a vital operation in a society to mainly deliver the ordered products from sources to the customers such that their requirements are satisfied. Satisfying the expectation of customers play a key role of logistics businesses in creating their client loyalty as well as maintaining their competitive advantage. In addition, the

logistics contributes to improve the customers' life by providing the convenient services. Basically, the level of satisfaction is dependent on the quality of services that the logistics service providers provide. Therefore, increasing requirements of customers require the logistics to develop corresponding services. Beside the right products with the quality of product guaranteed, the right reception location, the short delivery delay is one of important requirements demanded by the customers. For instance, the growing of e-commerce and online retailers permits the customers to access the product immediately. The online shipping is expected to benefit from reduced delivery time and make the greater choice, higher convenience and often lower prices. With this service, orders are delivered within a few hours after purchasing them, or in a chosen time window on the same day. In recent years an increasing number of 3PL companies have started developing and providing the same-day delivery services such as DHL [2], DPD [3], UPS [4], FedEx [5] and Amazon [6]. Consequently, by satisfying the needs of customers, the logistics contributes to improve the life quality of people.

Indirectly, the investments into logistics contribute to the development of the economic growth. In the study research conducted in [4], the authors examined the impact of logistics on the economic growth. Fig.1.2 sourced from [4] demonstrates impact mechanism of logistics investments on economic growth.

Accordingly, investments into logistics infrastructure have increased logistics capacity, provided rise of efficiency. improved the quality of services, and provided an increase in added values. So this situation has allowed lower logistics costs, shorter transportation time, and business expansion, for better efficiency and competitiveness force of countries. For instance, in 2012, the transportation of goods and warehousing cost has reached up to 144.6 billion EURO in France [7], approximately 10 percent of the French Gross Domestic Product (GDP).

The logistics activities generally involve closely two other sectors which are transportation and education. The transportation, considered as backbone of the logistics activities,

[2]DHL's same-day service, http://www.dhl.fr/en/express/export_services/export_same_day.html

[3]DPD's same-day service, https://www.dpd.com/de_en/home/products_services/express_service/domestic/same_day_delivery

[4]UPS' same-day service, https://www.ups.com/content/us/en/shipping/same-day-delivery.html

[5]FedEx's same-day service, http://www.fedex.com/us/fedex/shippingservices/package/sameday.html

[6]Amazon's same-day service, https://www.amazon.co.uk/gp/help/customer/display.html?nodeId=200173380

[7]Commission des comptes des transports de la nation, CCTN 2014, http://www.statistiques.developpement-durable.gouv.fr/

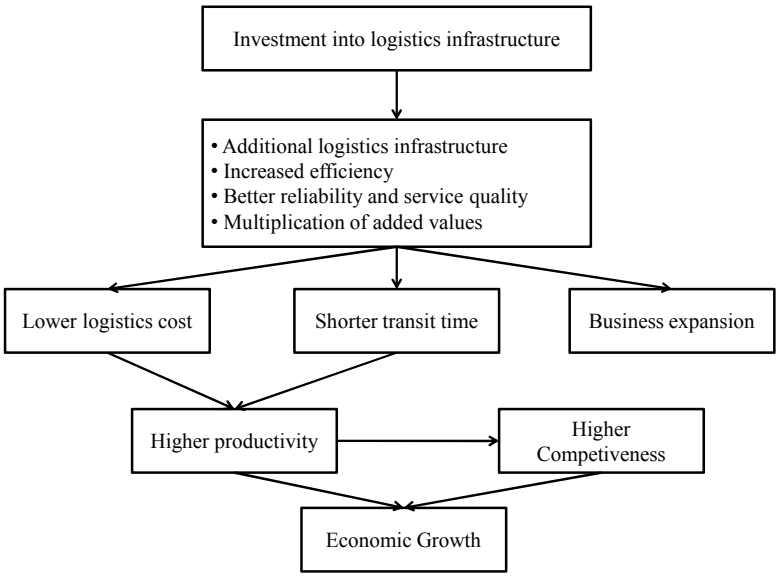


Figure 1.2: Impact of logistics on the economic growth

plays a key role in ensuring and maintaining quality of logistics services (i.e., leading-time, quality of order goods).For example, the fast development of e-commerce requires the logistics service providers to compete intensively for shorter delivery time, lower service price while guaranteeing the quality of ordered goods at the final destination. Investing modern transportation means (e.g., drones [8], autonomous guided vehicles (AGV) [5], [6] or alternative delivery solutions (e.g., last mile delivery [9], smart locker bank [7], etc.) are among the most important solutions for the providers in order to gain the advantage in the competition. On the other side, the expansion of logistics attracts a huge number of labors working in every activities of the logistics sector, thus the unemployment ratio is decreased considerably. The statistic data introduced in [8] indicated that about 30% of the working population in the UK are associated with work involving logistics practices. Logistics occupations cover a wide range of skill levels and specialties including equipment operators and mechanics, inventory managers, supply chain managers, business information systems, and distributions frames [9].

Obviously, the huge contribution of the logistics development is unarguable. However, in the next section, a review on negative impact of the current logistic systems is introduced.

[8]Deployment of Drone in DHL, http://www.dhl.com/content/dam/downloads/g0/about_us/logistics_insights/DHL_TrendReport_UAV.pdf

[9]Last mile delivery in future reported by McKinsey & Company, September 2016

### 1.1.3 The Negative Impact of Logistic Activities

Logistics is increasingly identified as a core element of the economic development of countries. Due to the growing large number of logistics operations, it is also subject to an increasing number of challenges to ensure efficiency and performance of such systems.These challenges come firstly from the unsustainability of logistics activities in the environment, economy and society points of view despite strong efforts by logistic organizations to raise efficiency. In [10], authors have identified challenges that have negative environmental, economical and/or societal impacts.

- In the environmental perspective, the major concerns of global are about amount energy consumed, the volume of greenhouse gasses (GHG) emitted. Despite policies to reduce GHG, pollution related to transportation continues to increase each year. For example, freight transportational one takes up 14% of all CO2 emissions which represents main source of CO2 emission in France [11]. Without any efficient solution to this problem, the emission is estimated to grow considerably due to about 33% increase every 10 to 15 years [12].

- From an economical perspective, the way that goods are moved in the current logistics system is hugely costly. The logistics cost is accumulated from several factors in which the dominant ones are accounted for transportation, inventory carrying, warehousing, order processing and administration. Fig.1.3 illustrates the logistics costs of businesses and equivalent percentages of the GDP that they account for in the U.S for 10 recent years.

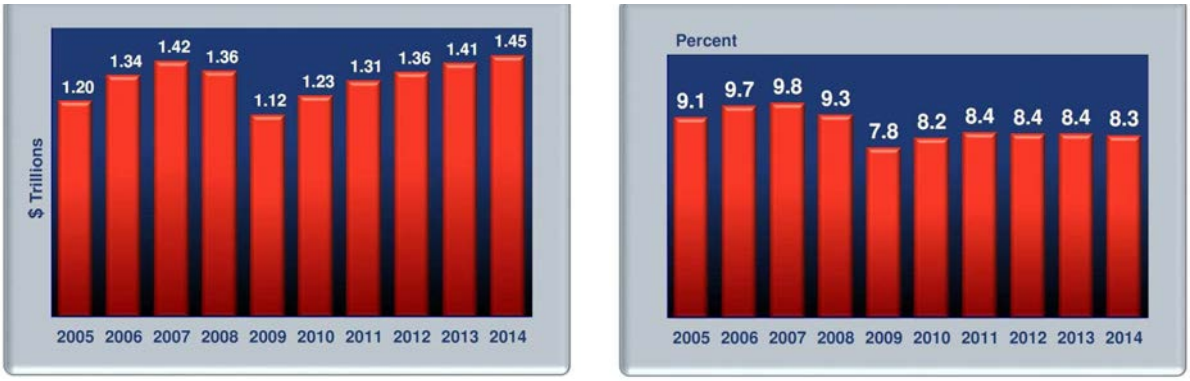


(a) Logistics cost for U.S business (b) Logistics percentage of the GDP of the U.S

Figure 1.3: Important contribution of logistics in economy development of the U.S for 10 recent years

Although the GDP related to the logistic is constant (from 2009 to 2014), we can observe the increase of the global logistic costs on the same period. Moreover, some

studies presented in [13] and [14] show the level of empty running or partially-loaded in the road freight industry. For instance, the level of empty running in the EU-27 road freight industry was 24% in 2010. In the same manner, the average lading factor was 57% in UK.

- The social perspective is shown through the fact that a high demand for truck drivers is increasing because road based transportation dominates continental transport means.For example, the America Trucking Association has estimated that the driver shortage in the U.S.A. will grow to 111,000 by 2014 [15]. The situation leads to case that so many truckers are nearly always on the road, so often away from home for long durations. Their family life, their social life, and their personal health are precarious. As an illustrative indication, a U.S. National Transportation Safety board study found that 58% of the accidents reported by driver were deemed to be fatigue and sleep deprivation related [10]..

The unsustainability of current logistic systems conducts different actors (logistic operators, service providers and researchers) to imagine and propose new solutions to develop a more sustainable supply chain. In the next Section, we review the state of the art paradigms of logistics which are being proposed and developed during the last decade in order to address these challenge.

## 1.2 Toward a Sustainable Logistics

In this section, we overview the main contributions and practical projects in the literature that can respond to some challenges or all of them.

### 1.2.1 Intelligent (Smart) Logistics

The terms intelligent logistics or smart logistics are often used to refer to the different logistics operations (inventory, transport or material management) which are planned, managed and controlled in a more intelligent way compared to conventional solutions. Moreover, the type and level of the intelligence varies among application and methods, ranging from product tracking and environmental sensing to problem recognition and automatic decision making and execution. Advanced technologies, especially the technologies in the information and communication domains play a key role in providing the intelligence characteristic. This section overviews the state of the art approaches and their practical projects realizing the concept of intelligent logistics.

[10] Johnston S.L. III, Consequence of Insomnia, Sleepiness, and Fatigue: Health and Social Consequences of Shift Work http://www.medscape.org/viewarticle/513572_2

- Intelligent Transportation System (ITS)

  The term Intelligent Transportation System (ITS) is used to refer to "*the latest technologies, infrastructure, and services as well as the operations, planning and control methods that are used for the transportation of passengers and freight*" [16]. For instance, EU Directive has proposed to design and realize an ITS for all European countries since 2010 [11]. The system applying ICT is used in all modes of transport including road, sea, air or interfaces of modes for supporting the efficient and secure mobility of goods and also people. The proposition is announced and called for developing and deploying during the context that the increasing in congestion on the European transport system and the related energy consumption and negative environmental impacts is at the warning level. The aim of the directive is "*to provide innovative services relating to different modes of transport and traffic management and enable various users to be better informed and make safer, more coordinated and 'smarter' use of transport networks*". The Directive 2010/40/EU Framework for the development of Intelligent Transportation Systems focuses on four priority areas:

  - Optimal use of road, traffic and travel data,
  - Continuity of traffic and freight management,
  - Road safety and security,
  - Linking vehicle and transportation infrastructure.

  For example, Interoperable EU-wide eCall emergency system [12] and Information and Reservation Services for Truck Parking [13] are siginificant services proposed and developed to improve efficiency, effectiveness, safety, security and environmental performances of freight transportation systems.

- Intelligent Cargo (iCargo)

  Among efforts to reduce the environment damage caused by inefficient ways of logistics activities, the EURIDICE project [14] funded by European Union is a potential

[11] Directive 2010/40/EU of the European Parliament and Council of the European Union, 7 July 2010, http://eur-lex.europa.eu/LexUriServ/LexUriServ.do?uri=OJ:L:2010:207:0001:0013:EN:PDF

[12] Interoperable EU-wide eCall emergency system, http://ec.europa.eu/transport/themes/its/road/action_plan/ecall_en

[13] Information and Reservation Services for Truck Parking, https://ec.europa.eu/transport/modes/road/consultations/2012-06-08-secureparkingplaces_fi

[14] EURIDICE project, https://ec.europa.eu/digital-single-market/en/news/intelligent-cargo-more-efficient-greener-logistics

solution. Based on the vision that normal products are replaced by intelligent products [17] with capabilities of self-aware, context-aware and interconnected, the aim of the project is "*to build an information services platform centered on the individual intelligent cargo item and on its interaction with the surrounding environment and the users*". Unlike traditional cargoes, the intelligent cargo possesses six significant capabilities as followings: self-identification, context detection, service access, status monitoring and registering, independent behavior and autonomous decision making. These characteristics enable the cargoes to form their network to connect to logistics service providers, industrial users and authorities to exchange transport-related information and perform specific services whenever required along the transport process. The key components of the ICT to realize the objective of the project include sensors, RFID, service oriented architectures (SOA), interoperability platforms for data interchange and collaboration between business partners, mobile technologies and GPS. The benefits of this approach can be described in following three main perspectives.

- The first is to enhance the end-to-end visibility of good flow by monitoring, tracing, tracking goods in real time. In combining with the IoT, a cargo tracking system is proposed in [18], [19], [20] enabling to capture the real time information relating to the location, time and status of the vehicles and carried intelligent cargo at anytime in anywhere. The captured information is used for the logistics operators to schedule and manage their assets efficiently in the case of empty trucks after accomplishing the delivery process. By this way, the economy sustainability of the freight transport is obtained.
- The second benefit of applying intelligent cargoes is to increase the efficiency of freight transportation networks due to improved synchronization between cargo movements, logistics services and control authorities.
- The third benefit is to improve sustainability of logistics system by reducing the negative impacts on environment caused by traffic congestion and pollution. The iCargo and vehicles beyond receiving the traffic and transportation information in the database is able to re-route their routing paths in order to avoid traffic congestion, thus reduce a considerable amount of $CO_2$ emissions.

### 1.2.2 Green Logistics

The term green logistics was originally used in the mid 1980s to indicate methods that use advanced technologies and innovated equipments to reduce mostly the environment issues such as greenhouse gas (GHG) emissions, noise and accidents mainly caused by inefficient

logistics operations [21]. To make the global logistics green, the environment aspect is concerned as the top priority in all logistics operations, in particular, transportation, warehousing and inventory operations [22]. These three activities are conducted in a series of researches and investigated in Operation Research (OR) models. Accordingly, to minimize the GHG emissions by the transportation, the operation is performed by optimizing four significant choices, namely, mode choice (i.e., plane, ship, truck, rail, barge or pipelines), usage of intermodal transport (i.e., types of containers), equipment choice (i.e., type and size of transportation unit) and fuel choice (e.g., gasoline, bio-fuels, electric, etc.). Whenever, the optimal selection of these handling equipments is set off, the minimum emission is obtained, thus the environment sustainability.

Warehousing and inventory operations are also activities impacting on environment directly. For instance, some goods require special or different storage conditions. Cooled and refrigerated condition for preservation of food, or heated storage for some oils are ensured by professional machines that in turn generate the environment footprint. Moreover, ingoing and outgoing goods need a lot of handling operations. These operations are supported by vehicles or special equipments. In warehouses, electric equipments like fork lift trucks are used the most because they create indirect emissions and they are flexible in short distance of moving. Meanwhile, long distance, heavy loads carried are reasons that diesel-fueled equipments must be used in the ports and terminals for transportations. Solutions to make the logistics operations in these areas green include reducing internal transport (i.e., long distance transportation) by allocating ports or terminals optimally, reducing the travel time in warehouse by an optimal scheduling or plan.

### 1.2.3 Reverse Logistics

Reverse logistics is defined by the American Reserve Logistics Executive Council as "*the processes of planning, implementing, and controlling the efficient, cost effective flow of raw materials, in-process inventory, finished goods and related information from the point of consumption to the point of origin for the purpose of recapturing value or proper disposal*" [23]. The main objective of this logistics paradigm is to recycle and/or reuse products in order to reduce the environmental impact. The reverse logistics complements to the forward logistics and their collaboration make a close-loop supply chain. It is an inherent requirement of the development of circular economy. So, previous concepts (smart and green) can be applied to generate a sustainable reverse logistic. Furthermore, the logistics assets such as pallets, boxes, transit packagings, etc., have to be recycled and reused like consumers goods that are transported. For instance, the Waste and Resources Action

Programme (WRAP) [15]are organized by the UK retailers, brandowners and suppliers to:

- reduce the carbon impact of grocery packaging by 10% through reduced packaging weight, increased recycling and increased recycled content,
- reduce household food and drink wastes by 4%,
- reduce grocery product and packaging waste in the grocery supply chain by 5% (solid and liquid wastes).

The programme conducted three significant projects to reuse the transit packagings:

- Argos: reusable sofa bags [16]
  The design of a reusable sofa bag went through a number of iterations during the project, but is essentially an envelope of reinforced bubble wrap with protective plastic outer covering and inner lining. During the trial the sofa bag was shown to be capable of at least seven uses. It reduced packaging, improved product protection and was welcomed by customers.
- B&Q: Carrierpacs for kitchen worktops [17]
  Kitchen worktops are a high value item, so the need to eliminate product damage in transit is critical. The Carrierpac is a bespoke design with polypropylene 'inner' and 'outer' components, and adjustable carrying handles. The most trips made by a single Carrierpac during the trial was 18 and the average number of uses was six. During the trial, no damage to worktops was reported.
- Reusable transportation and storage system for large kitchen appliances [18]
  This project examined the feasibility of replacing the current disposable packaging used for large kitchen appliances with an alternative reusable transportation and storage system, which could also provide a means of transporting "returns" and used appliances.

[15] WRAP (2010) The Courtauld Commitment, http://www.wrap.org.uk/category/initiatives/courtauld-commitment

[16]Reusable sofa bag, http://www.wrap.org.uk/sites/files/wrap/15203-06%20Argos%20CS%20LoRes.pdf

[17]Reusable "Carrierpac" packaging, http://www.wrap.org.uk/sites/files/wrap/Report%20-%20reusable%20transit%20packaging%20kitchen%20worktops.pdf

[18] Reusable transport and storage systems, http://www.wrap.org.uk/sites/files/wrap/1BL%20Usability%20Works%20TechReport%20Complete%2023rd%20April%2007.pdf

### 1.2.4 Physical Internet

The Physical Internet initiative [19] is proposed to design a logistic system to move, handle, store, realize, supply and use physical objects throughout the world in a manner that improves efficiency, effectiveness and sustainability simultaneously [24]. This paradigm is mainly founded on the interconnection of logistic networks and the encapsulation concept, in a similar way to the internetworking and transport of packets in the Digital Internet [25]. The latter encapsulates information in standardized data packets. Besides, all interfaces and protocols are designed and developed independently so as to exploit this encapsulation properly. In this way, data packets can be processed by different network equipment (e.g. routers or switches), and carried through different networks using various types of media. By analogy, the Physical Internet does not manipulate physical goods directly, but standardized modular containers (called $\pi$-containers) that encapsulate physical merchandises, and composite $\pi$-containers which can be composed of a set of unitary and smaller $\pi$-containers. The interfaces and protocols of Physical Internet are designed through $\pi$-facilities (such as $\pi$-hubs, $\pi$-movers, $\pi$-carriers, etc.) to obtain an efficient and sustainable universal inter-connectivity ( [25]). Therefore, the core of the Physical Internet concept is the handling of $\pi$-containers throughout an open global logistic infrastructure.

This emerging paradigm has been introduced by Montreuil in 2011 [24] to respond to the unsustainability of traditional logistic system. Our thesis will be a contribution to the development of this new approach. The Section 1.3 will be dedicated to introduce more details about the key elements and the concepts of the Physical Internet.

### 1.2.5 Synthesis of the Different Logistics Approaches

In efforts to solve the unsustainable problem of current logistics, several paradigms of logistics have been proposed. The intelligent logistics is an approach which exploits the intelligence concepts based on the introduction of advanced technologies (ICT). By this way, the overall efficiency of this logistics paradigm is improved significantly in terms of security, flow management, automation of processes. The main objective of green logistics is mainly to reduce the impact of logistics on the environment. The proposed solutions are based on the optimization approaches, for example, optimal scheduling of flows to minimize the GHG. The reverse logistics is part of the circular economy logic and creates a closed-loop logistic to cope with the re-utilization of logistics resources/assets effectively and efficiently. Finally, the Physical Internet paradigm is an approach at the global scale to cope with all the three dimensions of the sustainability: economy, environment and

[19] Physical Internet Initiative, www.physicalinternetinitiative.org

society. The approach is developed based on the combination of the previous mentioned paradigms: integration of ICT, optimization and re-utilization of logistics resources/assets in a global and shared infrastructure.

## 1.3 The Physical Internet network

Inspired by the Digital Internet, the objective of the Physical Internet aims to integrate current logistics networks, which are poorly interconnected, to be an open global logistic system. This network will be built based on the three key elements which are $\pi$-containers, $\pi$-hubs and $\pi$-protocols. This section focuses on describing these components and presents the actual roadmap towards realizing this future logistic network by 2050.

### 1.3.1 Components of PI network

Structured like the Digital Internet, the core of PI network is configured based on three components: $\pi$-containers, $\pi$-protocols and $\pi$-hubs.

#### $\pi$-container

On the operation perspective, the $\pi$-containers are transited most in through $\pi$-hubs under the control of the $\pi$-protocol. To support moving, handling $\pi$-containers, the logistics facilities and material handling systems are dedicated for the PI [10]. Accordingly, a key subset of physical elements including $\pi$-containers, $\pi$-nodes and $\pi$-movers functions as the foundation of the PI infrastructure. Locally, the $\pi$-movers (e.g. $\pi$-truck, $\pi$-trailer, etc.) serve as equipments to handle, carry, move the $\pi$-containers between $\pi$-nodes ($\pi$-stores, $\pi$-composers, etc.). Similar to the standard packets in the Digital Internet, the $\pi$-containers are physical entities which function primarily to contain the physical goods. In order to support the logistics activities in obtaining the sustainability, the $\pi$-containers are designed to be world standard, smart, green and modular [24] and cover the following fundamental characteristics [10]:

- Unitizing merchandise as their contents so that it is not dealt with explicitly by the Physical Internet;
- Coming in various modular sizes, from the cargo container sizes down to tiny sizes;
- Easy to handle, store, transport, seal, clench, interlock, load, unload, construct, dismantle, panel, compose and decompose;

- Smart tag enabled, with sensors if necessary, to allow their proper identification, routing and maintaining;
- Made of environment friendly materials, with minimal off-service footprint;
- Minimizing packaging materials requirements through the enabling of fixture-based protection and stabilization of their embedded products;
- Coming in various usage-adapted structural grades;
- Having conditioning capabilities (e.g. temperature) as necessary;
- Sealable for security purposes.

Fig. 1.4 illustrates the prototype model of $\pi$-containers along with the main properties required to design them.

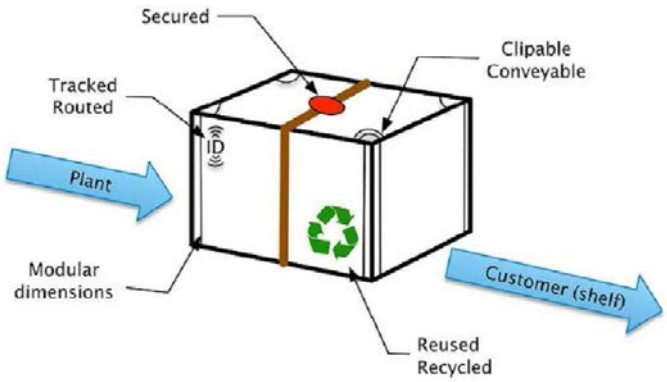


Figure 1.4: Structure of $\pi$-container prototype

The current containers including a wide range of small size parcels, cartons used in the giant logistics companies such as DHL, FedEx, UPS and larger world 20-400 foot shipping containers used in sea transportation, handling and storage do not respect all the specifications. In fact, standardizing a size range of $\pi$-containers is to be of utmost importance because of diversity of products and corresponding sizes. As a result, the cooperation of manufacturers is required to make an agreement to define a limited range of dimensions for all the types of products. Although the work takes a lot of efforts and time, the benefit that it brings to the logistics activities is quite huge. The research and then proof-of-concept study conducted in researches [26], [27] show that the space utilization is improved significantly by using the standardized modular $\pi$-containers in packing and loading process. Consequently, the problem of air transportation of current logistics is

handled. The project MODULUSHCA [20] funded by the 7th Framework Program of the European commission is the first project to design and develop $\pi$-containers (termed as M-boxes in this project) dedicated for fast-moving consumer goods (FMCG). Generally, the FMCG includes daily used goods of consumers with wide range of small/medium sizes such as pharmaceutical, consumer electronic, personal care, household care, branded and packaged foods, spirits and tobacco. The M-boxes are sized and designed by the methodological engineering process introduced in the research [28]. Fig.1.5 illustrates the prototype and physical model of the M-boxes designed by the projects.


Figure 1.5: Physical structure of $\pi$-container designed by MODULUSHCA project

In order to allow smooth and successful operation, a facility dedicated for the network must be constructed appropriately or renovated from the current logistics system. The facility including physical infrastructure and informational system should exploit the characteristics of $\pi$-containers as best as possible to improve the efficiency of the logistics operations. A new set of tangible equipments classified into $\pi$-containers, $\pi$-movers and $\pi$-nodes are proposed and presented in [10] as means for supporting the Physical Internet in the domain of material handling. In the context of Physical Internet network, $\pi$-containers are delivered from suppliers to final customers through an appropriate set of $\pi$-nodes by an appropriate set of $\pi$-movers. The effectiveness of the delivery mission is proved not only by the satisfaction level of the customers but also by the efficiency that the routing network of these $\pi$-containers offers in terms of delay and operation cost. The $\pi$-node as defined in [10] is generic noun to indicate a real location which is responsible for a main logistics operation. For instance, the main mission of a $\pi$-hub is to allow the transfer of $\pi$-containers from incoming $\pi$-movers to outgoing $\pi$-movers. Although serving

[20]MODULUSHCA project www.MODULUSHCA.com

| Layer | Digital Internet | Physical Internet |
|---|---|---|
| 1 | Physical | Physical |
| 2 | Data Link | Link |
| 3 | Network | Network |
| 4 | Transportation | Routing |
| 5 | Session | Shipping |
| 6 | Presentation | Encapsulation |
| 7 | Application | Logistics Web |

Table 1.1: The analogy of layer structure models between the Digital Internet and Physical Internet

the most significant logistics operation, several vital logistics operations naturally occur within the $\pi$-nodes such as unloading, composing to support the $\pi$-nodes in completing their missions successfully.

### $\pi$-protocol

Like the TCP/IP protocol of the Digital Internet, the $\pi$-protocol is a virtual entity consisting of world standard rules for controlling and managing the operations of the Physical Internet network. The rules include services offered to ensure the smooth operation of logistics network.

In other words, under the $\pi$-protocols, a shipment of goods can be containerized, the $\pi$-containers can travel across the network and the goods can be delivered to the recipient on time [29]. In the Digital Internet, the TCP/IP protocols define network services which are structured into seven layers according to the Open System Interconnection (OSI) reference model [21] adopted by the International Standardization Organization (ISO, 1994). An equivalent model is proposed for the Open Logistics Interconnection (OLI) to apply for the Physical Internet. Accordingly, the OLI model is also organized into seven layers: physical, link, network, routing, shipping, encapsulation and logistics web each of which provides specific services to support the particular logistics activities such as procurement, handling, realization (production, assembly, finishing, etc.), storage and transportation. Table 1.1 presents the layered structure of two models OSI and OLI [29].

The benefit of layering the services is to distribute the logistics management then the efficiency of logistics activities is optimized [29]. For example, the physical layer is responsible for ensuring the physical movement of $\pi$-containers smoothly. The layer provides information relating to the handling equipments ($\pi$-trucks, $\pi$-mover, etc.) and

[21] OSI model on Wikipedia, https://en.wikipedia.org/wiki/OSI_model

then guarantees the physical conditions (mechanical, electric) to accomplish the logistics activities of this layer (i.e. handling, moving). As the layer takes into account for these services solely, they are developed so that the quality of services is maximized.

#### $\pi$-hub

The third key element of the PI network is the $\pi$-hubs where $\pi$-containers are received, stored and sent like data packets in the digital hubs. The crucial role of the component is to ensure that each coming $\pi$-container is routed to next destination on time and correctly. The PI infrastructure is then composed of a set of interconnected $\pi$-hubs.

The design of cross-docking hub is essential for the successful development of the Physical Internet. Different types of PI hubs can be considered (e.g., road to rail, road to road, ship to rail) for uni-modal or multi-modal transshipments. Fig.1.6 adopted from [10] illustrates a design for a sea-road $\pi$-hub in the PI network.

Several logistics operations such as the loading/unloading or the composition/decomposition of $\pi$-containers are taken place in the $\pi$-hubs. Therefore, the design of an appropriate set of handling and storage systems ($\pi$-movers, $\pi$-carriers, $\pi$-facilities) is necessary for an efficient and a high-speed transshipment of $\pi$-containers [10].

The hybrid control architectures to control Physical Internet cross docking systems are proposed in the PI-NUTS (Physical InterNet cross-docking hUb conTrol System) project [22]. This project focuses on the control architecture to manage a $\pi$-hub with a dual and complementary objective. The first one is to obtain a globally "optimized control system" to ensure a good overall performance for a $\pi$-hub (e.g. reduction of the average throughput time of the freight, reduction of the $CO_2$ emissions), and the second is to permit to the $\pi$-containers to cooperate with other $\pi$-hub equipments (e.g. docks, conveyor systems,...) to be reactive and to be able to locally face perturbations.

### 1.3.2 Road-map toward PI realization

PI is an innovative concept in logistics. Several researches and studies since 2011 have contributed to demonstrate and give the proof of concept. Recently, the Physical Internet is a long-term vision for an end-to-end global logistic network, and several alliances like

[22] Yves SALLEZ, Physical InterNet cross-docking hUb conTrol System, http://www.agence-nationale-recherche.fr/?Project=ANR-14-CE27-0015

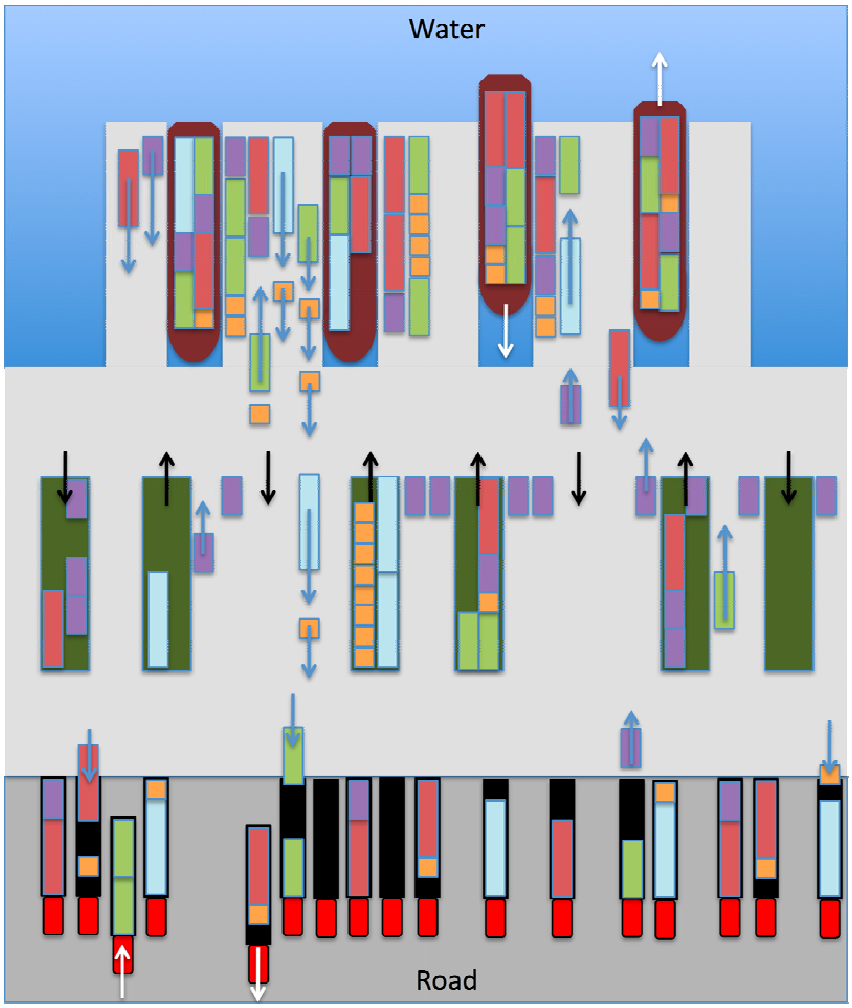


Figure 1.6: An example of inter-modal $\pi$hub connecting the water and road transportation

MHI [23] and ALICE [24] have already adopted the concept, and promote the Physical Internet concepts and practices. Fig.1.7 illustrates the roadmap toward realizing the concept of PI in 2050 by ALICE.

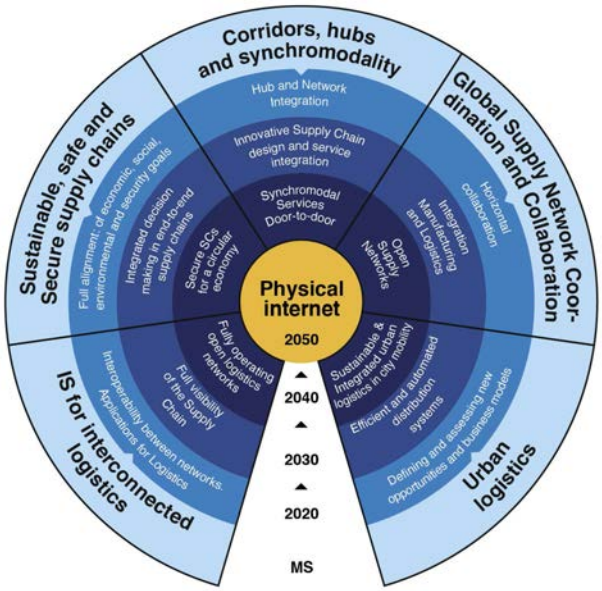


Figure 1.7: Roadmap towards Physical Internet by 2050 by ALICE

Looking to the future, the goal in 2020 is to realize interoperability between networks and IT applications for logistics. Around 2030, the supply chain should be fully visible. In 2040, the target marks the birth of fully functional and operating open logistics networks. Finally, in 2050 the physical internet has become our new reality. To reach these goals, more than 30 varying projects and research studies have been carried out. For example, Chill-on project [25] aims to improve the quality and safety, transparency and traceability of the chilled and frozen supply chain. The development of chill-on smart labels combined with the implementation of intelligent packaging concepts represents the centerpiece of the research activities. The Tiger project [26] has provided new logistics concepts for congestion of EU ports connecting see with inland terminal seamlessly. Tiger did the basis for accessing effectiveness and environment impact identifying proper sustainability criteria indicated which have been applying the real case demonstrations. Tiger demonstrated

[23]MHI, the largest material handling logistics, and supply chain association in the U.S., has created a community of industry thought leaders called the U.S. Roadmap for Material Handling & Logistics.http://www.mhi.org/

[24]ALICE (Alliance for Logistics Innovation through Collaboration in Europe), http://www.etp-logistics.eu/

[25]Chill-on project, http://www.chill-on.com/

[26]Tiger logistics, http://www.go2tigers.com/services/tiger-logistics

four cases with about twenty companies involved. Comcis project [27] demonstrates collaborative information services for container management and ensure that such services can be used in real-world operations if developed innovative ICT solution to access standardized consolidate and deliver information from multiple data sources and parties using data drawn from the entire supply chain. Comcis provided comprehensive and accurate logistics information allowing dynamic replanning increasing efficiency and resource utilization. Two demonstrations run by DHL [28] and ECT [29] have proved the ability to create a global vision on data related to containers for ocean freights unlocking extra values by improving accuracy and efficiency reducing terminal dwell times. Modulushca project [30] proposes to use a new framework of interconnected logistics especially designed for open resource sharing, notably thanks to open standard load units, real-time identification and routing through open facilities. In this framework, potentially all goods are encapsulated in smart, modular, eco-friendly and standard unit loads and are handled, stored, and transported as best fit in these unit loads through shared facilities and across open networks. The project ensures a global synchronization with concurrent projects in the U.S.A and Canada within the international physical internet initiative and pays the way for a common and early market implementation at the intercontinental level. The EU-funded project CO3 (Collaboration Concepts for Co-modality) project [31] has set up the horizontal collaboration basic tools and business models and tested them on the first pilot project. Results of these pilots show a serious decrease in logistics costs and seemed to output ranging from 15% to 25%. Companies like P&G, PepSiCO and many others are implementing the first pilots. Hybrid control architectures to control Physical Internet cross docking systems are proposed in the PI-NUTS (Physical InterNet cross-docking hUb conTrol System) project [32] aiming to efficiently transfer the $\pi$-containers through the intermodal hubs.

These are only a few examples but one by one all of these research projects and logistics are contributing pieces to the final goal of the PI concept. Joining in the research community to realize the Pi, in this thesis, we are focusing on exploiting $\pi$-containers and their characteristics to deal with the synchronization of physical and information flows in dynamic and complex PI network.

[27] Comcis project, http://www.comcis.eu/
[28] Comcis demonstration for DHL, http://www.comcis.eu/dhl.html
[29] Comcis demonstration for ECT, http://www.comcis.eu/ect.html
[30] Modulushca project, http://www.modulushca.eu/
[31] CO3 project, http://www.co3-project.eu/
[32] Yves SALLEZ, Physical InterNet cross-docking hUb conTrol System, http://www.agence-nationale-recherche.fr/?Project=ANR-14-CE27-0015

## 1.4 Contribution and Structure of the Thesis

### 1.4.1 Issues and Contributions

The Physical Internet operates handling of $\pi$-containers throughout an open global logistic infrastructure. This vision will require rethinking the global supply chain where modular $\pi$-containers will be manipulated over time (transport, store, load/unload, build/dismantle ...) but also, their subparts may be changed among the different nodes of the Physical Internet network (e.g. partial loading/unloading, containers splitting and merging). This composition/decomposition of $\pi$-containers is a key element to generate an efficient and sustainable global logistics chain [30], [31], [26]. Moreover, the Physical Internet is expected to exploit the capabilities of smart containers as much as possible, in order to enable decision-making processes on the spot that will open new opportunities such as real-time routing [32]. For instance,$\pi$-containers could adapt their routing plans in each $\pi$-hub, given new current information on opportunities and constraints. As a result, a significant challenge is then to maintain the $\pi$-container traceability in a highly dynamic transport and logistic system.

Technologies and electronic devices, such as bar code readers and radio frequency identification tags (RFID), have revolutionized the way to automatically and continuously identify logistics objects. These automatic identification systems also known as Auto-ID technologies are mainly used to detect the presence of nearby objects. In this process, tagged objects equipped with a barcode label or a RFID chip are localized when they are in proximity to optical or RF readers, respectively. Although Auto-ID technologies have been proven to be sufficiently adequate for localization in some logistics applications, such as inventory management, there are numerous other applications that cannot benefit from this technology due to some limitations. These limitations are mainly related to the environment in which tags and readers communicate [33], and also the location accuracy reduced to the presence or not of the object in the range. The localization precision also depends on the type of tags (passive, active and semi passive tags) and the number of reader used.

In this thesis we propose an approach using the smartness and activeness concept of PI-containers. The $\pi$-containers are equipped with electronic components that provide capabilities to each of them to sense, process and communicate. These $\pi$-containers become intelligent objects which interact directly with logistics operators or other $\pi$-containers. Through the increasing of its communication and decision capabilities, the $\pi$-container can play an "active" role by itself in the PI management. The activeness of PI containers is introduced by Y. Sallez in [32]. From these capabilities, new services – some of which can contribute to improve the synchronization of physical and informational

flows, can be developed. We focus here on the $\pi$-container composition and decomposition processes necessary to an efficient PI. The numerous handling processes can introduce a desynchronization between the physical and informational flows.

To overcome this problem, we propose a system able to generate and maintain automatically a virtual 3D layout reflecting the spatial distribution of $\pi$-containers. The objective is to identify but above all to be able to locate the exact position of stacked items. To do this, the reliance on wireless technologies and localization techniques is needed. However, the originality of our approach is to be independent of the quality of received signals, which is important in harsh environments and operating conditions encountered in logistics. Besides, no pre-installed localization infrastructure is required. Our approach is based on the use of smart $\pi$-container embedding wireless sensor nodes and the knowledge extraction from the obtained adhoc network. Once information collected, a Constraint Satisfaction Problem (CSP) can be formulated where each feasible solution of the CSP is a potential loading pattern. The resulting composite container model can be used to provide up-to-date information (permanent inventory) but also to detect any error during the encapsulation process, which might have a negative impact on the overall effectiveness and efficiency of the Physical Internet.

### 1.4.2 Structure of Thesis

The structure of thesis is organized in five chapters that are summarized as followings.

In the Chapter 1, we have presented the general context of this work that concerns on the status of the current logistic system. Besides the huge contributions of the system to the the global development, inefficiency of the logistics activities causes the universal challenge termed as unsustainability in economy, environment and society perspectives. The Chapter included the overview of the proposed logistics systems such as intelligent logistics, green logistics, reverse logistics and physical internet as significant solutions to response to the challenge. As proved to provide the solution globally, the Physical Internet configured by three key components: $\pi$-container, $\pi$-hub and $\pi$-protocol is reviewed in this Chapter as our scope of research. In order to improve the efficiency of the logistics activities, composite $\pi$-containers composed by sets of unitary $\pi$-containers are handled, moved, transport and stored instead of single $\pi$-containers. However, the misplacement of some $\pi$-containers during loading/unloading or composing/decomposing processes leads to desynchronization between physical and information flows of these containers. Due to the very high dynamic nature of the logistics activities, for example high frequency of physical transformation of composite $\pi$-containers, the core problem set up in our thesis is how to improve the synchronization level between two flows.

The problem can be solved by deploying the positioning systems that can track the

location of $\pi$-containers for real time control and intervention. The Chapter 2 is a literature state of art about the localization algorithms, techniques, technologies and their application of positioning logistics assets in logistics. Among the surveyed solutions for indoor positioning, methods based on range-free techniques seems to be more adapted to our problem due to two main reasons. Firstly, this approach does not require algorithms to estimate the accuracy distance between objects (ie.g., $\pi$-containers) and the reference point that is quite difficult to be deployed in harsh environments and operating conditions like logistics environment. Secondly, since $\pi$-containers are handled in groups, relative positions among them is more important for the PIMS to handle them efficiently, for example composing, decomposing, etc.

Therefore, based on proximity information translated from the neighbor relation of sensor nodes of $\pi$-containers, we will propose a methodology to reconstruct the relative positions of $\pi$-containers arranged in a finite space. The Chapter 3 presents the proposed approach based on $\pi$-containers equipped with wireless sensor nodes. During the composition or decomposition of a composite $\pi$-container, an ad-hoc wireless network is established from the set of nodes.The relative position of $\pi$-containers can be determined by the neighborhood relationships between these sensor nodes. Finally, from this information, a constraint set is formulated in a Constraint Satisfaction Problem (CSP) where each solution is a potential loading pattern. The methodology, the network protocols and the CSP model are developed and presented in this chapter.

To validate the above approach, proposed protocols and models, we consider, in the Chapter 4, several scenarios that represent real compositions of composite $\pi$-containers. The obtained results show that our proposed method yields quick and satisfactory results. The spatial distribution of staked $\pi$-containers can be retrieved with proximity information extracted from the network.

The chapter 5 concludes this dissertation, indicates the current limits of our work and perspectives to overcome these.

# Chapter 2

# Wireless-based Localization and Application in Logistics

## Contents

## 2.1 Introduction

Localization service is a new kind of application using geographical location information and then, providing context-aware information for users of electronic devices. With the ubiquitous availability of mobile equipments, the services play an important role in contributing to the convenience of human life. For example, by installing location based intelligence application in a smart phone, retail customers can access quickly to the nearest store location which holds the needed items. Generally, the basic process of localization of objects includes two steps [34–37]. The first step involves techniques of physical measurement such as distance, proximity, etc. between the target object and reference nodes (nodes with predefined locations). The reference nodes are always associated with wireless communication capability such as Wifi Access Points. Meanwhile, the targets can be communicating devices like mobile phones or objects supported by communicating devices such as RFID tags. In the second step, these primary data is used in positioning algorithm to estimate the final position of target. Based on the space environment used for localizing objects, there are two types of localization scenarios which are indoor and outdoor localization.

In outdoor environments, GPS (Global Positioning System) is used widely in location based application of various areas [38]. The system relies on at least four GPS satellites which are always known their own position to determine the location of object. Accordingly, the target is functioned as a receiver and receives the signal transmitted from the satellites. These signals, after transformed to other kind of data usually estimated distances are used in the positioning algorithm of receiver to obtain the final coordinates of target. With a large number of advantages such as coverage range (planet level), low cost, weather insensitive, etc., however, this system does not work well in indoor environments. This limitation is from the fact that the signals emitted by the GPS satellites are weak and unable to penetrate most building materials. This vision promotes a series of researches to design positioning systems for indoor spaces where objects including people are available and their location are requested most of their time for further applications. Thanks to the fast emergence of innovative technologies especially information and wireless communication technologies (ICT), various indoor localization techniques and algorithms used in the two steps of localization are developed [39].

The performance of indoor positioning system (IPS) depends mostly on the measurement results in the first step. This observation is originated from the fact that the system relies on the wireless signal for measuring the physical parameters which are inherently influenced by a set of constraints such as None Line of Sight (NLOS), multipath padding, interferences in indoor environment. Since these negative effects cannot be com-

pletely eliminated, hence the performance of indoor localization system can be improved by improving the measurement techniques firstly. Generally, some properties of wireless signals, such as arrival time, signal strength, and direction, are considered in measurement schemes. Accordingly, certain signal parameters, such as TOA (Time of Arrival), TDOA (Time Difference of Arrival), RSS (Received Signal Strength), and AOA (Angle of Arrival), proximity sensing are obtained for further using in the next step.

In the second phase, the physical position of the target object is obtained by positioning algorithms using the signal parameters obtained from the first phase as input data. Although there are several survey papers in the literature of indoor localization algorithms [34,35,40] and their classifications, the thesis takes into account the two kinds of localization techniques: range-free and range-based for considerations. Range-based schemes use metrics such TOA, TDOA, RSS, AOA to estimate the distance between two nodes. Meanwhile, proximity sensing between two nodes representing their communication connectivity or pattern matching is typically the basis for range-free algorithms.

Fig.2.1 overviews the techniques and associated algorithms for positioning in indoor environments in the literature.

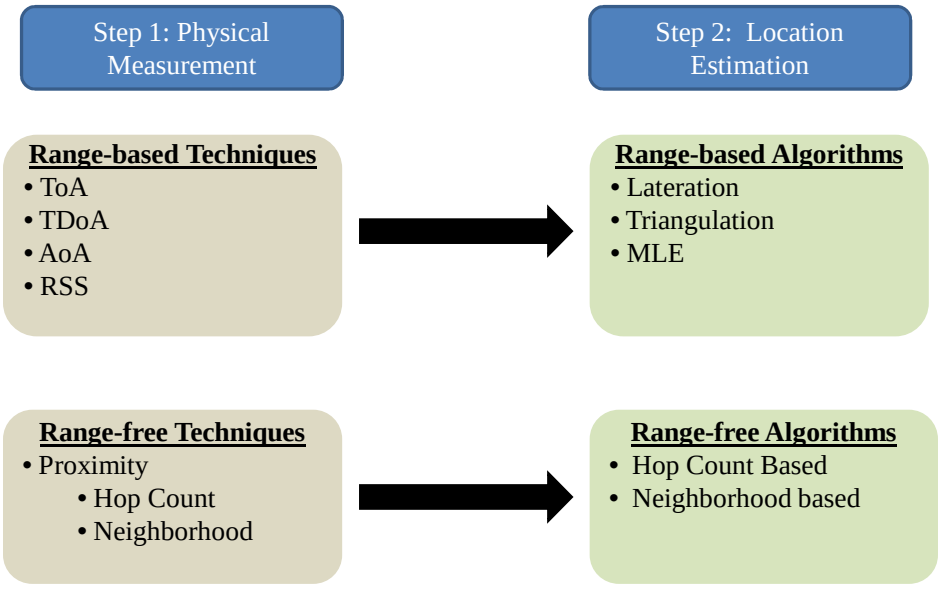


Figure 2.1: A typical procedure for localizing objects in indoor environment and classification

## 2.2 Physical Measurement Techniques

Generally, there are several physical attributes obtained based on the characteristics of wireless signals. Therefore, numerous methods are proposed to measure these attributes. This section focuses on two physical parameters: distance and proximity to presents existing techniques for measuring them.

### 2.2.1 Range-based Distance Measurement

- Time of Arrival (TOA)

  Commonly, for a signal with known velocity $\nu$, the distance ($D$) between transmitter and receiver can be derived as follow equation:

  $$D = \Delta t \times \nu, \tag{2.1}$$

  where $\Delta t$ denotes the travel time from the transmitter to the receiver. Since, ToA method depends on the time of arrival of signal at the receiver node and time of departure at the transmitter note, a synchronization protocol between two nodes is required to minimize their clock offsets as well as clock drift caused by imperfect hardware design. In addition, selection of signal path for measuring distance impacts the measurement result. Generally, majority of ToA based positioning techniques use the first path to range the transmitter and receiver [41]. However, this path is not the strongest [42, 43]. The observation challenges the ToA methods in the indoor environment where multipath is available inherently. This limitation finally contributes to poor performance of distance measurement.

  Among wireless signal technologies, the UWB (Ultra-Wide Band) technology used for the ToA technique achieves higher precision [44, 45] because the UWB signal transmitted by extremely short pulses and large bandwidth deals with multipath effects in indoor environment. Therefore, the distance is estimated with high accuracy.

- Time Difference of Arrival (TDOA)

  Instead of relying single signal, TDoA technique uses two different kinds of signals with speeds $\nu_1$ and $\nu_2$ respectively to transmit [46]. The following mathematical model is used to calculate the distance ($D$) between two devices:

  $$\frac{D}{\nu_1} - \frac{D}{\nu_2} = \Delta t_1 - \Delta t_2, \tag{2.2}$$

where $\Delta t_1$ and $\Delta t_2$ indicate the travel times of two signals from transmitter to receiver respectively.

Fig.2.2 illustrates this measurement technique .

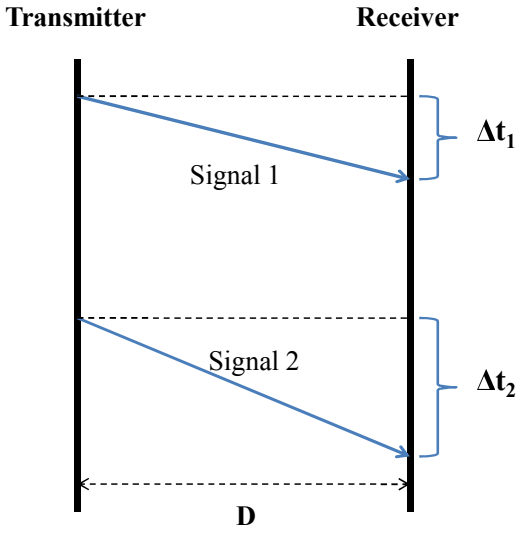


Figure 2.2: Distance Measurement based on TDoA Method

The most important advantage of TDoA method is that it does not require synchronization between two devices. However, the usage of two signals results in increasing the cost of device hardware.

- Round Trip Time (RTT)

  Instead of requiring time synchronization of two nodes as ToA method does, RTT based measurement approach only relies on local clock of each node to calculate the time difference. Fig. 2.3shows the flow of signal travel and time difference.

  The distance is obtained from following equation [47, 48]:

$$D = \frac{(\Delta t_{RTT} - \Delta t_p) \times \nu}{2}, \tag{2.3}$$

  where $\Delta t_{RTT}$ denotes the amount of time needed for a signal to travel from transmitter to the receiver and back again, $\Delta t_p$ represents processing time delay required by the receiver.

  Although the RTT based techniques are able to solve the problem of synchronization to a certain extent they still can suffer from the clock drift. To address this issue, nanotron technology presents a novel method called symmetric double sided two-way

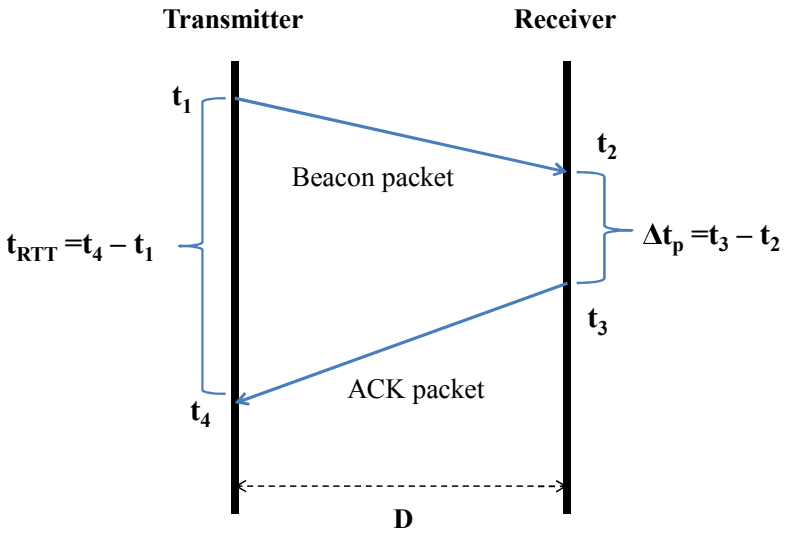


Figure 2.3: Distance Measurement based on RTT Method

ranging (SDS-TWR) [33]. The scheme uses two RTTs obtained by both transmitter and receiver symmetrically. Fig.2.4 shows the procedure of this method operation.

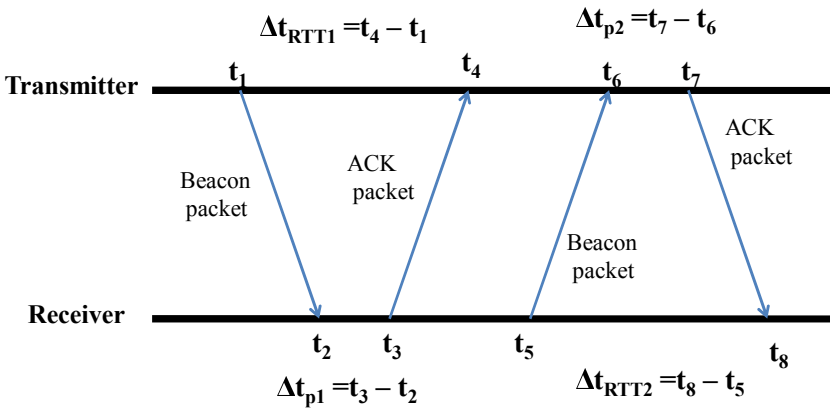


Figure 2.4: Distance Measurement based on SDS-TWR method

The distance between two nodes is derived by follow equation:

$$D = \frac{[(\Delta t_{RTT1} - \Delta t_{p1}) + (\Delta t_{RTT2} - \Delta t_{p2})] \times \nu}{4}, \tag{2.4}$$

[33]Nanotron Technologies, http://www.nanotron.com

by this way, the error caused by clock drift of two nodes is eliminated. Hence, the distance is measured with a high level of accuracy.

- Angle-based Methods

  Supporting arrays of antennas both reference nodes and target node can determine the direction of transmitted signals. By analyzing the phase or time difference between the signal's arrivals at different reference nodes, the AoA of signal can be achieved [34, 35, 37, 40, 49–51]. The AoA value, hen, is used to estimate the distance between the target and references. Considering a scenario in which two reference nodes $R_1$ and $R_2$ are used to get the distances between them and the target node T. Using the AoA measurement techniques, the AoA values are obtained as $\theta_1$, $\theta_2$ (Fg. 2.5). Applying trigonometry, the distances $D_1$ and $D_2$ are derived from the following equations:

$$D_1 = \frac{\Delta X \tan\theta_1 \tan\theta_2}{1 + \tan\theta_1 \tan\theta_2}, \tag{2.5}$$

$$D_2 = \frac{\Delta X \tan\theta_1 \tan\theta_2}{(1 + \tan\theta_1 \tan\theta_2)\sin\theta_2}, \tag{2.6}$$

  Although the AoA based measurement distance technique does not require time synchronization between nodes, it has existing limitations. Since AOA-based methods are highly sensitive to multi-path and NLOS, it is not suitable for indoor localization sometimes. As the distance increases, the localization precision will decrease. In addition, technologies based on AOA require additional antennas with the capacity to measure the angles. This increases the cost of the whole system.

- Received signal strength (RSS)-based Methods

  For wireless communication, the signal strength is attenuated over distance from the transmitter to the receiver. Many factors causing the path loss of signal such as shadowing, reflection are dependent on environment and unpredictable. Therefore, once a propagation of signal is modeled, the distance can be translated accordingly. An empirical mathematical model to calculate the distance $D$ according to signal propagation is as follows [52, 53]:

$$\rho(D) = \begin{cases} \rho(D_0) - 10n\log\frac{D}{D_0} - nW \times WAF & nW < C, \\ \rho(D_0) - 10n\log\frac{D}{D_0} - C \times WAF & nW \geq C. \end{cases} \tag{2.7}$$

  where $D_0$ is a reference distance, $\rho(D)$ and $\rho(D_0)$ the signal strengths received at $D$ and $D_0$ respectively, $nW$ the number of obstacles between the transmitter and

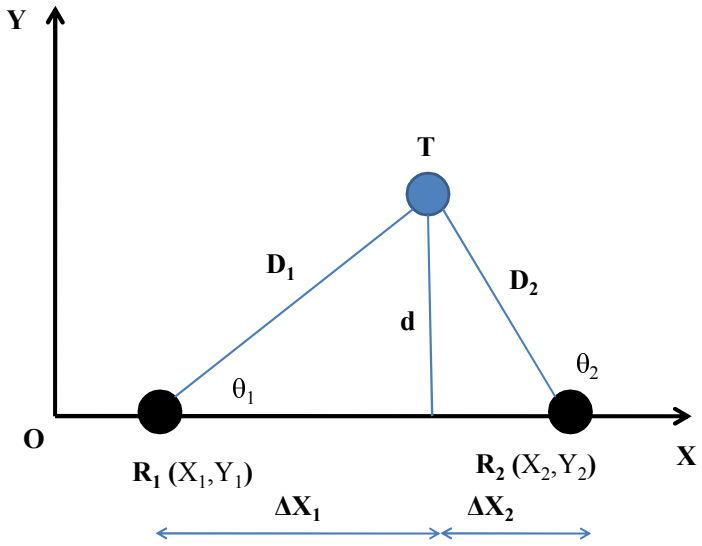


Figure 2.5: Distance Measurement based on AoA method

the receiver, $WAF$ the attenuation factor of the wall, $C$ the maximum number of obstacles between the transmitter and the receiver, and $n$ the routing attenuation factor which could be determined by both theoretical and empirical calculations. Advantages of distance measurement technique based on RSSI includes less communication overhead between two devices, lower implementation complexity and lower cost. However, since the signal property is environment dependent, the distance is estimated at lower accuracy.

### 2.2.2 Range-free Distance Measurement

In the proximity sensing technique, devices use wireless signal to sense and detect objects nearby. In particular, for a network of wireless nodes, a node is aware of its neighbors within its communication range by sensing capability. By this way, primary information about location of a node can be obtained by the reference nodes which always know their sensing range.

- Hop Count Measurement

  On the principle of wireless communication, two nodes require internodes (intermediate nodes) for forwarding information as the physical distance between them is less than their transmission range. By this observation, one hop is referred as one inter node on the path of communication between a source node and a destination node and hop count is number of internodes on the path.

In the localization scenario, thus, the distance between a target and a reference is calculated based on their hop count and an average per-hop distance. As given the location of two reference nodes, their physical distance and hop count can be derived. Consequently, the average per-hop distance can be obtained. Fig.2.6 presents an example to illustrate the measurement method based on hop count technique. The example considers a scenario in which a target is positioned with aid of two references and other internodes. The reference nodes calculate the average per-hop distance ($avgHD_{12}$) based on their physical distance $D_{12}$ and their hop count $HC_{12}$. The distances between the target and references, then are estimated as indicated in the Figure.

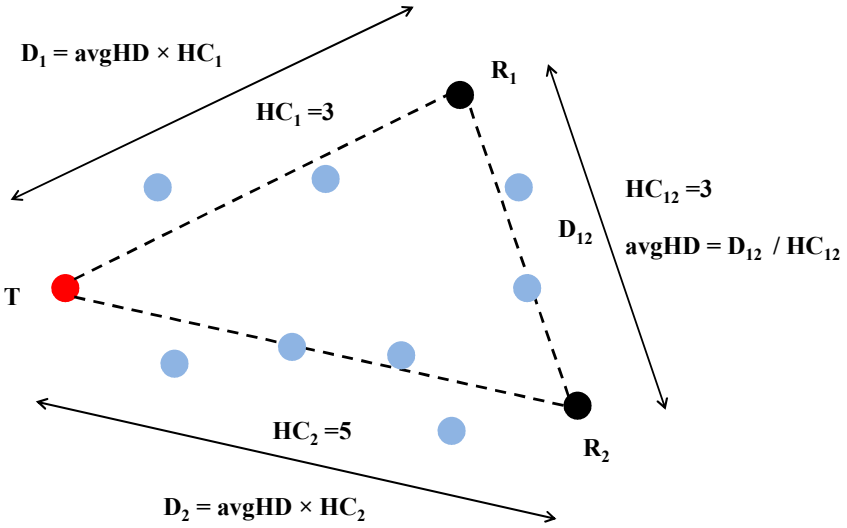


Figure 2.6: Distance Measurement based on hop count method

- Neighborhood Measurement

  Relying on the proximate connectivity, the target can be positioned based on number of its neighbors. One of the most basic schemes for localizing the target is that of one-neighbor proximity. Accordingly, the target upon receiving the location information of its neighborhood reference uses this information as its own location. Although the approach proves its simplicity of performance, the obtained location of object is coarse-grained. In order to achieve a fined-grained localization, a number $k$ ($k \geq 2$) of neighborhood references is required to provide more constraints of the predicted area where the target is placed. The approaches using the $k$ neighbors are referred as $k$-nearest-neighbor approaches. Considering an example as presented in the Fig.2.7 in which the red round is the target node needed to be determined its real position

and five black rounds are references being within the proximity range of target.

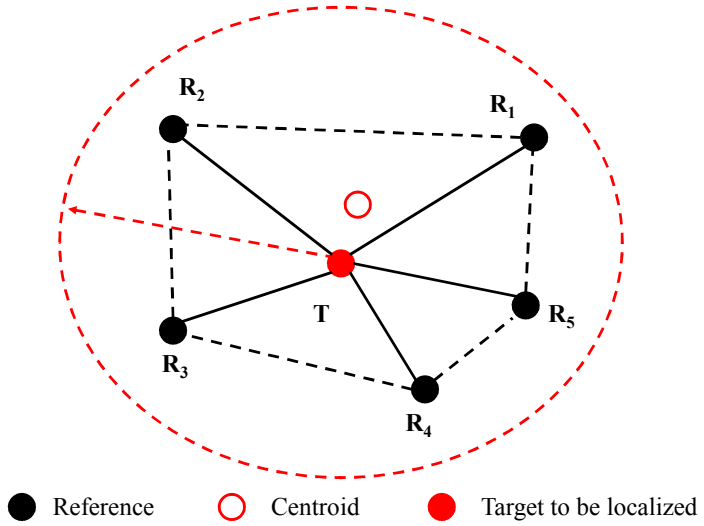


Figure 2.7: Localization based on k-neighbor proximity approach

Many algorithms are proposed to estimate the position of target based on the location information of these five references. Among them, the centroid algorithms [54] are used the most. This $k$-nearest-neighbor approximation obtains not only the efficiency of computational simplicity like the single-neighbor proximity approach but also more accurate localization results.

## 2.3 Location Estimation Algorithms

Based on the two measurement techniques in the first step, the position of the target is calculated by the two corresponding positioning algorithms: range-based and range-free. This section introduces the most popular approaches regarding to this classification.

### 2.3.1 Range-based Algorithms

Whenever the absolute distances between the target and references are estimated, they can be used in the positioning algorithms.

- Lateration

  The lateration based positioning algorithm [55–57] requires two (bilateration), three (trilateration) or more than three (multilateration) reference nodes to calculate the physical position of a target node. The technique indicates that the global position

of the target is within the intersection zone of rounds centered at the references. Therefore, the more reference nodes the algorithm use, the more accurate level the target position can obtain. The lateration technique localizes the objects in both 2D and 3D spaces. Fig.2.8 illustrates the trilateration algorithm for achieve the coordinates of a target in 3D space.

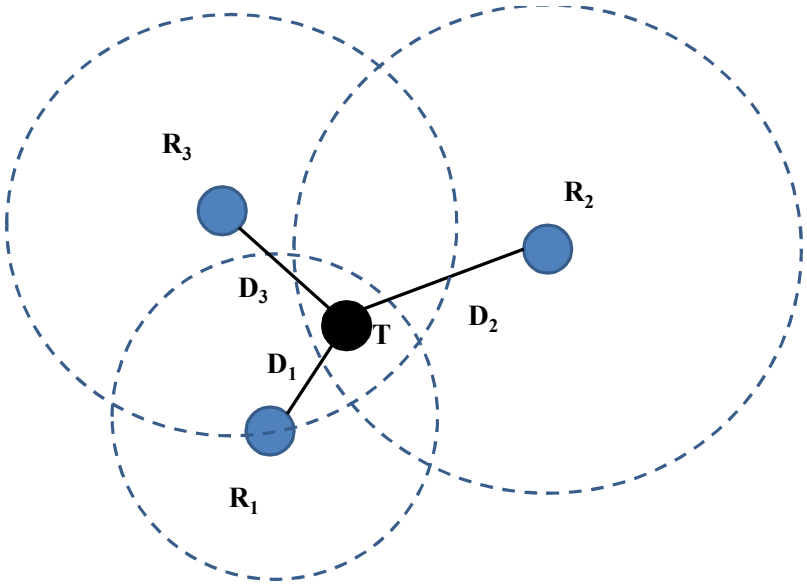


Figure 2.8: Trileteration-based positioning method

Based on the coordinates of three reference nodes: $R_1(x_1, y_1, z_1)$, $R_2(x_2, y_2, z_2)$, and $R_3(x_3, y_3, z_3)$, and the corresponding distances from each reference node to the target node: $D_1$, $D_2$, $D_3$, the coordinate of target node can be referred from the following equation systems:

$$\begin{cases} (x_1 - x)^2 + (y_1 - y)^2 + (z_1 - z)^2 = D_1^2 \\ (x_2 - x)^2 + (y_2 - y)^2 + (z_2 - z)^2 = D_2^2 \\ (x_3 - x)^2 + (y_3 - y)^2 + (z_3 - z)^2 = D_3^2 \end{cases} \tag{2.8}$$

where $T(x, y, z)$ denotes the unknown coordinates of the target $T$.

- Triangulation

  When AOA measurements are available, triangulation can be used to determine the position of the target node. Instead of measuring distances between nodes as lateration methods do, triangulation-based positioning is based on the measurement of angles, though they work in a similar manner. In most situations, triangulation

can be transformed to trilateration since the distance between nodes can be reconstructed from the bearings between them. However, compared to trilateration, only two reference nodes are needed for triangulation (in 2D), instead of three.

With triangulation, the position of the target node can be determined by the intersection of several pairs of angle direction lines [35]. As shown in Fig.2.9 where $R_1$ and $R_2$ represent reference nodes, after obtaining the angles $\theta_1$, and $\theta_2$, the physical position of $T$ (representing the target to be located) could then be calculated based on the predetermined coordinates of the reference nodes.

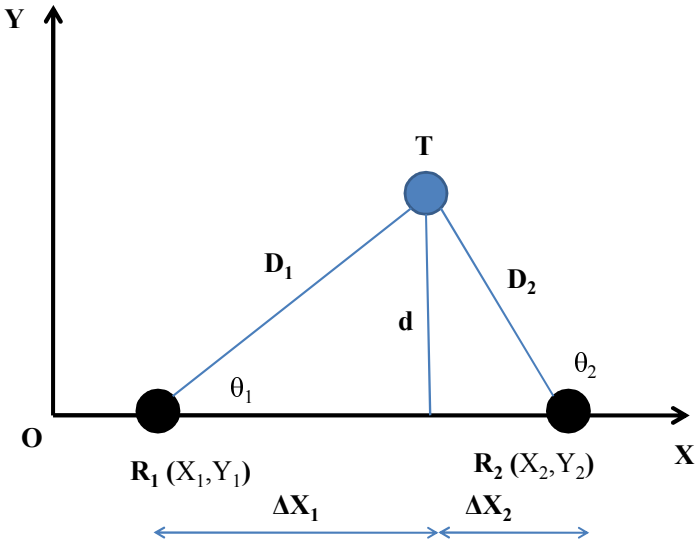


Figure 2.9: Triangulation based positioning method

- Maximum Likelihood Estimation MLE is a popular statistical method used for solving the problem of measurement invariance in localization. In other words, the MLE aims to minimize the differences between the measured distances and estimated distances [58,59] thus the positioning algorithm can obtain the fined grain localization.

### 2.3.2 Range-free Algorithms

Range-free approaches locate unknown objects without the knowledge of inter-node distance measurement. Saving the cost of ranging hardware, they are more cost-efficient than range-based ones. Basically, range-free schemes rely on the connectivity or proximity information to localize the target objects. The range-free algorithms generally require only simple operations and do not need additional hardware, which makes them attractive to be applied widely especially in wireless sensor networks.

- Neighborhood based Methods

  The most significant algorithm based on the neighborhood detection is the algorithm Centroid [60]. In this technique, the reference nodes are assumed to have equal weights and the target coordinate is estimated as the centroid of the locations of all references nodes. Considering to the example presented in the Fig.2.7, the position of target can be derived from following equations:

$$x_T = \frac{x_1 + x_2 + x_3 + x_4 + x_5}{5}, \tag{2.9}$$

$$y_T = \frac{y_1 + y_2 + y_3 + y_4 + y_5}{5}, \tag{2.10}$$

$$z_T = \frac{z_1 + z_2 + x_3 + z_4 + z_5}{5}, \tag{2.11}$$

  where $T(x_T, y_T, z_T)$ and $R_i(x_i, y_i, z_i)$, $i = 1 \ldots 5$ are coordinates of the target and the five reference nodes respectively. The classical Centroid algorithm is simple and easy to implement but the localization accuracy heavily depends on the percentage of deployed references. In order to taking into account influence of reference position to target, weighted centroid algorithms [61] are developed. By this way, the above equations can be modified as follows:

$$x_T = \frac{w_1 x_1 + w_2 x_2 + w_3 x_3 + w_4 x_4 + w_5 x_5}{w_1 + w_2 + w_3 + w_4 + w_5}, \tag{2.12}$$

$$y_T = \frac{w_1 y_1 + w_2 y_2 + w_3 y_3 + w_4 y_4 + w_5 y_5}{w_1 + w_2 + w_3 + w_4 + w_5}, \tag{2.13}$$

$$z_T = \frac{w_1 z_1 + w_2 z_2 + w_3 z_3 + w_4 z_4 + w_5 z_5}{w_1 + w_2 + w_3 + w_4 + w_5}, \tag{2.14}$$

  Where $w_i$, $i = 1 \ldots 5$ are weight factors representing a reflect that the smaller the distance between the target and references is, the greater the influence the references have on the target. The selection of the factor depends on the algorithms and number of references around the target nodes [61].

  A novel range free localization algorithm based on a number of neighbors presented in [62] is an approximate point-in-triangulation test (APIT). In this algorithm, the whole network is divided into triangular regions formed by any three-reference nodes (neighbors) of target (see Fig.2.10).The target node after receiving the information from its neighboring nodes determines whether it is inside/outside the triangle

formed by reference nodes and the final centric location of overlapping regions is considered as estimated location.

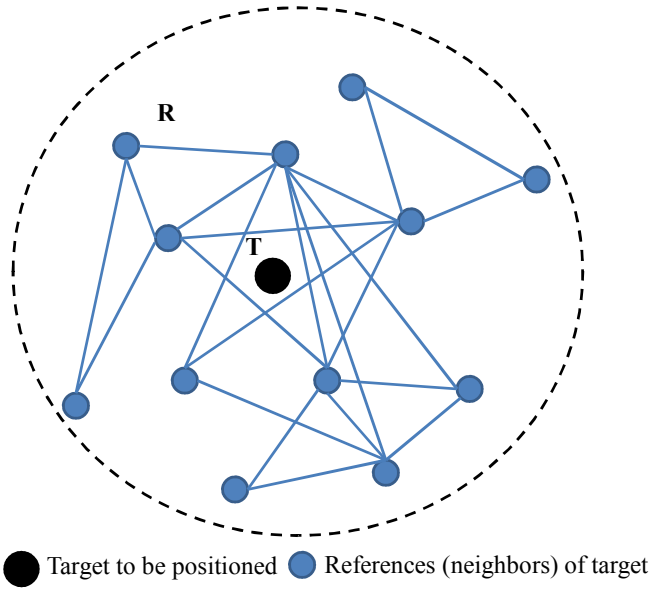


Figure 2.10: Triangulation based positioning method

This algorithm can obtain the best performance and low complexity operation in networks with random deployment of nodes. However, the localization accuracy level of the APIT method is sensitive to the presence of target that it is inside or outside of triangular regions. Therefore, as the density of nodes in network is increased, so does the accuracy level. Consequently, the network system cost is raised up.

- Hop Count based Methods

  A well-known range-free localization algorithm using the hop count measurement is DV-Hop proposed in [63]. In DV-Hop scheme, each reference node computes the distances to other reference nodes and then estimates its average hop distance based on the hop-count information. The target then utilizes the average hop distance to determine their distances to references and apply lateration technique to calculate the final location estimates. This scheme shows a simple implementation, however, it suffers from large location error due to invariance in the calculation of average hop distance.

  Consequently, many improvements of DV-Hop are suggested to increase the positioning accuracy level. One of the significant works proposed in [64] presents three

improved stages to address the large location error of the classic DV-Hop localization algorithm. First, the average hop distance is calculated by using least square method. Second, the distance between the target and reference nodes is calculated based on average hop distance of different reference nodes instead of using the first received average hop distance of the classical DV-hop. Third, the primary location of the target node is estimated using multi-lateration method with a number of chosen reference nodes. This step is repeated and then the final location of target is calculated as the average of primary location estimates. The simulation results prove the improvements of algorithm in enhancing greatly the localization precise level of target but in turn, the computational overhead is high.

## 2.4 Indoor Localization Systems based on Wireless Communication Technologies

The wireless signals are very sensitive to the indoor environment where inherent appearance of obstacles effect on the performance of transmitted signals such as multipath, interference, path loss, etc. Consequently, these results have a heavy impact on the accuracy of physical measurements and hence, the precise level of localization regardless the mentioned techniques used. The section summaries the most popular localization systems based on wireless communication technologies such as optical wireless and radio frequency.

### 2.4.1 Optical Wireless Localization Systems

- Infrared (IR)

Infrared radiation is a kind of electromagnetic radiation. The propagation of infrared wave is expressed through its wavelength range (30cm-740nm)and corresponding frequency range (3GHz-400THz).The IR wave possesses several negative properties which challenge in using it. For example, it cannot pass through opaque obstacles and thus requires LOS environment between an IR transmitter and an IR receiver for effective performance. In addition, the receiver must be within the short transmission range of the transmitter to detect and receive the sent signal. Besides, it is subject to interference of other sources of IR devices.However, the IR technology is applied widely in available consumer equipments such as mobile phones, TV, printers, PDAs, and so forth as they are usually equipped with IR sources. Everything can emit IR radiation, but with different levels such as wavelength, intensity,

etc. One of the most popular IR sources is infrared light emitting diode (IR-LED) emitters. Generally, the IR wave is invisible to human eye, but people can feel it as heat which radiates. Therefore, in order to sense and detect IR radiation, particular IR detectors, sensors or infrared cameras containing charge-coupled-device (CCD) imaging chips sensing the IR light are required. Based on these theoretical point views, there are two main methods to exploit the IR communication to uses in indoor positioning algorithms. The first method is to use the IR signals (active beacon) emitted from the emitters directly as wireless signals. The second is to sense the temperature radiated by the IR radiation by thermal sensors or CCD camera. Some significant systems based on the IR technology such as Avtive Badge [65], Firefly [34], and OPTOTRAK [35], IRIS_ LPS [66] are summarized in Table 2.1.

Using IR signal for designing IPS has several advantages. For instance, the whole simple infrastructure not only saves the cost of installation and maintenance but also provides a high accurate level of positioning. In addition, the IR emitters are small, light-weight and easy to be carried or tagged. However, there are some inherent limitations in these indoor IR positioning systems. The foreseen constraints come from the nature of IR signals. For example, they are interfered by other light sources such as fluorescents or sunlight or they cannot pass through opaque obstacles. These points prevents the IR based IPSs work well in environment where there are presence of other light sources or emitters are covered by any objects from their detectors. Moreover, the high cost of camera in the hardware components is one restriction of designing the IPSs based IR technology.

| Reference System | Signal Sensor, Camera | Measurement & Positioning Techniques | 2D/3D space | Accuracy Level |
|---|---|---|---|---|
| ActiveBadge | Sensor | Private | 3D | 6m |
| FireFly | Camera | Private | 3D | 3mm |
| OPTOTRAK | Camera | RSSI/Triangulation | 3D | 0.1-0.5mm |
| IRIS_ LPS | Sensor | AoA/Triangulation | 3D | 16cm |

Table 2.1: Some significant indoor positioning systems based on IR technology

- Visible Light

Visible light belonging to the electromagnetic radiation posses its wavelength between 400 nm and 700 nm and corresponding frequency range from 430 Hz to 750

[34]Firefly Motion Tracking System User's guide, http://www.gesturecentral.com/firefly/FireflyUserGuide.pdf

[35]OPTOTRAK Technology, Northen Digital Inc., http://www.ndigital.com/msci/products/optotrak-certus/

THz. Light sources can be from nature such as the Sun or artificial manufacture like bulbs, fluorescent lamps. Among them, light-emitting diode (LED) is emerged as a future light source due to its advantages such as long life, brightness and energy efficiency, friendly environment. By utilizing of on/off capability of LEDs and high speed modulation, the visible light can be used as a wireless communication technology [67]. The technology called visible light communication (VLC) standardized as the standard 802.15.17 by IEEE Wireless Personal Area Networks working group is gaining various researches for different applications like broadcasting, sensing networks, etc. [67, 68]. Among those services, proposed indoor positioning algorithms and corresponding systems outperforms traditional algorithms based on RF, IF, Ultrasound in terms of accuracy, interference sensitivity and security [69]. Generally, an IPS based on VLC comprises of three main components placed within a finite space such as a room, building, etc with a local coordinate system associated (see Fig.2.11).

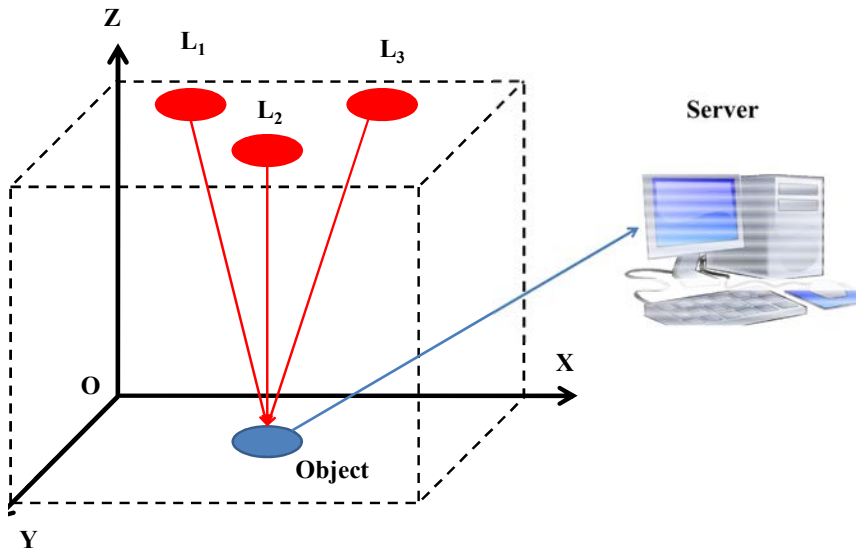


Figure 2.11: A general indoor positioning system based on visible light

The first is light emitters, usually Leds ( expressed as L1, L2, L3 in Fig.2.11) which transmit visible light signals periodically. The signals after encoded by processors of LEDs contain LED IDs and LED coordinates assumed to be known. The second component is objects to be localized. These objects upon receiving and decoding the light signals calculates their local coordinates by popular techniques like AoA, RSSI, ToA, TDoA. The third component, a server, implements a positioning algorithm to determine the global position of objects as receiving the information from the

objects. Depending on types of light signal receivers (objects), the VLC based IPSs can be classified into two classes: photodiode and camera based systems [70]. A photodiode is a kind of sensor being capable of sensing incident light and transform it into an electrical current. In addition, the current is proportional to the emitted light power. Consequently, by measuring the current at the receiver objects, the corresponding received signal strength can be derived. For the second class, the camera functioned as an image sensor is used to capture the LED emitters. By analyzing the series of taken images, the location and ID of LED transmitters can be obtained by the receiver objects. Thus, the achieved information can be used in the servers for further process of positioning the objects. Table 2.2 summaries some significant proposed IPSs based on the VLC technology.

| Reference System | Signal Sensor, Camera | Measurement & Positioning Techniques | 2D/3D space | Accuracy Level |
|---|---|---|---|---|
| Luxapose [71] | Camera | AoA/MLE | 3D | 0.1m |
| ALTAIR [72] | Camera | AoA/Triangulation | 3D | 0.4m |
| Epsilon [73] | Photodiode | RSSI/Trilateration | 3D | Under 0.4m |
| System in [74] | Photodiode | TDoA/A low-complexity Algorithm | 3D | Under 0.01m |
| System in [75] | Photodiode | AoA, RSSI/Trilateration | 2D, 3D | 2.3cm |
| System in [76] | Photodiode | RSSI/Trilateration | 2D | Under 0.4m |

Table 2.2: Some popular indoor positioning system based on VLC

As traditional light sources such as bulbs, fluorescents are speedy replaced by LEDs inside indoor spaces from buildings to warehouses thanks to their huge benefits in manufacturing as well as using them, there is a huge opportunity for realizing the proposition design for a ubiquitous, reliable, and cost-effective IPS through the exploitation of these light emitters. In addition, the systems can also provide high localization accuracy (extremely low positioning errors). These observations promote to development of IPS designs based on VLC technology.

### 2.4.2 Radio Frequency (RF) Localization Systems

Systems designed based on RF can cover larger distance since it uses electromagnetic transmission, which is able to penetrate opaque objects such as people and walls. Besides, a RF system can uniquely identify people or objects tracked in the system. In the literature, triangulation and fingerprint techniques are widespread used in RF based systems. Based on this technology, RFID (Radio Frequency Identification), WLAN (Wireless Local Area Network), Bluetooth, wireless sensor networks (WSN), UWB (Ultra Wide Band) are created. In addition, RF based technologies are further divided into narrow band based technologies (RFID, Bluetooth and WLAN) and wide band based technologies (UWB). Amongst these technologies, UWB is the most accurate and fault-tolerant

system that has a widespread usage in indoor localization. Some systems are based on these technologies comprising WhereNet [36] using RFID, RADAR [77], EKAHAU [37] and COMPASS [77] using WLAN, Ubisense [38].

- Radio Frequency Identification (RFID)

  RFID is an identification technology using radio signals to identify objects. An RFID system generally includes three components: RFID readers (or scanner), RFID antenna and RFID tags. The RFID tags are classified into two classes: active and passive tags. The main difference between the two kinds of tags is power sources on which they rely to operate. While a passive tag is activated only as receiving power provided by sent signals of the readers, an active tag with own internal power supply can continuously broadcast signals. Therefore, the passive tags are smaller, lighter and cheaper than the active tags, although, their communication range is shorter than the range of active ones. The tags are usually attached to objects and store information about objects. The RFID system operates under the protocol of two-way radio transmitter-receivers. In other words, the reader sends a request signal to the tag and then read the response of tag to retrieve the data.

  The IPSs based on the RFID technology can be structured by different ways. Alternatively, the readers, the tags or their combination can be deployed as the reference points with known positions. Thus, as the tags or readers are attached to the target objects to be localized, the system can obtain the rough position information about the objects upon receiving the information of references. However, due to the fact that most of tiny RFID reader chips are integrated popularly into handheld equipments such as PDAs, mobile phones, RFID based IPSs are oriented to deploying RFID tags as reference nodes.

| Reference System | Measurement & Positioning Techniques | 2D/3D space | Accuracy Level |
|---|---|---|---|
| WhereNet | ToA/Triangulation | 3D | 3cm |
| LANDMARC [78] | RSS/Triangulation | 3D | 1-2m |
| System in [79] | Private | 3D | 2cm |

Table 2.3: Some significant indoor positioning systems based on RFID technology

  Although the IPSs using the RFID technology are simple and light-weight, positioning techniques requires numerous infrastructure components such as more deployed

[36] WhereNet, Zebra Technology Company, https://www.zebra.com/us/en/solutions/location-solutions/enabling-technologies/wherenet.html

[37] Ekahau positioning system, http://www.ekahau.com/userData/ekahau/documents/solution-brochures/Ekahau-RFID-over-WiFi-RTLS-Solutions.pdf

[38] Ubisense positioning system, http://ubisense.net/en

tags or readers.

- Wifi

Wifi is a wireless communication technology using a series of standards in IEEE 802.11 operating in the two licensed bands 2.4 GHz and 5 GHz according to ISM band release. Wireless Local Area Network (WLAN) based on this wireless technology is deployed widely in public areas such as building, hospital, stations, etc. Therefore, exploiting the available infrastructure of WLAN is the primary advantage of IPSs based on Wifi signals. By this way, all Access Points (AP) play a role in being reference nodes with location-awareness. Meanwhile, objects to be positioned are equipped with a Wifi communication module to transmit RF signals. The strengths of signals are measured by APs and sent directly to a server. Based on these measurements, a positioning algorithm is operated to determine the position of object. Fig.2.12 illustrates a typical structure of IPS based on Wifi technology and their operation.

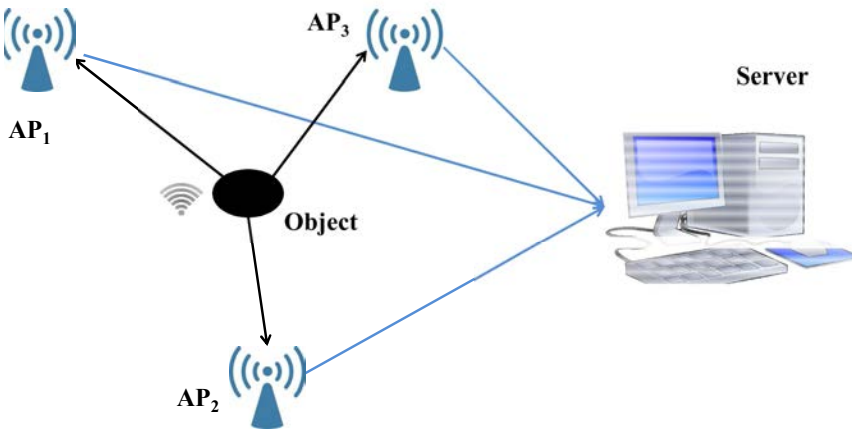


Figure 2.12: A general indoor positioning system based on Wifi technology

Depending on measurement techniques and positioning algorithm used, different IPSs are proposed. Table 2.4 summaries some significant system proposed and developed recently.

The two main goals in developing an IPS are high accuracy level and at the same time acceptable cost.Wifi-based indoor positioning system is seen as a low cost solution since it reuses the available hardware of WLANs. In addition, consumer

| Reference System | Measurement & Positioning Techniques | 2D/3D space | Accuracy Level |
|---|---|---|---|
| RADAR | RSSI/ Triangulation | 2D | 2.26cm |
| EKAHAU | RSSI/Triangulation | 2D | 1m |
| COMPASS | RSSI/ FingerPrinting | 2D | 1.65m |
| Horus [80] | RSSI/ FingerPrinting | 3D | 3.5cm |
| ActiveCampus [81] | RSSI/ FingerPrinting | 2D | 4cm |
| PlaceLab [82] | RSSI/ FingerPrinting | 2D | 8cm |
| OIL [83] | RSSI/ FingerPrinting | 2D | 5cm |

Table 2.4: Some significant indoor positioning systems based on Wifi technology

electronic devices such as mobile phones, laptops, TVs, PDAs support communication wirelessly by wifi, thus they can be used to locate human or objects. However, in the indoor environment with appearances of interferences, the precise level of IPSs is quite low within several meters. Using fingerprinting is a solution to address this issue but complexity and cost of systems are increased considerably.

- Zigbee

Zigbee-a wireless technology standard is usually associated to wireless sensor network (WSN). The network is built on the physical and media access control (MAC) defined by IEEE 802.15.4 standard. Based on the specification, the standard uses unlicensed ISM radio band: 2.4 GHz supporting a low rate of transferring 250 kbit/s. Generally, the WSN consist of a number of sensors placed randomly in a finite space. Sensors such as MicaZ, TelosB are electronic devices with capability of sensing, communicating wirelessly and computing. WSNs are widely deployed for various applications in different fields due to their ability in monitoring and controlling remotely. Among them, location based services like tracking, detecting and determining positions of events are interested in designing the application layer of network.

For building an IPS based on Zigbee (WSN) technology, several sensor nodes with known location are chosen to be the references. Meanwhile, a target object equipped with or without sensors interacts with reference nodes. The information about the target received at the references then is forwarded to a base station for further processing to obtain position of target. Fig.2.13 shows the techniques.

| Reference System | Measurement & Positioning Techniques | 2D/3D space | Accuracy Level |
|---|---|---|---|
| OPT [84] | RSS/Triangulation | 2D | 1.5-1.8m |
| System in [85] | RSSI/Triangulation | 2D | 3m |
| System in [86] | RSSI/Triangulation | 2D | 3m |

Table 2.5: Some significant indoor positioning systems based on Zigbee technology

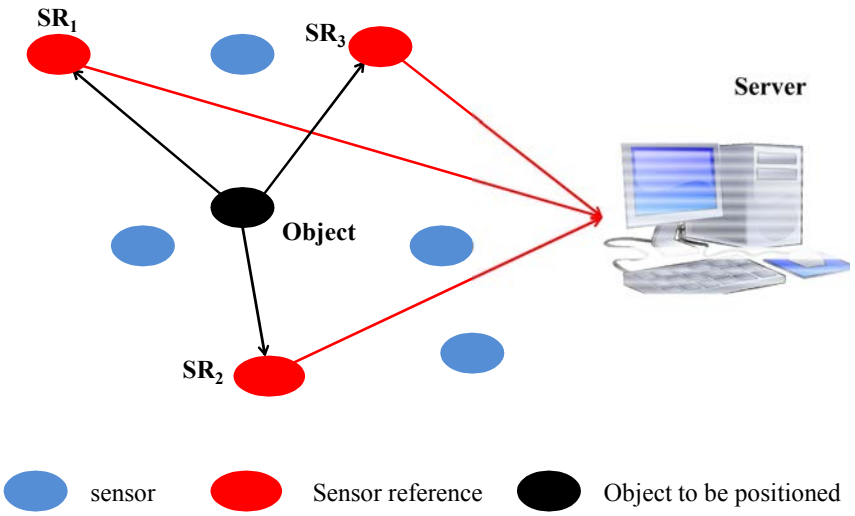


Figure 2.13: A general indoor positioning system based on Zigbee technology

- Bluetooth

  Bluetooth or the IEEE 802.15.1 standard is another kind of wireless communication technology deployed popular in wireless Personal Area Network (WPAN). The maximum communication range that latest technology (Bluetooth 2.0) can support is up to 100m. Meanwhile, in normal conditions, the range is only about 5-10 m. However, sharing information using Bluetooth takes more advantages such as high security, low cost, low power and light-weight. Therefore, Bluetooth are embedded into the most of electronic handheld devices (e.g. mobile phones, PDAs, laptops). An IPS based on the Bluetooth technology relies on the Access Points as references. Meanwhile, objects to be positioned requires a Bluetooth module such as tags to communicate with the references. The signals sent from the objects and received at the references are input data for a server to estimate the position of objects. Some typical systems are based on these technologies comprising Topaz [39], ZONITH [40] or a system proposed in [87]. Table 2.6 summaries the systems and their significant characteristics.

- Ultrasound

[39] Topaz positioning system, http://www.tadlys.co.il/pages/Product_content.asp?iGlobalId=2
[40] ZONITH Indoor Positioning, http://zonith.com/wp-content/uploads/ZONITH-Indoor-Positioning-System-Brochure.pdf

| Reference System | Measurement & Positioning Techniques | 2D/3D space | Accuracy Level |
|---|---|---|---|
| System in [87] | RSS/FingerPrinting | 2D | 2-10m |
| Topaz | RSS/Triangulation | 2D | 5m |
| ZONITH | RSS/Triangulation | 2D | 6m |

Table 2.6: Some significant indoor positioning systems based on Bluetooth technology

In contrast to electromagnetic waves, sound is a mechanical wave that expresses an oscillation of pressure transmitted through any medium except a vacuum such as air or water. In the wide range frequency of wave, the human ear can detect the sound wave with the range from 20Hz to 20 KHz referred as audible range of hearing. The sound with frequency above the audible range (i.e.,more than 20 KHZ) is called an ultrasound. Comparing to the RF signals, the ultrasound has some advantages such as slow propagation speed, passing through most of objects (e.g., walls, water) which can be exploited effectively to use in IPSs. Table 2.7 presents some popular indoor positioning systems based on Ultrasound technology which include Active Bat [65], Criket [78], Sonitor [41].

| Reference System | Measurement & Positioning Techniques | 2D/3D space | Accuracy Level |
|---|---|---|---|
| Active Bat [65] | ToA/ Triangulation | 2D/3D | 3cm |
| Criket [78] | ToA/Triangulation | 2D/3D | 1-2cm |
| Sonitor | Private | 3D | 8-10cm |

Table 2.7: Some significant indoor positioning systems based on Ultrasound technology

Although low cost is the one of the most benefits of the systems based on ultrasound technology, the accuracy level is lower than that of IR-based systems due to the reflect influence and noise interference. Additionally, in order to address the issues of synchronization and coordination, the RF technology is usually required in the system design, which in turn results in increasing the cost of the whole system.

## 2.5 Application of Localization in Logistics

The main logistics activities such as storing, handling and transporting merchandises or their containers usually take places in finite spaces like warehouses, shipping containers, or terminal ports. In fact, there are a huge number of goods or their containers stacked or placed by a manner so that it can facilitate next processes like handling or moving the requested objects. However, due to the high dynamic nature of merchandise flows (inbound and outbound), managing them is prone to usual errors such as wrong orders, incorrect position or misplaces. Therefore, a reliable and robust system for identifying

[41] Sonitor positioning system, http://www.sonitor.com/

and localizing the requested objects in real time is necessary to be deployed. In addition, location information can further be used to improve efficiency of processes such as handling, controlling, monitoring. In this situation, an IPS mentioned in the previous section can be matched to realize the mission. Depending on many factors such as specific indoor spaces (warehouses, TEU containers), performance requirements, specific application, technology type used, etc., an IPS can be designed appropriately. This section is based on particular applications for logistics activities to review current positioning systems designed and developed to provide the services.

### 2.5.1 Conditioning Monitoring

A series of three systems using WSNs are proposed [88–90] to monitor environment conditions inside TEU containers containing sensitive goods such as fruits, vegetables or refrigerated foods. To do this, the used containers adopted from the design of University of Bremen are equipped with a RFID system and a WSN [91]. The network consists of two types of sensors. The first type includes all sensors placed arbitrarily on pallets carrying directly the physical goods or their boxes. These sensors are requested periodically to report their sensed parameters of ambient environment and their locations to a central base station for further supervising and controlling. In order to determine the position of sensors attached on the pallets, the second type of sensors is used. This kind of sensors including 20 Tmote Sky sensors are fixed on the side walls of the container and considered as reference (anchor) nodes with known locations. Fig. 2.14 (sourced from [90]) illustrates the configuration of reference sensors in the TEU container.

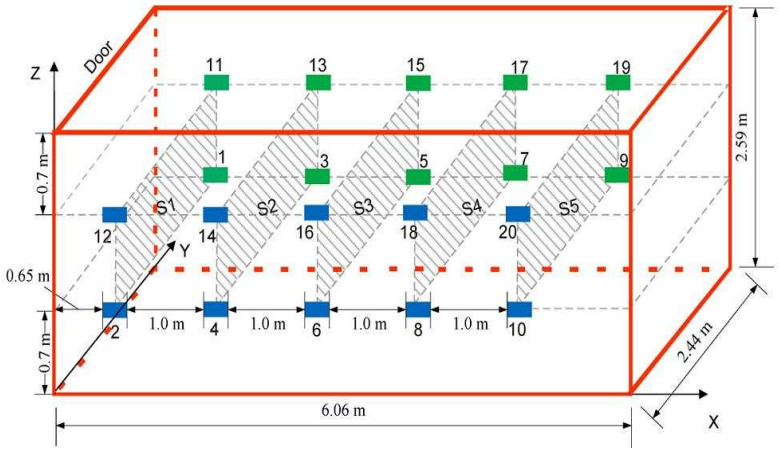


Figure 2.14: Deployment of 20 reference sensors (green and blue rectangular marks) in the container

In the algorithm presented in [88], by collecting the RSSI values of wireless signals transmitted from the anchors each sensor estimates the corresponding distances between them. The distances then are used in the multi-lateration algorithm to determine its position in the container. Although the algorithm is simple, the performance is limited by low precise level of distance measurement due to RF signal damping and reflection inside the container. To address the issue, a dynamic RSSI filtering is used in [89, 90] to eliminate the error during the process of measuring the distances. As the result, this dynamic method obtains the higher accuracy level of localization. Therefore, the exact distribution of environment measurements at the corresponding places of sensors allows the system to monitor effectively and adjust appropriately in order to ensuring the quality of the goods under the optimal environment condition.

### 2.5.2 Handling Facilitation

In warehouses, the majority of activities such as moving, handling pallets horizontally are performed by automated guided vehicles (AGVs). Meanwhile, storing or retrieving the pallets in or from a high racks requires standard forklifts or special AGVs in combination with manual support in driving and controlling. In order to enable automatic pallet engagement, a monocular vision based system is proposed for positioning and orienting pallets [92]. In the system, a single camera attached on the fork carriage top of a forklift is capable of captures the images of target pallet being engaged at any height (Fig.2.15 sourced from [92]).

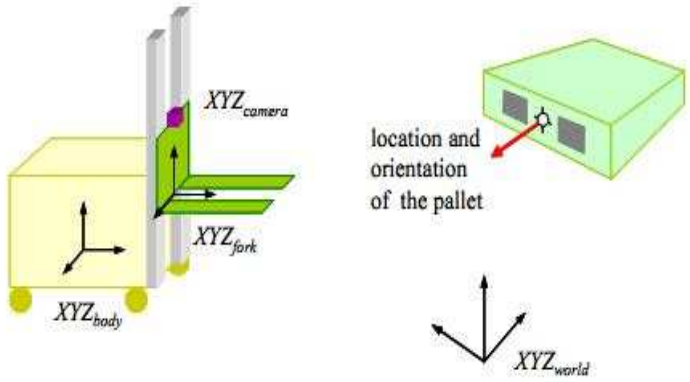


Figure 2.15: Virtual configuration of vision based systems for positioning and orientating pallet automatically

The information extracted from the captured images is used in developed algorithms

called back-project to find the orientation and 3D location of the pallet. The experiment results show that a high accurate level of positioning can be obtained as the forklift is near the target pallet. Practically, the system not only engages the pallets but also can be used for supporting processes like loading or unloading truck effectively.

### 2.5.3 Inventory Management

Besides physical goods, there are many types of assets used in logistics activities such as handling equipments (e.g., forklift, pallet jacks, etc.), returnable transportation items (e.g., pallets, etc.) and so forth. The asset management involving monitoring state and location of the assets plays an important role in expediting the product flow, thus increasing the efficiency of logistics processes. Among other things, warehouses are gained the particular interest since most of logistics activities take places in these locations. In other words, movements as well as states and positions of assets are changed frequently. These alternated data are required to be updated automatically in warehouse management systems (WMS) for further supervising and appropriate controlling. However, the updating process is common to faults to occur since it relies on the manual performance such as barcode scanning, order sorting.

A WSN based system nanoLOC proposed in [93] allows addressing the issues by detecting storage or retrieval of pallets and then estimating new bin locations of storage pallets on a three-level bay in a warehouse. Technically, the system designed for the bay include four wireless sensors fixed on its two sides, one base station and other sensors equipped with the pallets and the handling equipments (i.e., forklifts). Fig.2.16 sourced from [93] illustrates the deployment of the sensor nodes. On the operation perspective of the system, once the pallet carried by the forklift is detected to be lifted up, its associated sensor reports the retrieval load to the WMS. Similarly, the storage pallets and their new bin locations are reported when they are put down on the rack. In the both cases, certainly the pallets are identified by an Auto-ID technology such as barcode or RFID. Meanwhile, the location information is obtained by a range-based algorithm. First of all, the pallet sensor calculates distances from it to the four anchors based on the SDS-TWR technique. Finally, these distances are sent to the base station to determine the location of pallets by the tri-lateration technique along with an Extended Kalman Filter (EKF) estimation. For further testing and evaluation, the proposed system is installed in the demonstration storage of the Fraunhofer-Institute for Material Flow and Logistics using euro-pallets.

On the aspect of positioning performance, experiment results show that the system can achieve a precise localization around half a meter. Although the result meets the requirement of a metering precision in the warehouses, the LOS between pallet sensors and

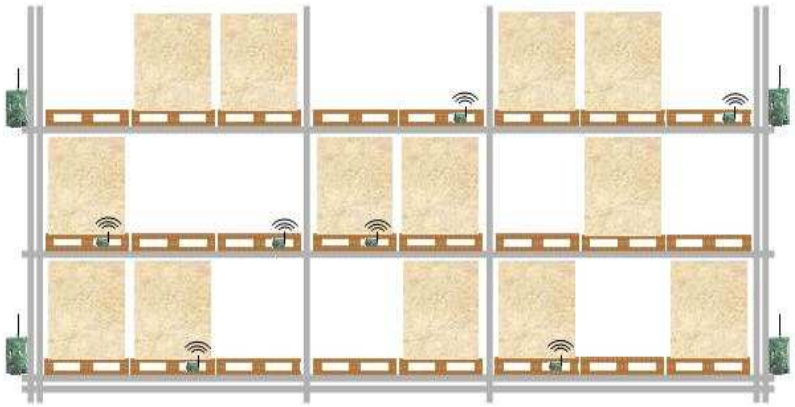

Figure 2.16: Deployment of sensor nodes in a storage rack of pallets and boxes

the anchors must be ensured in the deployment of sensors. More importantly, the system can benefit the efficiency and effectiveness of the WMS by automatically supervising the inbound and outbound flows of items in real time.

### 2.5.4 Tracking Logistics Assets

Tracking systems for logistics application enable locations of assets to be monitored in real-time regardless processes like storing, moving, transporting that they are participating. In current practice, two tracking systems based on GPS and Auto-ID technologies (e.g. RFID, Barcode, etc) are used the most. Since each system is not compatible for logistics activities completely, their own applications are shared in different ranges of objects. In other words, while the Auto-ID system is suitable for cataloging individual items, cases and pallets, the GPS can be used to track logistics assets at a broader level. The separation comes from several points of views. First of all, from technical perspective, short communication range of devices in the Auto-ID systems allows them operate effectively in indoor spaces (e.g., warehouse, large containers) and in contrast, the GPS can monitor the positions of large containers, fleet of trucks in outdoor environment due to its very long range of wireless communication. In addition, high cost and low precise level of localization are main causes preventing the GPS from using in the enclosed, inside spaces.

For practical tracking based RFID technology, an intelligent lot-tracking (LotTrack) system [94] is deployed in cleaning rooms of wafer factories where the chain of production processes are managed based on the dispatch list instead of an automated material handling system. The dispatch list represents the order the wafer boxes to be processed. Since there is a huge number of boxes (up to thousands of boxes) in the lists which need

to be handled, keep tracking of positions of boxes is required to ensure the production processes. The LotTrack system developed by Swiss company Intellion takes the mission. The system comprises of three main components. The first component called Distag is a smart RFID tag attached on the wafer boxes. The Distag contains a control panel enabling local interaction with the factory operators, a signaling module (LED) displaying the order or priority of boxes according to the production schedule. The second component is an array of antennas mounted on the ceiling of the cleaning room along the factory's interbay and intrabay. This component contains ultrasound emitters and provides the communication channel between the Distags with RFID readers. The last component is a central server store the backend software to link shop-floor activities and the integrated with the manufacturing execution system (MES). The server supports a dashboard for visualizing all transport and storage activities relating to the wafer boxes. The LotTrack operates as following. The ultrasound emitters transmit periodically a ping signal. These ping signals are received by the Distags on the wafer boxes. Using the physical measurement techniques, the Distag compute the travel time of the ultrasound waves together with corresponding RSS and then temporarily store the results locally. The data is sent back to the RFID receivers in the antenna lines and then to the central server successively. In the central server, a complex algorithm computes the real-time position information of wafer boxes. The accuracy level of positioning provided by LotTrack is up to 0.5m. The systems are deployed in many companies like Infineon, STMicroelectronics, and OSRAM. The main advantage of LotTrack solution is to reduce cycle times and working-in-progress (WIP), increase operator efficiency and enable automatic authentication of production lots at the equipment.

Using the GPS to manage and track delivery vehicles along with shipping containers is one example where the technology can create real benefits and cost savings. Particularly, the technology can keep logistics activities in the loop on whether a truck is on road or whether it might be delayed due to inclement weather or certain accidents, using that intelligence to make the appropriate controls. In addition, the GPS system allows the third party logistics companies to make decisions timely based on service times and service-level requirements (i.e., priority). By this way, the service quality for customers is ensured.

Besides the two mentioned technologies, a proposed tracking system in [95, 96] uses WSNs to determine the position of shipping containers in ports and terminal. In this system, six wireless sensors are placed on the edges of each container. In addition, a base station upon receiving the two flows of information from the sensors is used to calculate the relative position of containers. The first information flow expresses the neighborhood relation between containers obtained by neighbor detection function of sensors. The

second describes the geometrical constraints of containers. By setting up a coordinate system inside the container, the information is transformed to be a mathematical model. Therefore, as the position of a container is known, the location of the other containers can be obtained. The demonstration of system is implemented by using Tmote Sky sensors programmed in nesC in TinyOS operating system and a base station running a java based software to provide a graphic user interface (see Fig. 2.17(Sourced from [95, 96])).

Figure 2.17: A graphic user interface retrieved from the works

The results of demonstration prove the effectiveness of techniques in precisely localizing the real containers as well as responding quickly to any change of container configuration (e.g., adding, removing containers). Due to the simplicity of configuration, the system can be applied in practical activities of logistics at ports and terminal where huge number of containers are imported, stored and exported frequently.

### 2.5.5 Safety and Security

Considering work places such as chemical industry manufacturer in which maintaining the safety condition in handling and storing special materials is the most important concern. The observation comes from the fact that the two processes are constrained by regulatory requirements about perceptive volume of carried materials and their locations in the places. For instance, the maximum allowable volume of liquid corrosive (acid) material stored inside a biopharma production factory is 1000 gallons, and a flammable material must not be placed in a 20-feet proximity range of an oxidizer source. Therefore, monitoring the states and positions of materials in a certain space continuously allows keeping its safety under control. One system in [97] based on a WSN is proposed to monitor positions of pallets carrying the materials in a warehouse. By this way, the system is capable of operating in real time to detect the constraint violation and then broadcast alarm signals. On the design perspective, the system includes a set of sensors and a base station. The

sensors are classified into two functioning types. The first type is mounted on the ceiling of warehouse to function as Beacons. The other referred to as Motes is placed on the pallets to indicate their positions.

Fig.2.18 adapted from [97] illustrates the node deployment.

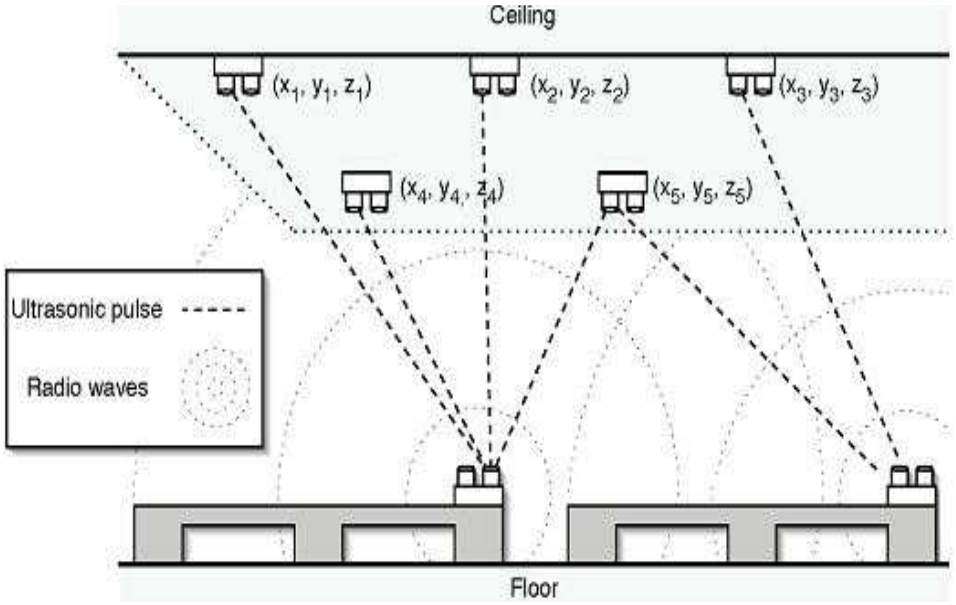


Figure 2.18: Deployment of sensors and pallets in a warehouse

For localizing the Mote positions, the Beacons estimate the distances between them and the Motes by using AoA techniques. These distances are used in positioning techniques combining probability and MLE methods to obtain the final location of the Motes. The experiment results show that the system can achieve the high accuracy level (0.33m). The results can detect the spatial violation of pallets effectively because their wide size is about 1m. However, the system is needed to improve the increasing the performance time. In addition, since the Motes use ultrasound signals to transmit, they require LOS environment inside the warehouse. As a result, the deployment is taken into account of the observation.

## 2.6 Conclusion

In this chapter, we overviewed the main techniques, algorithms and technologies used to localize physical objects in indoor environments. The algorithms can be classified with two groups: range-based and range-free. In the range-based algorithms, determining the position of target relies on the signal features (RSSI, ToA, TDoA, or AoA) to estimate

the distance. Meanwhile, the range-free algorithms only use the connectivity or proximity information to localize the targets. Table 2.8 resumes some positioning systems introduced in Section 2.5, that are proposed and used for specific applications in logistics. Most of the mentioned systems are based on range-based algorithms which provide a good positioning precision in regards to the application.

| **Systems** | **Technologies** | **Techniques** | **Algorithms** | **Advantage** | **Disadvantage** | **Logistics Application** |
|---|---|---|---|---|---|---|
| LotTrack [94] | RFID, Ultrasound | RSSI/Private | Range-based | High accuracy level (0.5m) | Support 2D positioning, require addition infrastructure | Tracing and Tracking items |
| nanoLoc [93] | Zigbee | SDS-TWR/Private | Range-based | High accuracy (0.5m), support 2D/3D positioning | Complex Algorithm | Asset Management |
| [88] | Zigbee | Static RSSI/Multilateration | Range-based | Simple Algorithm, support 2D/3D positioning | Low accuracy (1.2m) | Condition Monitoring |
| [89, 90] | Zigbee | Dynamic RSSI/Multilateration | Range-based | High accuracy (0.8m) | Additional Hardware and system cost | Conditioning Monitoring |
| [95, 96] | Zigbee | Proximity, Equality & Inequality system | Range-free | Simple algorithm, support GUI in 3D positioning | Using a large number of sensors | Tracing & Tracking assets |
| [92] | Vision-based (camera) | Vision | Range-free | High accuracy & simple infrastructure | Require a high quality camera with short range interaction | Handling Facilitation |
| [97] | Zigbee | AoA/MLE & Probability | Range-based | High accuracy, support 3D positioning | Require LoS environment | Safety and Security |

Table 2.8: Summary of proposed systems applied for localizing assets in logistics

From the above related works, the wireless sensor technology and WSNs benefit from their wide applications in positioning logistics assets. In Physical Internet, $\pi$-containers are equipped with wireless sensors to support the smartness characteristics. We exploit the wireless communication and processing abilities of sensor nodes to develop a system that localizes unitary $\pi$-containers inside their composite $\pi$-container. This system can operate in autonomous manner that allows the positioning process take place everywhere (i.e., inside $\pi$-trucks, composite $\pi$-containers, $\pi$-pallets, etc.) and at any time, without the need of a dedicated infrastructure. We exploit the neighborhood information between nodes in the wireless sensor network to determine the physical layout of the composite $\pi$-container. Indeed, the range-free positioning techniques will be more suitable than the range-based methods since the ranging measurements can be affected negatively by the perturbed environment (i.e., various obstacles, high noisy condition, highly interference).

In addition, the range-free positioning systems are cost-effective because they benefit from no additional infrastructure (i.e., access points) required.

In the next chapter, we develop our proposed approach based only on proximity information between wireless nodes to localize the $\pi$-containers stacked in a finite space such as composite $\pi$-containers, H-containers, and $\pi$-pallets.

# Chapter 3

# Problem Statement and Proposals

## Contents



## 3.1 Problem Statement

Logistic processes such as partial loading/unloading or composing/decomposing of $\pi$-containers play an important role for a successful Physical Internet. In fact, in a $\pi$-hub, a set of $\pi$-containers can be composed or loaded so that their combination is unit loads for efficient handling, moving, storing. In addition, these $\pi$-containers can be unloaded and decomposed and then recomposed for further routing to the different next destination in

another $\pi$-hub. Since exchange of $\pi$-containers is the core activities taken place continuously in the $\pi$-hubs, high frequency of transformation processes can introduce a desynchronization between the physical and information flows of the $\pi$-containers. In other words, the real composition characteristics of a composite $\pi$-container (number and relative position of stacked $\pi$-containers) can differ from the information obtained and stored in the Physical Internet Management System (PIMS). For example, a unitary $\pi$-container that will be dismantled in the next $\pi$-hub should be placed at the outermost place of their composite $\pi$-containers for facilitating further the decomposing process. However, the information does not reflect adequately the real position of the unitary $\pi$-container where it is encircled by other unitary $\pi$-containers. In this case, orders, orientations and relative positions of unitary $\pi$-containers are taken into account during arranging and stacking them since they impact on the efficiency of the decomposition or dismantle processes. In order to overcome this problem, **we propose a system to generate and maintain automatically a virtual 3D layout which represents exactly the spatial distribution of unitary $\pi$-containers within the composite $\pi$-container**. Fig.3.1 shows an example illustrating the stated problem of retrieving 3D layout of spatial arrangement of 9 unitary $\pi$-containers within the composite $\pi$-container.

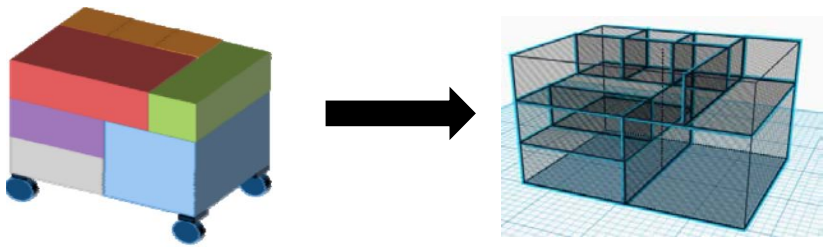

Real composition of 9 unitary π-containers

Corresponding 3D layout of the composite π-container

Figure 3.1: An example for illustration of the problem: retrieving 3D layout of $\pi$-container arrangement

To adapt to a very dynamic environment of the Physical Internet, the layouts must be obtained in an autonomous manner (i.e., without human intervention) at any time and in any place (e.g., in $\pi$-hubs, $\pi$-movers during transportation, $\pi$-stores, etc.). The layouts can be sent to the PIMS periodically or to humans and artificial operators such as handling robots when requested in on-demand manner. Therefore, this model (3D layout) can be used to generate guidance information for loading/unloading systems (e.g., paletization/depaletization robots). Other value-added services can be declined such as permanent inventory by the different stakeholders of the logistics chain, or the monitoring of the global state of the composite $\pi$-containers (degradations, opening tentatives,

incompatibility between goods, etc.).

In the following sections, we describe main factors which impact on the process of constructing the layouts. The factors mainly come from the characteristics of $\pi$-containers in both physical and information perspectives.

### 3.1.1 Physical characteristics of $\pi$-containers

- Standardized Dimensions

  As mentioned in the Chapter 1, $\pi$-containers are designed to be modular and world standardized. These characteristics are exploited in the PI processes (i.e., loading and composing) to optimize the space utilization, thus minimize the air packaging problem. The standardized dimensions of $\pi$-containers are classified into three different groups: small, medium and large sizes which characterize three corresponding types of containers: P-containers, H-containers and T-containers. To support efficient encapsulation of $\pi$-containers, the dimensions are designed and optimized such that a set of P-containers ( or H-containers) after composing can be fully fit in inner space of a H-container ( or T-container) respectively. In our proposition, we consider to construct the layouts of H-containers which are filled fully by a limit set of unitary $\pi$-containers (P-containers) or smaller composite $\pi$-containers. The external maximum size of H-containers is usually 1.2 m and that of P-containers is on the set $\{0.12, 0.35, 0.48, 0.6, 0.12\}$.

  Note that, we can extend our approach for efficiency constructing 3D layouts of T-containers composed by a set of H-containers.

- Stackability

  Stackability refers to ability of $\pi$-containers by which they can be piled up on the top of others during composing or loading processes to form composite $\pi$-containers or block of $\pi$-containers with perfect cube shapes. The ability supported by interlocking structure and modularity allows a set of $\pi$-containers to snap together to a stable block. However, stackablity is imposed by rotation allowance. In general, the rectangular shape of $\pi$-containers enables them to be rotated in orthogonal directions (8 possible rotations). The flexible rotation capability permits $\pi$-composers to have more options in creating efficient unit loads having different sizes. However, in fact, the rotation orientation of $\pi$-containers can be constrained by orientation requirement of the contents encapsulated inside the $\pi$-containers. Practically, the rule represented by the sign or label "**this way up**" on the cover of current packing boxes (Fig.3.2) is noted during packing, stacking or loading process. As a result,

the imposition causes a decrease of number of rotation possibilities.


(a) Traditional carton box (b) M-box in MODULUSHCA project

Figure 3.2: The sign "**This way up**" is printed on the cover of packing box for guiding the direction of packing, stacking and loading (Sourced from the Internet). In this case, the boxes have fixed vertical orientation, they are allowed to rotate by 90° horizontally.

In addition, all the $\pi$-containers have to be placed orthogonally inside the composite $\pi$-containers (with their sides parallel to the sides of the composite $\pi$-container), to facilitate the loading and unloading operations.

- Material

To be green is one of requirements that designing the $\pi$-containers must be respected to obtain the sustainability of logistics in the environment perspective. The material used to make the $\pi$-containers has major impacts on the designing criterion such as lightweight, reusable ability. In fact, depending on the embedded physical goods, the material is selected properly in order to firstly protect the embedded products effectively. For example, there are scenarios in which $\pi$-containers covered by special materials (steel, alumina material) are used to contain and protect special contents (e.g., exotic, hazardous liquids, etc.). Secondly, when the $\pi$-containers are equipped with the wireless communication components (i.e., RFID tags, wireless sensors, etc.), data exchange (i.e., reading product identifier, transferring sensed data) enabled by wireless signal propagation can be effected by the materials of the $\pi$-containers. In the scope of our thesis, we consider the P-containers used for the FMCGs [28] are mostly made up by carton, plastic, wood material that can benefit from effective wireless communication (i.e., low level of obstacle severity). This characteristic is clarified in the following section.

### 3.1.2 Instrumentation of $\pi$-containers

The intelligence of the $\pi$-containers is enabled by exploiting the generic capabilities (e.g., sensing, data storing, processing, communicating) of the wireless sensor mote equipped physically to them. When interfaced with professional sensor boards (i.e., humidity, temperature, etc), the sensing capability of the node allows the ambient environment condition of the container to be monitored periodically. In our scope of thesis, this function of node is not considered and left for other deep researches. Integrated with a memory, the sensor node can store and maintain relevant data. Applying for the PI network, since $\pi$-containers are equivalent to the data packets flowed in the Digital Internet networks, information relating to fundamental specification of $\pi$-container should be stored in the memory such as container identifier, container dimension, container category. In addition, to support routing protocols effectively, routing information (i.e. previous/next/final destination address) of the $\pi$-container provided by the PIMS is also added to the storage. Processing capability enables the nodes to perform specific tasks and provide corresponding additional functionalities for the containers. Meanwhile, enabled by integrated wireless transceivers, the $\pi$-container can communicates with other $\pi$-containers or $\pi$-facilities (e.g., $\pi$-trucks, $\pi$-composers, handling robots, etc.) through the wireless communication of their nodes. Practically, an example of integration of all these capabilities is the Intelligent Container (so called InBin as Fig.3.3) recently developed by the Fraunhofer Institute for Material Flow and Logistics [42] to support transporting the perishable food products efficiently.


Figure 3.3: Intelligent containers designed and introduced by the Fraunhofer Institute

Above all, dual capabilities including processing and communication allow cooperation of the nodes to perform joint algorithms. In the PI, this potential characteristic should be exploited as much as possible in order to provide value-added services since composition of $\pi$-containers is taken place frequently in $\pi$-nodes. Made up of materials such as woods, cartons, plastics, sensor nodes enables their $\pi$-containers communicate effectively. Thus,

[42] inBin project, http://www.industrie40.iml.fraunhofer.de/en/ergebnisse/inbin.html

a corresponding adhoc network consisting of these sensor nodes can be formed inside a composite $\pi$-containers. Fig.3.4 illustrates the deployment of sensor nodes for $\pi$-containers and an adhoc wireless network that is formed from the connections of wireless nodes.

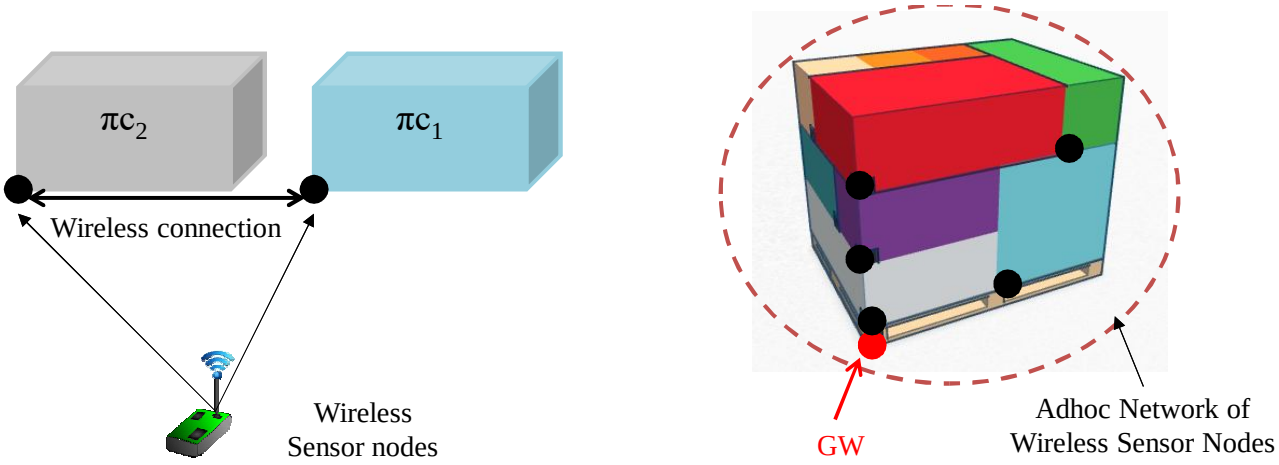


Figure 3.4: Sensor nodes embedded into $\pi$-containers allows them to communicate together and forms an adhoc network inside the composite $\pi$-containers

This kind of networks is ubiquitous in the PI network since unitary $\pi$-containers are composed and embedded fully in H-containers for efficient handling, loading, and transporting. Therefore, in order to mange the composite containers efficiently, the sensor nodes of H-containers act as communication gateways (GW) that collects data from the internal sensor network and provides an access point for the PIMS, handheld devices or external networks.

## 3.2 Methodology and Assumptions

Traditionally, container loading tools are used to find the optimal solution for loading a set of smaller rectangular boxes into a shipping container so that the space utilization is maximized [98]. This type of problem well known as container loading problem (in short, CLP) can be developed for different scenarios (e.g. loading in multiple containers, bin packing problem, etc.) with different kinds of constraints (e.g. weight, priority order, etc.) [99–103]. The problem can be solved by different optimization algorithms whose common structure includes a defined objective function (minimize the empty space in the container or maximize the space utilization) and a set of constraints. As a result, a solution will be called loading pattern that describes an optimal way to arrange the boxes inside the container .

In the PI, similar patterns (e.g., composite $\pi$-containers) are frequently created by $\pi$-composers that composes a set of unitary $\pi$-containers (P-containers) to be efficient unit loads. In this thesis, we propose an approach to retrieve the spatial distribution (named as 3D layout) of unitary $\pi$-containers that are arranged inside a finite space (composite $\pi$-containers or compact H-container). In contrast to the CLP, our approach faces many following challenges since all the $\pi$-containers are allocated in the H-container as a "black box".

1. The number of unitary $\pi$-containers is unknown.

2. The dimension of unitary $\pi$-containers is unknown.

3. The way to arrange the unitary $\pi$-containers (objective function in the CLP and other constraints such as weight distribution constraints) is unknown.

Thanks to the instrumentation of $\pi$-containers, the two first challenges can be resolved. Accordingly, when a sensor node is mounted physically on the unitary $\pi$-container, it can store information relating to the specification of $\pi$-containers (i.e., identifier number, dimension, material, etc.). In addition, since the sensor nodes can interact with the GW, the GW can know the number of $\pi$-containers available inside the H-container. Meanwhile, the third challenge can be released if the $\pi$-composer provides the unknown information. However, in our methodology, we keep the information to be unknown in order to obtain the generality of our approach. In addition, since the retrieved 3D layout used to validate the conformity with the layout predefined by the $\pi$-composer, our approach remains independent to the 3D construction scheme issued by the $\pi$-composer. Thus, based only the number of unitary $\pi$-containers, their dimensions, and dimension of the H-container, we can model the stated problem as a constraint satisfaction problem (CSP) that consists of the geometrical constraints as follows:

1. Non-overlapping constraints: The unitary $\pi$-containers do not ovelap.

2. Within-container constraints: The unitary $\pi$-containers lie entirely within the H-container.

Assumed to be freely rotated, the CSP can have many solutions since the unitary $\pi$-containers can be oriented without violation of the two conditions.

The main objective of our approach is to find a unique representation of the exact composition of the $\pi$-composite. That is equivalent to the unique solution obtained from the modeled CSP. Thus, in order to reduce the feasible solution of CSP or obtain the unique solution, we introduce a new kind of constraints originated from the networking

aspects: the proximity constraints. These constraints can be obtained thanks to instrumentation of the $\pi$-containers and the algorithm performance of networks to determine the neighborhood information for all the unitary $\pi$-containers. Fig.3.5 below illustrates the proposed approach to obtain the 3D layout of the composite $\pi$-container.

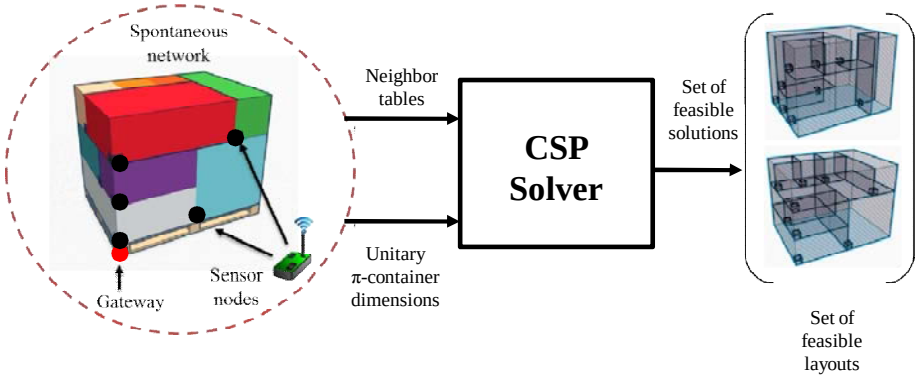


Figure 3.5: The proposed model for obtaining the 3D layout of $\pi$-container arrangement

The proximity relationships of nodes in the WSN can be obtained after several successive operations performed in collaboration between the GW and the nodes, and under following assumptions:

- The transmission range of the nodes is influenced by several factors like the operating frequency, the transmission power or the antenna gain. We consider here the transmission range as the distance where the communication between two nodes can be set up, and beyond which the quality of the communication exceeds a given stability.

- Each sensor node equipped with one omnidirectional RF antenna can adjust its communication range through the control of the transmission power level [104]. To verify that this assumption is reasonable, we realized some experiments using a MICAZ platform [43]. The nodes are based on a 2.4 GHz IEEE 802.15.4 compliant RF transceiver offering 32 transmission power levels. The experimentation has been realized under different conditions (e.g. sensor's line-of-sight or obstacles). A communication distance from a few centimeters to several dozen meters is achieved in consonance with the range of the RF power values. The detailed results will be presented in the Appendix A. To conclude, each unitary $\pi$-container with the external

[43] MicaZ Platform Specification, http://www.memsic.com/userfiles/files/Datasheets/WSN/micaz_datasheet-t.pdf

dimensions mentioned in section 3.1.1 can adapt its transmission range and detect the proximity of other $\pi$-containers in the H-container, and communicate with them.

As a result, position constraints between the unitary $\pi$-containers which will be used in our CSP, can be obtained after several successive operations performed in collaboration at the gateway and node levels:

1. The first operation concerns the identification of the number of unitary $\pi$-container that composed the composite $\pi$-container. This can be achieved by the implementation of a discovery mechanism named as counting algorithm in our proposed methodology to count the number of nodes available in the network. This task initiated by the GW is performed by broadcasting an announcement request, and after receiving it, each node replies with a packet that contains the identifier of the unitary $\pi$-container. The identifier can also be used to ensure that the detected unitary $\pi$-container belongs to the composite $\pi$-container and prevent counting the $\pi$-containers from other H-containers. This can be achieved by checking the identifier number that the GW embeds it in the packet and the stored identifier number that the sensor of unitary $\pi$-container stores in routing information. Due to the small dimensions of the composite $\pi$-container and the long transmission range of sensors, a multi-hop communication manner is not necessary. Thus all the unitary $\pi$-containers can be discovered at the same time with a value of power transmission adapted to the dimension of the composite $\pi$-container. The algorithm can be repeated at different time to be tolerant to possible missing counting due to packet losses in the network.

2. After that, each node detects and identifies the proximity of other nodes. The same discovery mechanism can be used to search their neighbors. A node broadcasts discovery packets so that they reach all nodes in the neighborhood area. At this step, we only assume bidirectional communication links. That is, sensor nodes $\boldsymbol{i}$ and $\boldsymbol{j}$ are neighbors if node $\boldsymbol{i}$ can receive the messages sent from node $\boldsymbol{j}$ and vice versa. The algorithm can also be repeated at different time to be tolerant to possible interferences. The symmetric neighbor relation implies that sensor nodes use the same transmission power level. Each node can obtain a local neighbor list that gives the relative position between the unitary $\pi$-containers. This information is essential to generate pertinent allocation constraints for our CSP, thereby reducing the number of feasible solutions. This point will be discussed in the followings of this section.

3. The GW attached to the composite $\pi$-container can be used as a reference of our localization system. Hence, the position of all the $\pi$-container can be derived from

this absolute position if the relative positions are known. Forwarding mechanisms based on a multi-hop routing tree are commonly used in wireless sensor networks to transfer collected data throughout the network. Such technique is used to collect the local neighbor lists at the gateway where they are combined together to generate a global neighbor list, before to be expressed as position constraints in our CSP.

After these successive operations, the GW can compute the global connectivity graph and send it to the base station (or handled device). Then, the modeled CSP can be formulated where:

- The neighbor table gives position constraints between the unitary $\pi$-containers, but also with the composite $\pi$-container. It represents allocation restrictions in the CSP problem.
- The container size provides basic geometric constraints. The unitary $\pi$-containers lie entirely within the composite container and do not overlap. Each one may only be placed with their edges parallel to the walls of the composite $\pi$-container.

Also, each feasible solution of the CSP is a potential loading pattern, and the resulting virtual 3D layout can be generated through a graphical user interface. Fig.3.6 shows the global input/output information flows and corresponding tasks for the devices in the system of model.

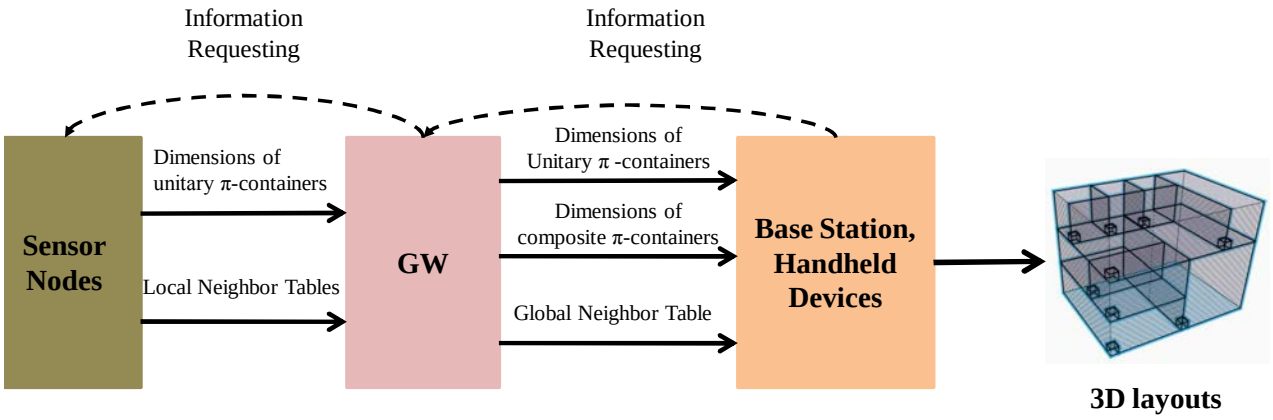


Figure 3.6: Input/Output flows of information corresponding to the consecutive steps for implementing the proposed model

Once these information is stored in the sensor nodes, when it is requested by the base station or handheld devices, these data will be processed and filtered in order to provide

the requested information to the BS: dimensions of $\pi$-containers, etc. With all this data, the 3D layouts can be obtained by the BS or handheld devices after executing the CSP.

The advantage of our approach is that the properties of the received signals, e.g., signal strength or angle of arrival, are not considered in the successive operations to localize the $\pi$-container. The position is only determined from geometrical and neighborhood information of the $\pi$-containers, which is important in harsh environments and operating conditions encountered in logistics. However, the number of feasible solutions issued from the CSP solver is directly linked to the pertinence of the global neighbor list, and therefore, the choice of the transmission range is important.

Indeed, two nodes are neighbors if they can communicate, i.e. the distance between them is lesser than or equal to the transmission range. Therefore, with a transmission range smaller than the smallest dimension of the $\pi$-containers, lot of nodes will be unable to find neighbors in close proximity. This is illustrated Fig. 3.7 where a composite $\pi$-container is composed by six unitary $\pi$-containers ($\pi c_1$, $\pi c_2$, $\pi c_3$, $\pi c_4$, $\pi c_5$, $\pi c_6$).

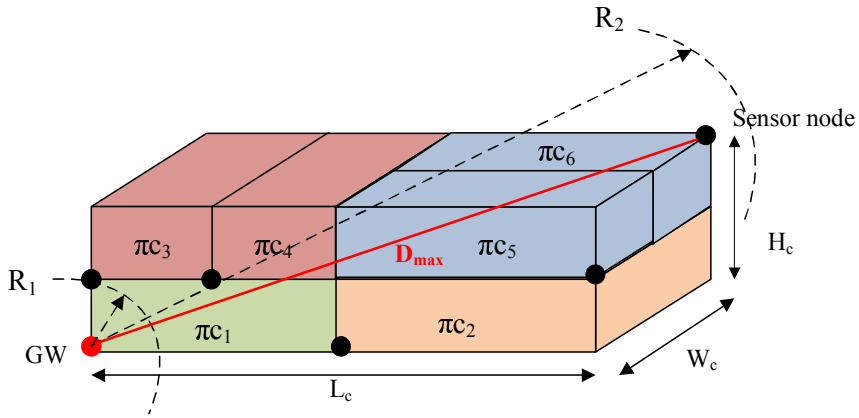


Figure 3.7: Ranging $R_1$ and $R_2$

The distribution of the sensor nodes (black rounds) corresponds to the arrangement obtained when the composite $\pi$-container is set up. The global neighbor list is modeled by an undirected graph for different transmission range Rc. A vertex represents a sensor node belonging to a $\pi$-container, and edges, the neighbor relationships between them. The neighbor graph obtained with a transmission range R1, inferior to the smallest dimension of the the $\pi$-containers, is an edgeless graph (with no edges) (Fig. 3.8a).

Therefore it will be impossible to specify position constraints in our CSP. The number of feasible solutions, i.e., virtual 3D layouts for the composite $\pi$-container, will correspond to every possible arrangement of the $\pi$-containers into the composite $\pi$-container. Similarly, if the transmission range is superior to the length of the composite $\pi$-container diagonal, all nodes are neighbors one of another. The neighbor graph will be a complete

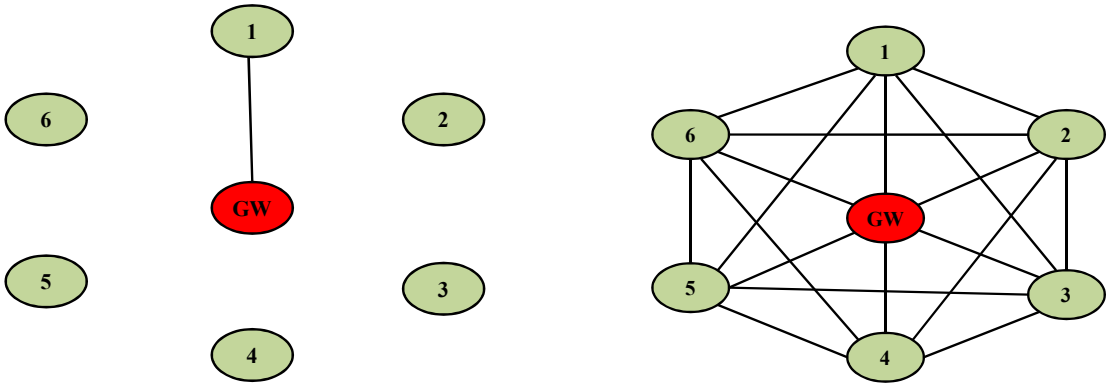


(a) $Rc < R_1$ (b) $Rc \geq R_2$

Figure 3.8: Connectivity Graphs of the network in two values of ***Rc***

graph, as depicted Fig. 3.8b with R2. A lot of solutions, where the position constraints will be satisfied, can be found from a simple permutation or rotation of $\pi$-containers. Thus, the transmission range must be adapted according to the $\pi$-containers dimensions in order to obtain pertinent and sufficient position constraints. The following sections describe each process (with proposed algorithms) and the modeling of the CSP.

## 3.3 WSN Algorithms for Data Collection

This section presents the proposed algorithms to obtain the set of data (number of $\pi$-containers, dimensions, neighborhood relation) necessary to execute our CSP.

### 3.3.1 Counting of Number of Unitary $\pi$-containers

In our proposed methodology, being aware of number of unitary $\pi$-containers constituting the composite $\pi$-container plays a key role to obtain a precise 3D layout which is in conformity with the real spatial arrangement of the unitary $\pi$-containers. Since each unitary $\pi$-container is equipped with a sensor node, the number of unitary $\pi$-containers can be derived by counting number of the sensors which can be obtained by several algorithms proposed in traditional sensor networks [105–109].

In the literature, algorithms for estimate or count the number of nodes deal mostly with networks at large-scale. The main purpose of the task is to estimate the size of the network and then to use this parameter for adaptable setting and configuration of application served by the network. Most of the proposed algorithms are operated in decentralized manner and they can be classified into three classes: probabilistic polling algorithms, random walk based algorithms, and gossip-based algorithms [105]. In the

first type of algorithms as proposed in [106], the basic idea is to probe the network in a probabilistic way and to infer the size of the network based on the set of replies. To this end, the sink node broadcast messages, the nodes send back a response with a probability depending on the probability parameter set in the broadcast message. By this way, each node can estimate the number of its neighbor in its overlay. At the end of algorithm, the sink collects all the data sent by all the nodes and filters the final size of the network. The simulation results obtained from this algorithm performance shown the estimated number with high accuracy level. However, in term of networking perspective, more overhead used causes inefficient energy consumption of the nodes. In the random walk based algorithm [107], a node with the smallest identifier sends a packet containing an initial counter value on a random walk to a node with higher identifier, and each node that is passed on the walk increase by 1 to the counter. When the random walk returns to the initiating node it can estimate the network size based on the counter value. This algorithm is simple to implement but it suffers from the drawbacks that it relies on identifier assignments of the nodes. In the gossip-based algorithms proposed in [108, 109], the network size is estimated from averaging an initial value over all nodes when this value is embedded in all Beacon packets flooded in the network. Although the algorithms are operated in decentralized manners which are expected to decrease the overhead during networking implementation, the estimation accuracy is quite low.

In contrast to our network model characterized by small-scale (a limited number of unitary $\pi$-containers inside a H-container), the exact counter is a prerequisite condition required by the proposed system to generate the exact 3D layout. Therefore, these above proposed algorithms mainly applied to estimate the size of dense networks are inefficient to apply in our model. In this case, we propose an centralized algorithm that aims for the GW to detect the existence of all nodes in the network. From the networking perspective, one node can be detected by the GW through their one-hop or multi-hop communication. In the first manner, the presence of the node is detected when it and GW can communicate directly. Otherwise, the node presence is reported to the GW thanks to overlay nodes that are aware of both it and the GW. In term of networking performance, multi-hop communication mechanism benefits from energy efficiency for the network when the transmission power is lower. However, some node can be hidden from the rest of network if it can not reach to the other nodes in network [109–111]. To overcome this problem in our network, one-hop communication is used for all the nodes to ensure that they can communicate directly to the GW. As a result, the node presence can be detected based on the ping-pong communication scheme as illustrated in Fig.3.9.

By exploiting this simple mechanism, we propose the counting algorithm that aims for the GW to detect and count all the nodes in the network. In the initialization process,

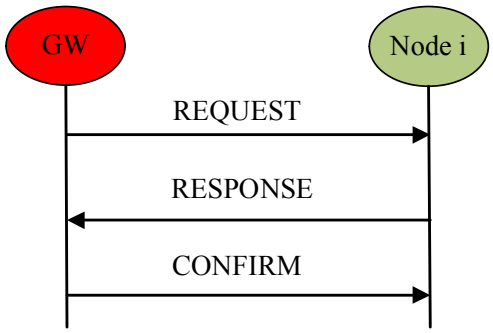


Figure 3.9: Ping-Pong scheme using 3 types of messages: request, response, confirm enables the GW to detect the presence of a node $i$. Accordingly, after receiving a request message issued by the GW, a node $i$ can announce its presence by sending a response message. Finally, the GW confirms the existence of the node in the network when receiving this response.

one important task of the GW is to choose an appropriate value of Rc such that all nodes in the network can communicate in one-hop manner. In fact, all the nodes can use the maximum transmission power to support the wireless communication with the maximum communication range, however, the energy inefficiency is resulted in. For example, the sensor nodes are no longer deactivated since their energy powered by uncharged batteries is drained quickly. In addition, long range of communication leads to more interferences that, in turn impact negatively on the performance of proximate networks (e.g., high ratio of packet loss, etc,). In our model, since the nodes are distributed within the inner space of a rectangular box shaping the composite $\pi$-container, all the nodes can communicate with the GW in one-hop manner if their minimum communication range is equal to the length of space diagonal line of rectangular denoted as $D_{max}$. In geometry, the length can be calculated by the GW since it stores the dimension of the composite $\pi$-container. From this distance, a corresponding power level to enable the nodes to communicate within this distance can be computed by the GW.

After the one-hop range of communication is selected, the algorithm starts by exchanging packets. In our proposed algorithm, we define two types of packets, namely HELLO_CNT and ACK_CNT packets generated by the GW and the nodes respectively. The structure of packet payloads is summarized as Table 3.1.

Based on the ping-pong mechanism, the presence of nodes can be detected by the GW throughout exchange of these two packets as scheduled in Fig.3.10.

Following the sequence diagram, the GW and the nodes in the network execute their own algorithms as proposed and sketched in Algorithm 1 and Algorithm 2 respectively.

According to the ping-pong mechanism, the GW broadcasts HELLO_CNT packets

| Node Type | Packet Type | Packet Fields | Number of Bytes | Description |
|---|---|---|---|---|
| GW | HELLO_CNT | **id** | 2 | Identifier |
| | | **pkt_type** | 2 | Packet type |
| | | **pw_level** | 1 | Power level |
| | | **no_pkt** | 2 | Number of packets sent by GW |
| | | **list_nodes** | $2 \times N_{max}$ | List of detected nodes |
| Node $\boldsymbol{i}$ | ACK_CNT | **id** | 2 | Identifier of node $\boldsymbol{i}$ |
| | | **id_gw** | 2 | Identifier of GW |
| | | **pkt_type** | 2 | Packet type |
| | | **dim** | 6 | Dimension of $\pi$-container $\boldsymbol{i}$ |
| | | **reserved** | 50 | Reserved for other applications |

Table 3.1: Payload of packets used in the counting algorithm

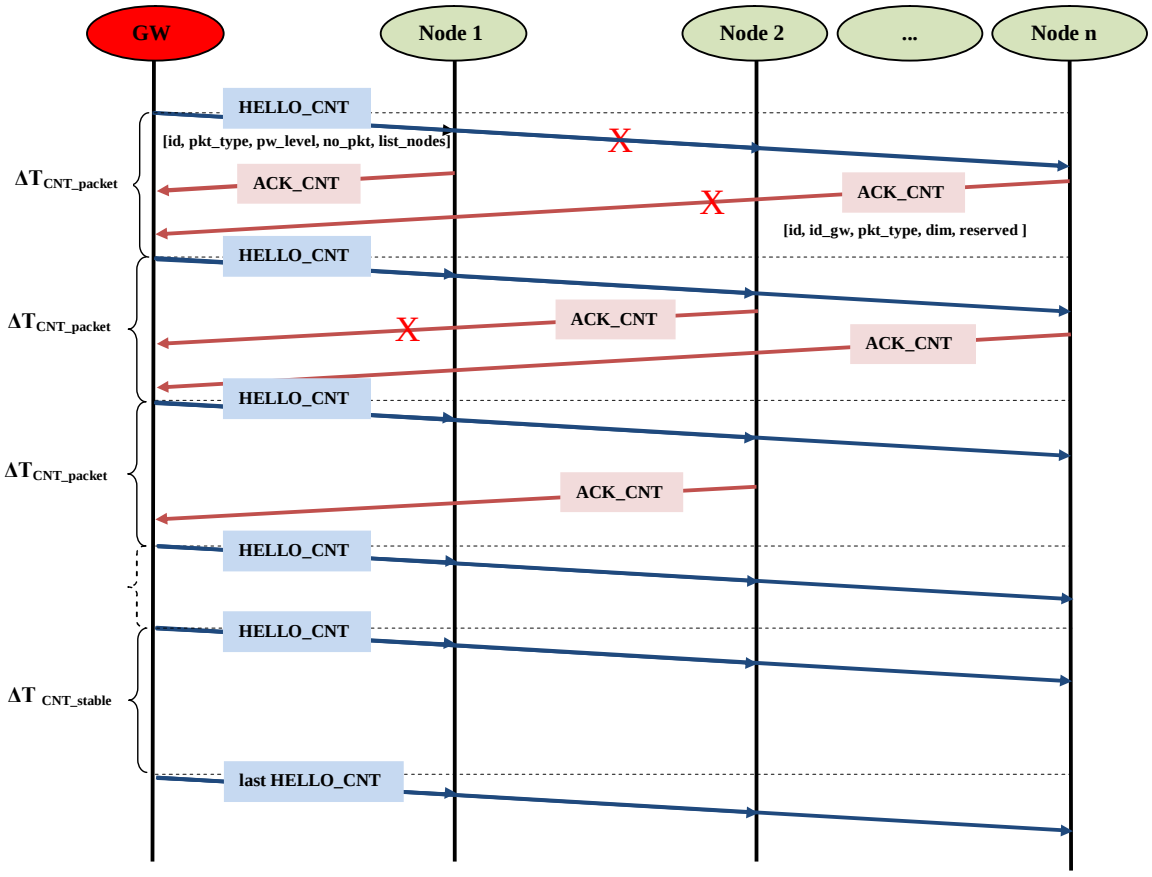


Figure 3.10: Sequence diagram for packet exchange between GW and nodes in the counting algorithm

**Algorithm 1:** Pseudocode for the GW in counting algorithm

**Input** : Dimensions of composite $\pi$-container
**Output**: **list_nodes**

Initialization: **no_pkt** =1, **pw_level**(GW) $\leftarrow$ P($D\_max$), **list_nodes**={0};
**if** ***list_nodes*** *is unstable during* $\Delta T_{CNT\_stable}$ **then**
    GW broadcasts a HELLO_CNT packet with rate 1 packet per $\Delta T_{CNT\_packet}$;
    During $\Delta T_{CNT\_packet}$:
    **if** *GW receives a validated ACK_CNT packet sent by a node* ***i*** **then**
        **if** $ID_i \in$ ***list_nodes*** **then**
            GW discards the packet;
            $mode(GW) \leftarrow LISTENING$;
        **else**
            $list\_nodes \leftarrow ID_i$;
        **end**
    **else**
        GW discards the packet;
        $mode(GW) \leftarrow LISTENING$;
    **end**
    $no\_pkt \leftarrow no\_pkt + 1$;
**else**
    $no\_pkt \leftarrow 0$;
    GW broadcasts the last HELLO_CNT packet;
    return **list_nodes**;
    Finish Counting Algorithm;
**end**

**Algorithm 2:** Pseudocode for a node ***i*** in counting algorithm

**Input** : Dimensions of unitary $\pi$-container $i$
**Output**: **list_nodes**

**while** *Node* ***i*** *doesn't receive the last HELLO_CNT packet* **do**
    **if** *node* ***i*** *receives a validated HELLO_CNT packet* **then**
        **if** $ID\_i \in$ ***list_nodes*** **then**
            Node ***i*** discards the HELLO_CNT packet;
            $mode(node\boldsymbol{i}) \leftarrow LISTENING$;
        **else**
            $pw\_level(node\boldsymbol{i}) \leftarrow pw\_level(GW)$;
            Node ***i*** transmits an ACK_CNT packet;
        **end**
    **else**
        $mode(node\boldsymbol{i}) \leftarrow LISTENING$;
    **end**
**end**
Store **list_nodes**;
$mode(node\boldsymbol{i}) \leftarrow LISTENING$;
Finish Counting Task;

periodically to request the acknowledgment packets (ACK_CNT packets) of the nodes in the network. The packet generation interval is denoted as $\Delta T_{CNT\_packet}$. The payload of this packet includes 5 fields: **id, pkt_type, pw_level, no_pkt, list_nodes**. The field **id** embedding the ID of the GW is used for the other nodes to validate HELLO_CNT packets sent by the GW. Thus, these coming packets will be processed if they contain the **id**; otherwise the GW discards the packets (Line 13, Algorithm 1). The field **pw_level** stores the power level equivalent to the transmission power to support one-hop communication in $D_{max}$ range. When nodes receive the packets, they extract this field and configures their corresponding power transmission. All packets exchanged in this algorithm (hereafter, in following algorithms) are distinguished by its type encoded in **pkt_type** field. By this way, after receiving a packet, nodes know how to process the received packet and perform its appropriate task. The field **no_pkt** indicates number of packets sent by the GW during the algorithm runs. The value of **no_pkt** will increase by 1 (Line 15 of Algorithm 1) after a HELLO_CNT packet is sent. When its value is set to be 0 (Line 17 of Algorithm 1) and updated in the last HELLO_CNT packet for the purpose of signaling to the rest nodes that the counting algorithm finishes. Finally, the field **list_nodes** stores and maintains the nodes detected by the GW after a series of packets exchanged. Whenever a new node **i** is detected, its identifier will be added to the list (Line 10, Algorithm 1).

For all the nodes in the network, they maintain their listening mode (Line 11, Algorithm 2) until they receive HELLO_CNT packets. A validated received packet that must contain the identifier of the GW is processed; otherwise, it will be discarded (Line 4, Algorithm 2). As soon as a validated packet is received by node ***i***, the content of packet is extracted and processed. Accordingly, Any invalided arrival packet is discarded if a node **i** receives the receives the HELLO_CNT packet successfully, and it then replays a ACK_CNT packet successfully. That means the GW detected its appearance and it is stored in the **list_nodes**. Node **1** in Fig.3.10 illustrates this case. Prior to sending ACK_CNT packets, the node configures its transmission power based on the power level of **pw_level** provided by the GW. Replying ACK_CNT packets is not only to announce the presence but also provide necessary data for the GW. In our model, the payload of this packet includes 5 fields: **id, id_gw, pkt_type, dim, reserved**. The field **id** is used to contain the identifier of unitary $\pi$-container. Meanwhile, the field **id_gw** refers to the identifier of the GW. To support efficient routing, the $\pi$-containers are assigned and scheduled by the PIMS such that they are aware of what H-container handle them in next operations. Therefore, through extracting this field of arrival packets, the GW can recognize what $\pi$-containers lie inside it. In other words, the GW can confirm the validation of the received packet and then process it. T field **dim** provides the dimension

of the unitary container (i.e., length, width and height of the container). This information is used to formalize the constraints of the CSP. The field **reserved** is used for additional applications requested by the GW, for example, the temperature, humidity measurements of environment sensed and measured by the corresponding sensors of the nodes.

Due to the nature of wireless communication (packet lost, packet errors caused by collision, interference, noise, etc), after the GW broadcast a *HELLO_CNT* packet, any node in the network may have following scenarios during $\Delta T_{CNT\_packet}$:

1. It receives the HELLO_CNT packet successfully, and then replies a ACK_CNT packet unsuccessfully. As a result, to the end of the algorithm, it couldn't be detected by the GW. Node **n** in Fig.3.10 illustrates this case.

2. It does not receive any HELLO_CNT packet, therefore it does not reply a ACK_CNT packet, and finally it could not be detected. Node **2** in Fig.3.10 illustrates this case.

To overcome these problems, we repeat the above packet exchanges in the next $\Delta T_{CNT\_packet}$ intervals in order to assign opportunities for nodes to announce them. Upon broadcasting the HELLO_CNT packets, **list_nodes** is maintained and updated to avoid retransmission of ACK_CNT packets sent by the discovered nodes.

The algorithm is finished if one of two stop criteria is reached as shown in Fig. 3.11.

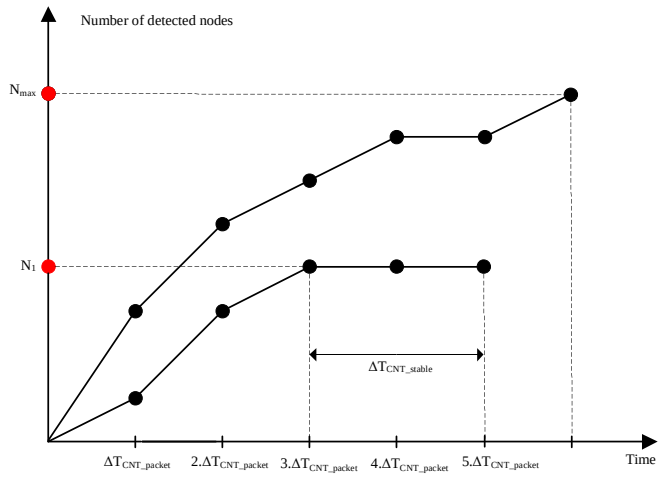


Figure 3.11: An example illustrating the two criteria for the GW to stop the counting algorithm: (1) The number of detected nodes reaches $N_{max}$ that can be computed by the GW prior to execution of the counting algorithm; (2) The number of nodes detected is $N_1$ that remains unchanged during a period $\Delta T_{CNT\_stable}$ measured in two consecutive intervals $\Delta T_{CNT\_packet}$.

1. The **list_nodes** is stable (unchangeable) during an interval of time $\Delta T_{CNT\_stable}$. In our proposition, this interval is measured as a number of consecutive packet generation intervals. Within this period, the GW keeps on sending HELLO_CNT packets but no responses of the other nodes are received. There are two cases in this situation: (1) all nodes of the network are already detected and stored in **list_nodes** and the nodes do not need to reply ACK_CNT packets; (2) some nodes of the network are detected and stored in **list_nodes** and no new nodes are detected during the period $\Delta T_{CNT\_stable}$ due to packet lost, packet errors. Therefore, the period plays a key role in obtaining the exact counter of nodes in the network. Generally, the longer the period is the more precise the node counter is. The length of period will be examined and analyzed in the simulation scenarios.

2. The maximum number of nodes ($N_{max}$) is obtained. Since, unitary $\pi$-containers and H-container are modular, thus there is a maximum number of unitary $\pi$-containers with the smallest size composed and filled fully in the H-container. Upon aware of this information, the GW is enable to stop the algorithm if the number of elements in the **list_nodes** reached $N_{max}$. This situation will be examined in the Chapter 4.

The nodes will finish their mission in the algorithm when receiving the last HELLO_CNT packet with the field *no_pkt* set to 0. The final **list_nodes** updated in this packet is extracted and stored in the memory of nodes. Therefore, all the nodes including the GW are aware of the global information of the network (i.e., number of nodes, their identifier number, etc.). The information is useful for next algorithms since the nodes can validate source of any arrival packets or the nodes can know the status of the network (i.e., which algorithm is processed and which nodes are processing the algorithm, etc.).

The GW and nodes process these packets and implement our counting algorithm as summarized as Algorithm 1 and Algorithm 2 respectively.

### 3.3.2 Joint Algorithm for Neighbor Discovery (ND) and Neighbor Table Forwarding

Traditionally, neighbor discovery is one of vital protocols performed by all nodes in the multi-hop network to primarily detect their neighbor nodes geometrically distributing within their communication range. The aim of the protocol is to create and maintain neighbor tables of nodes. Since all nodes are not supported by one-hop communication, the data collected by the sink or the GW of the network is forwarded through a series of neighbors of nodes. In other words, the neighbors can functions as relay agents to

transfer the information [112–115]. Generally, any neighbor of a node can be chosen to be the relay node from its neighbor set. However, in order to improve the performance of network, a relay node is chosen when it possesses advantage characteristics such as high residual energy, stable communication links to other. Although, awareness of all neighbors of each node aids at selecting the optimal neighbor for relaying, discovering them is time consuming and inefficient in energy especially in dense networks

In our model, the objective of the algorithm is to allow all the nodes (including the GW) to discovery all their own neighbors and then to forward successfully these neighbor lists to the GW. Since the neighborhood relationship between a pair of nodes can be translated to the relative position of their corresponding $\pi$-containers, the algorithm is required to obtain the an accurate neighbor lists.

In this section, a joint algorithm combining discovering neighbor and forwarding algorithms in the WSN (hereafter, this algorithm is shortened as joint algorithm) is proposed with the priority target of obtaining the exact possible number of neighbors for each node and then transmitting successfully the neighbor tables to the GW. In order to meet the strict requirement, upon collecting the global information of the network and the $\pi$-container specification, the GW coordinate the operation of nodes in discovering neighbors and then forwarding these neighbor tables back to GW by token based mechanism. The mechanism is enabled since the GW is aware of network topology (number of nodes, their IDs, etc.) obtained from the counting algorithm. Accordingly, all the nodes already stored in the **list_nodes** are assigned their task to implement the joint algorithm after receiving the token assigned by the GW. Instead of allowing all the nodes to perform the joint algorithms at the same time, they will do one by one. Although this mechanism may be time consuming, reduce the packet collision and packet loss, packet errors due to high interference permits all the nodes to discover their entire neighbors. In addition, a limit number of nodes in the network agrees with the proposed scheme to be deployed.

For different values of one-hop communication range Rc, different corresponding neighbor lists are obtained from the algorithm, thus a corresponding set of relative position constraints is derived. These constraints, in turn, impact on number of solutions to the CSP. Therefore, selection of one hop communication Rc is important task of the GW in order to obtain the sufficient global neighbor list of the network. The good selection of Rc is verified and analyzed in the Chapter 4 that implements simulation of different scenarios.

The Algorithm 3 sketches main steps to perform our proposed joint algorithm with objective to obtain the global neighbor list precisely.

After choosing a value of one hop communication Rc in the initialization process, the GW is the first node to discovery its neighbors. Algorithm 4 sketches the main steps

**Algorithm 3:** Pseudocode performed by the GW in the Joint Algorithm

```
   Input  : list_nodes, Rc
   Output: global_nbr_list
1  Initialization: pw_level(GW) ← P(Rc), global_nbr_list = {0} ;
2  GW performs the ND algorithm firstly as Algorithm 4;
3  global_nbr_list ← list_nbr(GW) ;
4  while list_nodes ≠ 0(empty) do
5      next_node ← node i;
6      list_nodes ← list_nodes − {node i};
7      pw_level(GW) ← P(D_max);
8      GW unicasts a TOKEN_NBR to node i;
9      Node i performs the NDP as Algorithm 5;
10     pw_level(node i) ← P(D_max);
11     Node i broadcasts REPORT_NBR packet;
12     global_nbr_list ← list_nbr(node i) ;
13 end
14 return global_nbr_list;
15 Finish Algorithm;
```

that the GW performs the neighbor discovery through the sequence of packet exchanges between the GW and nodes scheduled as the diagram in Fig.3.12.

**Algorithm 4:** Pseudocode performed the GW to discovery its neighbors

```
   Input  : list_nodes, Rc
   Output: list_nbrs
1  Initialization: pw_level(GW) ← P(Rc), list_nbrs = {0} ;
2  while list_nbrs is unstable within ΔT_NBR_stable do
3      GW broadcasts HELLO_NBR packet with rate 1 (packet) per ΔT_NBR_packet (second);
4      During ΔT_NBR_packet;
5      if GW receives a ACK_NBR packet sent by node i then
6          if ID_i ∈ list_nbrs(GW) then
7              GW discards the packet;
8          else
9              list_nbrs(GW) ← ID_i;
10         end
11     else
12         mode(GW) ← LISTENING;
13     end
14 end
15 GW broadcasts last HELLO_NBR packet;
16 return list_nbrs(GW);
17 Finish Algorithm;
```

By using the same mechanism of packet exchange as introduced in the counting algorithm, the GW and nodes transmit and receive the packets defined as Table 3.2 and Table 3.3.

Accordingly, after choosing a value of **Rc**, the appropriate power level is set up by the GW before broadcasting the HELLO_NBR packet periodically. We denote the packet generation interval in this algorithm as $\Delta T_{NBR\_packet}$. Structured similarly as

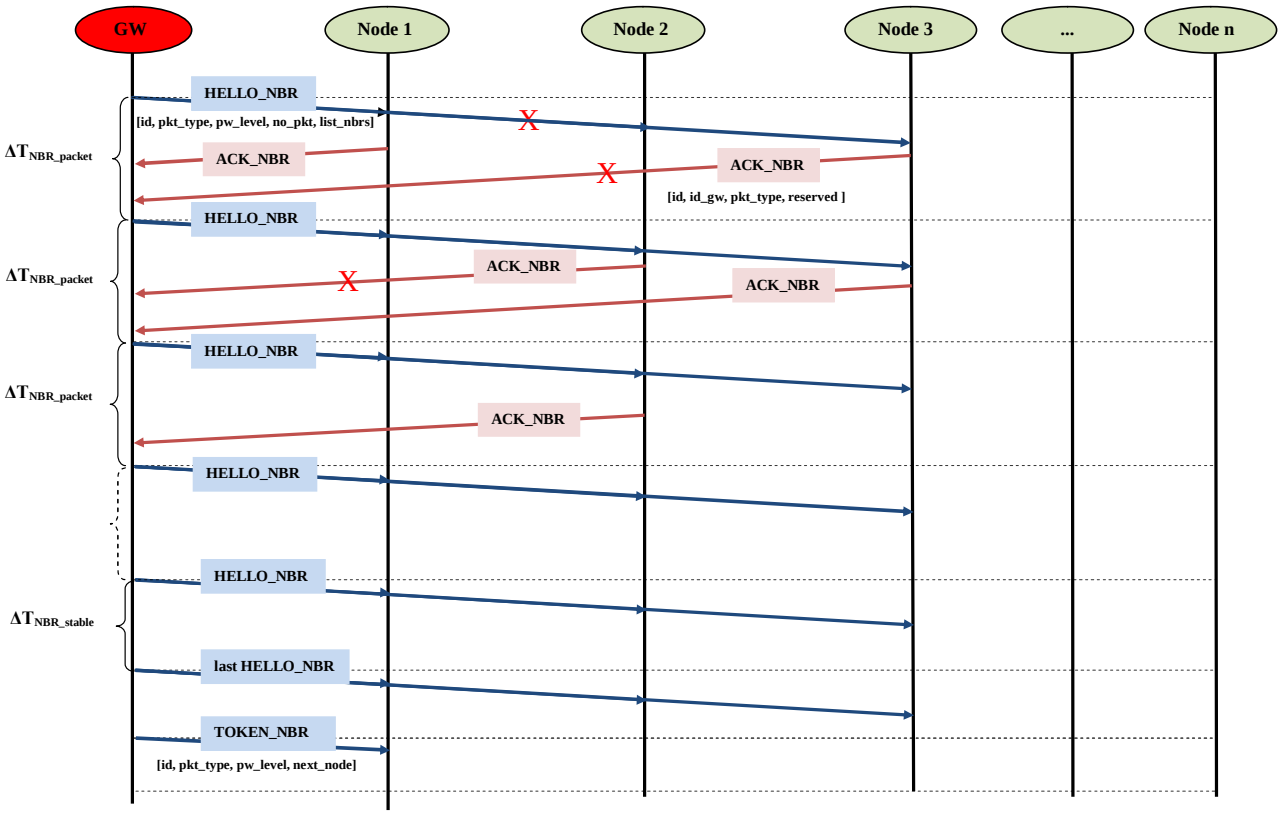


Figure 3.12: Sequence diagram for packet exchange between GW and nodes in the ND algorithm of the GW

| Node Type | Packet Type | Packet Fields | Bytes | Description |
|---|---|---|---|---|
| GW | HELLO_NBR | **id** | 2 | Identifier of GW |
| | | **pkt_type** | 2 | Packet type |
| | | **pw_level** | 1 | Power level |
| | | **no_pkt** | 2 | Counter of beacons |
| | | **list_nbrs** | 2 | Neighbor list of the GW |
| | ACK_NBR | **id** | 2 | Identifier of GW |
| | | **pkt_type** | 2 | Packet type |
| | | **reserved** | 50 | Reserved for other application |
| | TOKEN_NBR | **id** | 2 | Identifier of GW |
| | | **pkt_type** | 2 | Packet type |
| | | **pw_level** | 1 | Power level |
| | | **next_node** | 2 | Next node for neighbor discovery |

Table 3.2: Payload of packets used by the GW in the NDP algorithm

| Node Type | Packet Type | Packet Fields | Bytes | Description |
|---|---|---|---|---|
| Node ***i*** | HELLO_NBR | **id** | 2 | Identifier of nodes ***i*** |
| | | **pkt_type** | 2 | Packet type |
| | | **id_gw** | 2 | Identifier of GW |
| | | **pw_level** | 1 | Power level |
| | | **no_pkt** | 2 | Counter of beacons |
| | | **list_nbrs** | 50 | Neighbor list of the node ***i*** |
| | ACK_NBR | **id** | 2 | Identifier of node ***i*** |
| | | **id_gw** | 2 | Identifier of GW |
| | | **pkt_type** | 2 | Packet type |
| | | **reserved** | 50 | Reserved for other applications |
| | REPORT_NBR | **id** | 2 | Identifier of node ***i*** |
| | | **pkt_type** | 2 | Packet type |
| | | **id_gw** | 2 | Identifier of GW |
| | | **list_nbrs** | 2 | Neighbor list of nodes ***i*** |
| | | **reserved** | 50 | Reserved for other applications |

Table 3.3: Payload of packets used by all other nodes in the NDP algorithm

HELLO_CNT packet, the payload of HELLO_NBR packet includes 5 fields: **id, pkt_type, pw_level, no_pkt, list_nbrs**. Their functions are described as mentioned in the counting algorithm. Notably, the field **list_nbrs** is used to stored and maintained the neighbors of GW within the selected **Rc**.

During this period, when nodes receive this packet, they will process the packet if the packet contains the identifier number of the GW. Indeed, the power level extracted from the **pw_level** of the packet is translated to the corresponding transmission power for the nodes.

After that, they choose their own time randomly to reply to the GW by sending ACK_NBR packets. The ACK_NBR packet contains 4 fields in the payload: **id, id_gw, pkt_type, reserved**. We maintain the field **reserved** for supporting exchanging the data for other applications.

When the GW receives a valid ACK_NBR packet sent a node **i** containing the right identifier number of the GW (i.e., **id_gw**), it will store the node **i** in its neighbor list **list_nbrs** and updates this information in the global neighbor list (*global_nbr_list*).

The operation of packet exchange is kept the same for next $\Delta T_{NBR\_packet}$ periods. All nodes try to reply by sending ACK_NBR packets if they are not already stored in the **list_nbrs**, otherwise, they discard every arrival packets and maintain LISTENING mode to wait for other coming packets.

To finish the neighbor discovery task, the GW is based on a stable duration $\Delta T_{NBR\_stable}$ measured by a number of consecutive $\Delta T_{NBR\_packet}$ intervals. Accordingly, within this

duration, the GW keeps broadcasting HELLO_NBR packets, however, no ACK_NBR packets are received. Therefore, the accurate **list_nbrs** is impacted by the length of the period that will be verified in the Chapter 4 by simulation implementation. The termination of the ND task of GW is informed to its neighbors by sending the last HELLO_NBR embedding 0 to the field **no_pkt**.

After completing neighbor discovery, the GW starts to launch the token based mechanism that assigns the turn for the nodes to perform the joint algorithm. Accordingly, it selects randomly a node in the **list_nodes** as a next node to perform the algorithm, embeds its identifier in field **next_node** of TOKEN_NBR packet and then sends it to this node by unicast communication scheme. The important fields: **id, pkt_type and pw_level** embeds the corresponding data to the packet before transmitting it. Notably, the field **pw_level** contains the power level to support transmission within the selected **Rc** instead of $D_{max}$. In order to ensure that this packet is reached to this next node, the GW configures the power level such that the communication range is up to $D\_max$. Upon receiving the TOKEN_NBR packet, the node executes the joint algorithm as summarized in the Algorithm 5.

**Algorithm 5:** Pseudocode Perfomed by a node ***i*** in the Joint Algorithm

**Input** : $pw\_level(GW)$
**Output**: $list\_nbrs$
**while** $list\_nbrs$ *is unstable within* $\Delta T_{NBR\_stable}$ **do**
  $pw\_level(node_i) \leftarrow pw\_level(GW)$;
  $Node_i$ broadcasts HELLO_NBR frequently with rate 1 (packet) per $\Delta T_{NBR\_packet}$ (second);
  During $\Delta T_{NBR\_packet}$;
  **if** $node_i$ *receives an ACK_NBR packet sent by* $node_j$ **then**
    **if** $ID_j \in list\_nbrs(node_i)$ **then**
      $node_i$ discards the packet;
    **else**
      $list\_nbrs(node_i) \leftarrow ID_j$;
    **end**
  **else**
    mode(node ***i***) ← LISTENING;
  **end**
**end**
mode(node ***i***) ← LISTENING;
return $list\_nbrs(node_i)$;
Finish Algorithm;

Fig.3.13 illustrates the packet exchange sequence between a node, for example node 1 and other relate nodes.

In this case, the node 1 plays a role as the GW performing the neighbor discovery previously. Accordingly, the node sets up the transmission power extracted from the field **pw_level** of the TOKEN_NBR packet, then it periodically broadcasts HELLO_NBR packets including 6 fields: **id, id_gw, pkt_type, pw_level, no_pkt, list_nbrs** and

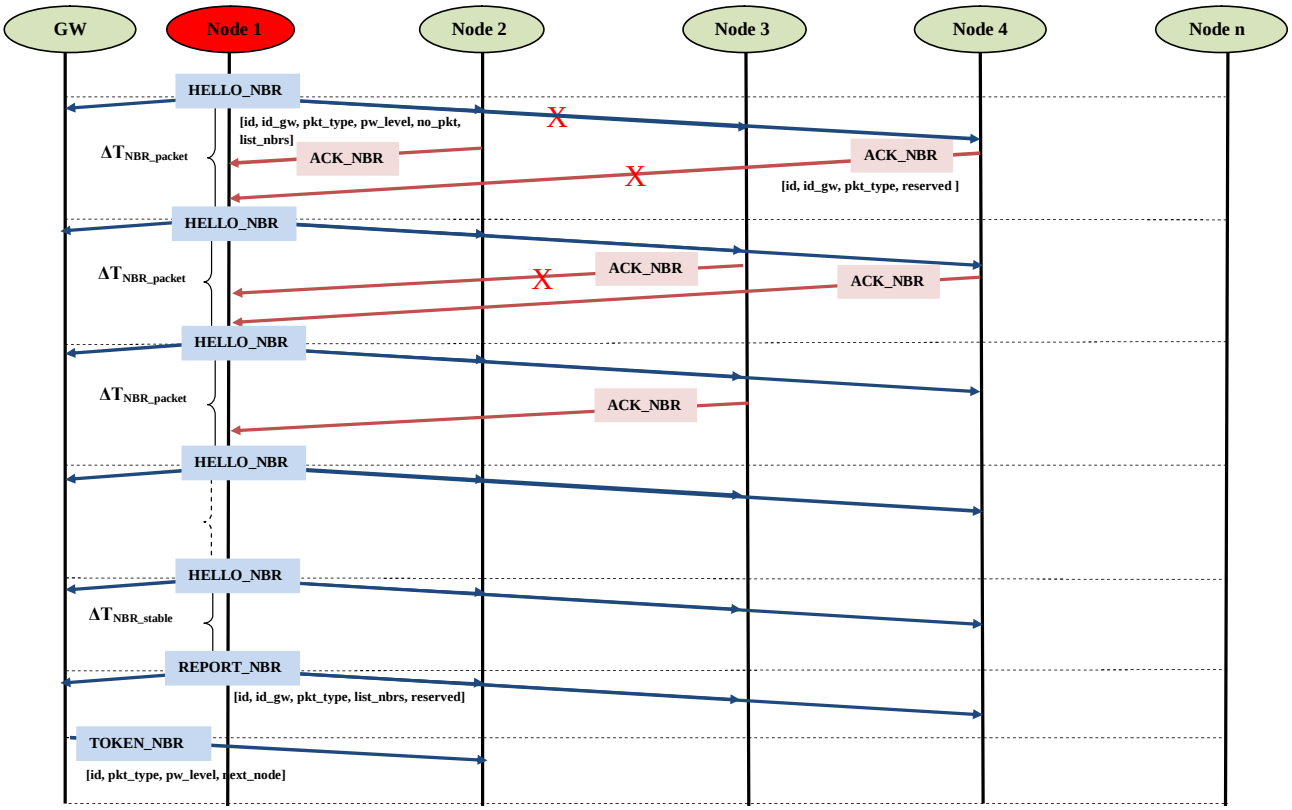


Figure 3.13: Sequence diagram for packet exchange between GW and nodes in the ND algorithm of the other nodes

waits for the acknowledgment packets sent by its neighbors. The same mechanism to process the packets is applied to the node as described in the performance of the GW to discover its own neighbors. The neighbor discovery task is finished if the **list_nbrs** is stable within $\Delta T_{NBR\_stable}$. After that, the node 1 sets up the transmission power as $P(D_{max})$ to broadcasts REPORT_NBR packet to all the node in the network. The payload of packet includes 5 fields as following: **id, id_gw, pkt_type, list_nbrs, reserved**. This operation aims to two purposes: (1) It forwards the **list_nbrs** to the GW directly and (2) It informs to all its neighbors that its algorithm execution terminates instead of sending the last HELLO_NBR.

After receiving the neighbor list of a node, the GW updates the global neighbor list and continues its assignment role to select a next node to do the joint algorithm. The final global neighbor list is created when all the nodes in the **list_nodes** complete the

joint algorithm.

### 3.3.3 Conclusion

In order to collect the necessary data so support the formulation process of CSP, the two algorithms are proposed. The counting algorithm aims for the GW to know entire nodes present in the network that is equivalent to the entire unitary $\pi$-containers stacked in the H-container. Meanwhile, in the second algorithm, given a communication range, the nodes in the network discover their neighbors in this range, and then forward their neighbor lists to the GW. At the GW, the neighbor lists are translated to neighbor relations relating to the relative positions of unitary $\pi$-containers. This information is used to formulate the neighbor constraints of unitary $\pi$-containers in the CSP.

The most important objective of the two algorithms is to obtain the accuracy of collected data: accurate number of $\pi$-containers and accurate global neighbor table with respect to a chosen Rc. Besides, other networking performances are concerned to evaluate the efficiency and effectiveness of the proposed algorithms. For example, the end-to-end delay that is needed for the GW to collect the expected data or total energy is consumed by a node after running the two algorithms. These terms are important to evaluate the application capability of our proposed methodology in practical application. By simulation, the evaluation is conducted in the Chapter 4.

## 3.4 Mathematical Formulation of CSP

The needed information including number of $\pi$-containers, dimensions of $\pi$-containers and proximity of $\pi$-containers is collected at the GW after the two successive algorithms proposed in the previous sections finish. This section exploits this information to model the CSP.

Assume that a set of $\pi$-containers with modular dimensions is currently stacked in a composite $\pi$-containers with given external dimensions. To explain the proposed methodology works, let us assume that we are looking inside the composite $\pi$-containers from its front side - this is the closest side to the managers or the robots. Using a 3D coordinate system (3D-CS) $OXYZ$, we also assume that the origin is placed at the front-left-bottom (FLB) corner of the composite $\pi$-container. The length ($L_c$), width ($W_c$) and height ($H_c$) of the composite $\pi c$ will be depicted, respectively, along the $OX$, $OY$, $OZ$ axes as Fig.3.14. We also designate the FLB corner of each $\pi$-container as the origin of its own coordinate system. This position denotes the orientation of a $\pi$-container, and corresponds to the initial location of the wireless sensor node. A set of neighborhood relations is defined

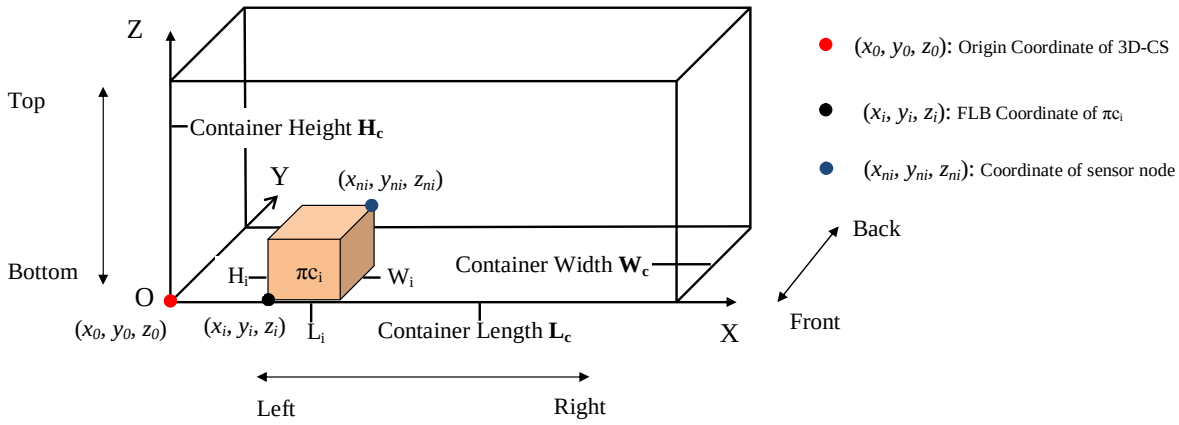


Figure 3.14: Three dimensional coordinate system integrated to the composite $\pi c$

from the global neighbor graph for a given value of the transmission range. In addition, we consider that $\pi$-containers can be freely rotated into different orientations. The objective of the CSP problem is to find the absolute coordinates and the orientation of each $\pi$-container, while satisfying the following set of constraints:

1. Each $\pi$-container is stacked in the composite $\pi$-container.
2. Each $\pi$-container must be orthogonally placed into the container.
3. The overlap among the $\pi$-container is prohibited.
4. All neighborhood relations about the unitary $\pi$-containers and the composite $\pi$-container must be respected.

A solution to the CSP is a complete assignment that satisfies all the constraints. The following sections provide a summary of parameters and variables, and include a mathematical model of the Constraint Satisfaction Problem. This model is based on the mathematical formulation proposed by Chen, Lee and Shen (1995) [103] to formulate the general CLP. This model has been adapted to consider the neighborhood constraints.

### 3.4.1 Parameters and Variables

All parameters used to formulate the CSP are defined as followings:

- $n$ : Total number of unitary $\pi$-containers stacked in the composite $\pi$-container (Its value is determined from the counting algorithm proposed in Section 3.3.1).

- $\pi c_i$: The set of $\pi$-containers, where $i \in \{0, ..., n\}$ and $\pi c_0$ is denoted as the composite $\pi$-containers.
- $(x_0, y_0, z_0)$: Origin of the 3D Cartesian coordinate system, with $x_0 = y_0 = z_0 = 0$.
- $(L_i, W_i, H_i)$: Non-negative external dimensions indicating the length, width, and height of the $\pi c_i$.
- $(L_c, W_c, H_c)$: Non-negative external dimensions indicating the length, width, and height of the $\pi c_0$.
- Rc: Communication range of sensor nodes.
- V: The $i \times j$ matrix with $\{i, j\} \in \{0, ..., n\}$. The matrix elements $V_{ij}$ denote the neighbor relationship between $\pi c_i$ and $\pi c_j$. Their values can be deduced as following equation 3.1:

$$V_{ij} = \begin{cases} 0 & \text{if } i = j \\ 1 & \text{if } \pi c_i \text{ and } \pi c_j \text{ are neighbors,} \\ -1 & \text{otherwise} \end{cases} \tag{3.1}$$

The variables used in to formulate the CSP are defined as followings:

- $(x_i, y_i, z_i)$: Continuous variables indicating the coordinates of the FLB corner of $\pi c_i$.
- $(x_{ni}, y_{ni}, z_{ni})$: Continuous variables indicating the coordinates of the sensor node attached physically to the $\pi c_i$.
- $(l_{xi}, l_{yi}, l_{zi})$: Binary variables indicating whether the length of $\pi c_i$ is parallel to the X-axis, Y-axis, or Z-axis. The value of $l_{xi}$ is equal to 1 if the length of $\pi c_i$ is parallel to the X-axis; otherwise, it is equal to 0.
- $(w_{xi}, w_{yi}, w_{zi})$: Binary variables indicating whether the width of $\pi c_i$ is parallel to the X-axis, Y-axis, or Z-axis. The value of $w_{xi}$ is equal to 1 if the width of $\pi c_i$ is parallel to the X-axis; otherwise, it is equal to 0.
- $(h_{xi}, h_{yi}, h_{zi})$: Binary variables indicating whether the height of $\pi c_i$ is parallel to the X-axis, Y-axis, or Z-axis. The value of $h_{xi}$ is equal to 1 if the height of $\pi c_i$ is parallel to the X-axis; otherwise, it is equal to 0.

  It is clear that the binary variables, $\{l_{xi}, l_{yi}, l_{zi}, w_{xi}, w_{yi}, w_{zi}, h_{xi}, h_{yi}, h_{zi}\}$, are dependent and used to determine the orientation of $\pi c_i$. For example, if the length $(L_i)$, width $(W_i)$, and height $(H_i)$ of the $\pi c_i$ are parallel to the X, Y and Z axes,

respectively, then $l_{xi}$, $w_{yi}$ and $h_{zi}$ are equal to 1 and all the other variables are null. Consequently, the relationships between these variables need to be verified.

- $(Right_{ij}, Left_{ij}, Behind_{ij}, Front_{ij}, Below_{ij}, Above_{ij})$: The set of six binary variables that are used to determine the relative positions of $\pi c_i$ and $\pi c_j$ inside $\pi c_0$. Binary variables is equal to 1 if the $\pi c_j$ is to the right of, to the left of, behind, in front of, below, or above the $\pi c_i$, respectively; otherwise, 0. These variables will be used to ensure that containers do not overlap. Fig.3.15 illustrates these relative positions.

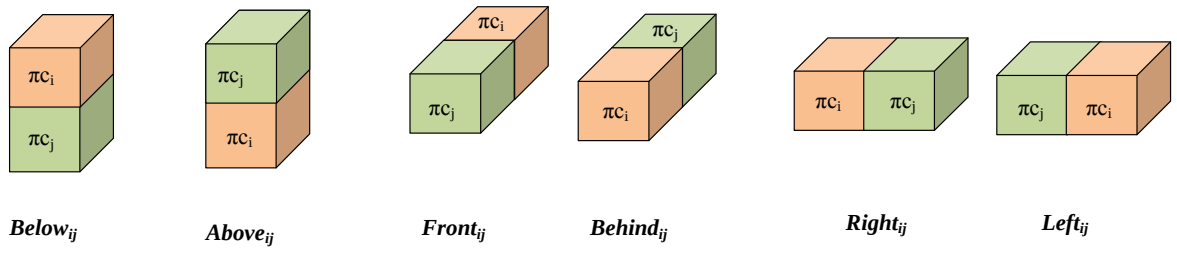


Figure 3.15: Relative positions between $\pi c_i$ and $\pi c_j$

### 3.4.2 Mathematical Formulation

From the parameters and variables described above, the constraints of the CSP are formulated mathematically as follows:

**Non-overlap constraints**:

$$\forall\{i,j\}, 1 \leq i,j \leq n : Right_{ij} \cdot [x_j - (x_i + l_{xi} \cdot L_i + w_{xi} \cdot W_i + h_{xi} \cdot H_i)] \geq 0 \quad (3.2)$$

$$\forall\{i,j\}, 1 \leq i,j \leq n : Left_{ij} \cdot [x_i - (x_j + l_{xj} \cdot L_j + w_{xj} \cdot W_j + h_{xj} \cdot H_j)] \geq 0 \quad (3.3)$$

$$\forall\{i,j\}, 1 \leq i,j \leq n : Behind_{ij} \cdot [y_j - (y_i + l_{yi} \cdot L_i + w_{yi} \cdot W_i + h_{yi} \cdot H_i)] \geq 0 \quad (3.4)$$

$$\forall\{i,j\}, 1 \leq i,j \leq n : Front_{ij} \cdot [y_i - (y_j + l_{yj} \cdot L_j + w_{yj} \cdot W_j + h_{yj} \cdot H_j)] \geq 0 \quad (3.5)$$

$$\forall\{i,j\}, 1 \leq i,j \leq n : Above_{ij} \cdot [z_j - (z_i + l_{zi} \cdot L_i + w_{zi} \cdot W_i + h_{zi} \cdot H_i)] \geq 0 \quad (3.6)$$

$$\forall\{i,j\}, 1 \leq i,j \leq n : Below_{ij} \cdot [z_i - (z_j + l_{zj} \cdot L_j + w_{zj} \cdot W_j + h_{zj} \cdot H_j)] \geq 0 \quad (3.7)$$

$$\forall\{i,j\}, 1 \leq i,j \leq n : Right_{ij} + Left_{ij} + Behind_{ij} + Front_{ij} + Below_{ij} + Above_{ij} \geq 1 \quad (3.8)$$

$$(3.9)$$

**Constraints about coordinates of sensors and correspondent $\pi$-containers**:

$$\forall i, 1 \leq i \leq n : ((x_i + l_{xi} \cdot L_i + w_{xi} \cdot W_i + h_{xi} \cdot H_i) - x_{ni}) \cdot (x_i - x_{ni}) = 0 \tag{3.10}$$

$$\forall i, 1 \leq i \leq n : ((y_i + l_{yi} \cdot L_i + w_{yi} \cdot W_i + h_{yi} \cdot H_i) - y_{ni}) \cdot (y_i - y_{ni}) = 0 \tag{3.11}$$

$$\forall i, 1 \leq i \leq n : ((z_i + l_{zi} \cdot L_i + w_{zi} \cdot W_i + h_{zi} \cdot H_i) - z_{ni}) \cdot (z_i - z_{ni}) = 0 \tag{3.12}$$

**Constraints of neighbor relations**:

$$\forall \{i, j\}, 0 \leq i, j \leq n : V_{ij} \cdot \sqrt{(x_{ni} - x_{nj})^2 + (y_{ni} - y_{nj})^2 + (z_{ni} - z_{nj})^2} \leq V_{ij} \cdot Rc \tag{3.13}$$

**Within-container constraints**:

$$\forall i, 1 \leq i \leq n : x_i + l_{xi} \cdot L_i + w_{xi} \cdot W_i + h_{xi} \cdot H_i \leq L_c \tag{3.14}$$

$$\forall i, 1 \leq i \leq n : y_i + l_{yi} \cdot L_i + w_{yi} \cdot W_i + h_{yi} \cdot H_i \leq W_c \tag{3.15}$$

$$\forall i, 1 \leq i \leq n : z_i + l_{zi} \cdot L_i + w_{zi} \cdot W_i + h_{zi} \cdot H_i \leq H_c \tag{3.16}$$

**Binary constraints**:

$$\forall i, 1 \leq i \leq n : l_{xi} + l_{yi} + l_{zi} = 1 \tag{3.17}$$

$$\forall i, 1 \leq i \leq n : w_{xi} + w_{yi} + w_{zi} = 1 \tag{3.18}$$

$$\forall i, 1 \leq i \leq n : h_{xi} + h_{yi} + h_{zi} = 1 \tag{3.19}$$

$$\forall i, 1 \leq i \leq n : l_{xi} + w_{xi} + h_{xi} = 1 \tag{3.20}$$

$$\forall i, 1 \leq i \leq n : l_{yi} + w_{yi} + h_{yi} = 1 \tag{3.21}$$

$$\forall i, 1 \leq i \leq n : l_{zi} + w_{zi} + h_{zi} = 1 \tag{3.22}$$

We can distinguish the constraints related to the neighborhood relations between nodes and those related to geometric feasibility conditions to place the $\pi$-containers. The inequalities (3.2)-(3.8) are non-overlapping conditions which ensure that all the $\pi$-containers do not overlap. The constraints (3.10)-(3.12) represent the relation between the FLB coordinates of $\pi$-containers and the coordinates of the sensor nodes. The sensor node can potentially be placed at one the eight corners of the $\pi$-container since it can be freely rotated. The constraint (3.13) certifies that all neighbor relationships have been respected. The constraints (3.14)-(3.16) ensure that all $\pi$-containers are within the composite $\pi$-container. Finally, the constraints (3.17)-(3.22) ensure that the binary variables which determine the position of the $\pi$-containers are properly controlled to reflect practical positions.

On finite domains, constraint satisfaction problems can be typically solved using search algorithms. The most used techniques include backtracking and constraint propagation [116]. In the first approach, all variables are initialized sequentially within their domains. By this way, different possible combinations of variables assignments are tested to examine the satisfaction of the all constraints until all possible solutions are found. In the second scheme, constraints between different variables are propagated to transform the original

CSP into an equivalent problem that is easier to solve. Accordingly, the domain size of variables is reduced since redundant values from their domains are removed. Depending on the domain size of variables, a proper search algorithm can be applied. In the Chapter 4, under the scenarios set up for simulation, we examine the search space of variables to apply the suitable algorithm to solve the CSP. The performance of the algorithm is investigated and analyzed in terms of time complexity and the number of solutions found within this time duration.

## 3.5 Conclusion

The typical physical characteristics of $\pi$-containers such as modularity and interlock capability allows composing specified sets of $\pi$-containers to be composite $\pi$-containers which are new unit loads with flexible sizes. These unit loads are created to support handling, transportation and storage activities since their sizes fits in the handling tools such as $\pi$-handlers, $\pi$-movers, $\pi$-carriers. Creating these unit loads becomes frequent since huge traffic flow of $\pi$-containers is going in/out of $\pi$-nodes ($\pi$-hubs, $\pi$-stores) continuously. In these cases, there requires an efficient mechanism of managing the $\pi$-containers in order to improve the efficiency of logistics activities.

The proposed methodology in this Chapter aims to retrieve the spatial distribution of unitary $\pi$-containers assigned inside a composite $\pi$-container (H-container). Given a set of $\pi$-containers (e.g., P-containers) fulfilled completely within an H-container, spatial locations of $\pi$-containers are imposed by two types of geometric constraints. The first is non-overlapping: the $\pi$-containers do not overlap and the second is within-the composite $\pi$-container: all $\pi$-containers lie entirely within the composite $\pi$-container. Therefore, these positions can be derived from solutions to constraint satisfaction problems (CSP). However, the two conditions are insufficient to determine exactly the position of $\pi$-containers. By exploiting the capabilities of sensor motes (i.e., communication, data storing, processing) equipped with $\pi$-containers, relative positions of $\pi$-container representing the neighbor relationship of sensors provide additional constraints which increase the tightness of constraints in the CSP. This model leads to find the absolute coordinates and the orientation of each $\pi$-container, which satisfy the neighbor relationships between the sensor nodes.

# Chapter 4

# Simulation Results and Analysis

## Contents



Based on different scenarios described in this Chapter, we have implemented the proposed algorithms deployed for the WSN and then solved the CSP to verify the performance of our proposed methodology.

## 4.1 Scenarios and Implementations

### 4.1.1 Scenarios

In all scenarios presented to our simulation models, 9 types of unitary $\pi$–containers introduced in [26] are reused to examine. These $\pi$–containers are composed by different manners so that the composite $\pi$–container is filled fully in a volume with predefined size. For ease of modeling, the dimensions of $\pi$–containers are normalized to be integer number since they are orders of a unit size. For example, when the unit size is set as the minimum size of dimensions of $\pi$–containers (0.12 m) as proposed in [10], normalized dimensions of a $\pi$–container $[2 \times 3 \times 2]$ corresponds to $[0.24 \times 0.36 \times 0.24]$m in real size. Fig.4.1 introduces the 9 types of unitary $\pi$–containers and the composite $\pi$–container along with their normalized dimensions. Note that, the black round sign in the corner of each $\pi$–container represents the sensor. The coordinate system in three dimensions $OXYZ$ is associated in the composite $\pi$–container to determine orientations of the $\pi$–containers easily.

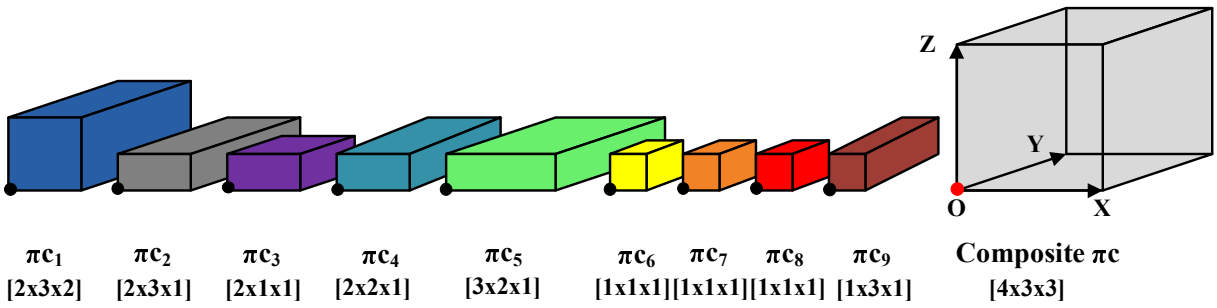


Figure 4.1: Normalized dimensions of 9 unitary $\pi$–containers and corresponding composite $\pi$–container

Three basic scenarios considered are illustrated in the Fig.4.2.

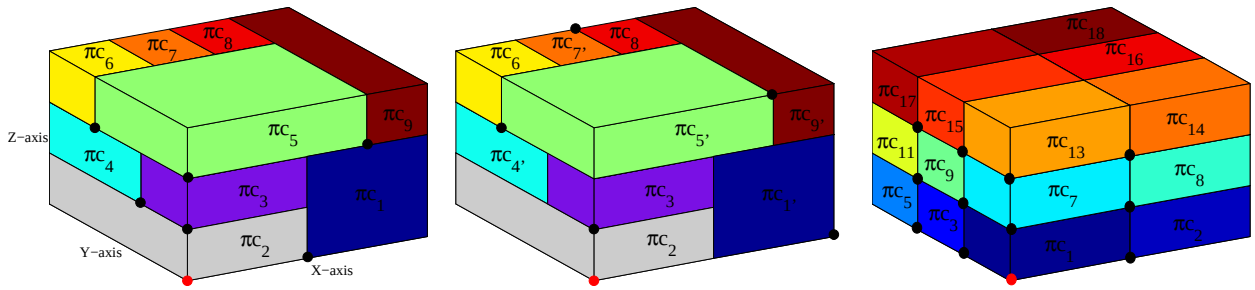


(a) Scenario Model 1 (b) Scenario Model 2 (c) Scenario Model 3

Figure 4.2: Three scenario models considered to study

For obtaining the generality, the three scenarios take into account both the types of $\pi$-containers to be composed: heterogeneous $\pi$–containers (where different dimensions of $\pi$–containers are considered) or homogeneous $\pi$–containers (where the $\pi$–containers are all identical in terms of their dimensions and orientation). Accordingly, the first and second scenarios classified as the first type use all the nine types of unitary $\pi$–containers, meanwhile the third one belonged to the second type uses 18 identical $\pi$-containers with dimensions $[2 \times 1 \times 1]$ to fill fully in the composite $\pi$–container.

Relating to the relationship between the FLB coordinate of $\pi$-container and coordinate of its sensor nodes, in the scenarios 1 and 3, the FLB coordinates of $\pi$-containers are identical to those of the sensor nodes. This perspective is feasible in practical logistics activities since the orientations of unitary $\pi$-containers must respect to a predefined rule of stacking (e.g. "**This way up**!" rule) during the stacking/loading processes. No rotation of the $\pi$-containers is allowed in these two scenarios. On other words, $(x_i, y_i, z_i)$ is equal to $(x_{ni}, y_{ni}, z_{ni})$ in the proposed mathematical model. This constraint will reduce research space and running time of the algorithm to solve the CSP.

Meanwhile, the scenario 2 takes into account the rotation allowance of some $\pi$-containers during composing or loading. Accordingly, these $\pi$-containers can be rotated by 90° or 180° on the horizontal (or vertical) plane freely without concerning any constraint of orientation for composing/stacking. Fig.4.2 reveals the difference between layouts in the scenario 1 and the scenario 2. Although the layouts of two scenarios is the same, orientations of some $\pi$–containers ($\pi c_1$, $\pi c_5$, $\pi c_7$, $\pi c_9$) marked by a prime symbol (') are changed. As a result, the change leads to the difference between the FLB coordinates of $\pi$–containers and the coordinates of sensor nodes. By integrating a three dimension coordinate system with the composite $\pi$–container, the FLB coordinates of $\pi$–containers, the coordinates of associated sensor nodes and the oriented dimensions of $\pi$-containers for the three scenarios can be derived as summarized in Table 4.1.

### 4.1.2 Simulator Tools and Parameters

#### Network Simulators

There are several network simulation software or platforms used by researchers to predict network system performance under proposed algorithms and protocols. Widely used network simulation software includes Network Simulation 2 (NS-2), Network Simulation 3 (NS-3), OMNeT++, and OPNET. The addition of LR-WPAN (Low Rate-Wireless Personal Area Network) module to the NS-3 makes the NS-3 network simulator [44] suitable for the performance analysis of a WSN given CSMA/CA medium access specification

[44] NS-3 Simulator, https://www.nsnam.org/

| Layout Model | $\pi c_i$ | Oriented Dimensions $[L_i \times W_i \times H_i]$ | FLB Coordinates of $\pi c_i$ $(x_i, y_i, z_i)$ | Coordinates of node $i$ $(x_{ni}, y_{ni}, z_{ni})$ |
|---|---|---|---|---|
| Scenario Model 1 | $\pi c_1$ | $[2 \times 3 \times 2]$ | $(2, 0, 0)$ | $(2, 0, 0)$ |
| | $\pi c_2$ | $[2 \times 3 \times 1]$ | $(0, 0, 0)$ | $(0, 0, 0)$ |
| | $\pi c_3$ | $[2 \times 1 \times 1]$ | $(0, 0, 1)$ | $(0, 0, 1)$ |
| | $\pi c_4$ | $[2 \times 2 \times 1]$ | $(0, 1, 1)$ | $(0, 1, 1)$ |
| | $\pi c_5$ | $[3 \times 2 \times 1]$ | $(0, 0, 2)$ | $(0, 0, 2)$ |
| | $\pi c_6$ | $[1 \times 1 \times 1]$ | $(0, 2, 2)$ | $(0, 2, 2)$ |
| | $\pi c_7$ | $[1 \times 1 \times 1]$ | $(1, 2, 2)$ | $(1, 2, 2)$ |
| | $\pi c_8$ | $[1 \times 1 \times 1]$ | $(2, 2, 2)$ | $(2, 2, 2)$ |
| | $\pi c_9$ | $[1 \times 3 \times 1]$ | $(3, 0, 2)$ | $(3, 0, 2)$ |
| Scenario Model 2 | $\pi c_1$ | $[2 \times 3 \times 2]$ | $(2, 0, 0)$ | $(4, 0, 0)$ |
| | $\pi c_2$ | $[2 \times 3 \times 1]$ | $(0, 0, 0)$ | $(0, 0, 0)$ |
| | $\pi c_3$ | $[2 \times 1 \times 1]$ | $(0, 0, 1)$ | $(0, 0, 1)$ |
| | $\pi c_4$ | $[2 \times 2 \times 1]$ | $(0, 1, 1)$ | $(2, 1, 1)$ |
| | $\pi c_5$ | $[3 \times 2 \times 1]$ | $(0, 0, 2)$ | $(3, 0, 3)$ |
| | $\pi c_6$ | $[1 \times 1 \times 1]$ | $(0, 2, 2)$ | $(0, 2, 2)$ |
| | $\pi c_7$ | $[1 \times 1 \times 1]$ | $(1, 2, 2)$ | $(2, 3, 3)$ |
| | $\pi c_8$ | $[1 \times 1 \times 1]$ | $(2, 2, 2)$ | $(2, 2, 2)$ |
| | $\pi c_9$ | $[1 \times 3 \times 1]$ | $(3, 0, 2)$ | $(4, 3, 2)$ |
| Scenario Model 3 | $\pi c_1$ | $[2 \times 1 \times 1]$ | $(0, 0, 0)$ | $(0, 0, 0)$ |
| | $\pi c_2$ | $[2 \times 1 \times 1]$ | $(2, 0, 0)$ | $(2, 0, 0)$ |
| | $\pi c_3$ | $[2 \times 1 \times 1]$ | $(0, 1, 0)$ | $(0, 1, 0)$ |
| | $\pi c_4$ | $[2 \times 1 \times 1]$ | $(2, 1, 0)$ | $(2, 1, 0)$ |
| | $\pi c_5$ | $[2 \times 1 \times 1]$ | $(0, 2, 0)$ | $(0, 2, 0)$ |
| | $\pi c_6$ | $[2 \times 1 \times 1]$ | $(2, 2, 0)$ | $(2, 2, 0)$ |
| | $\pi c_7$ | $[2 \times 1 \times 1]$ | $(0, 0, 1)$ | $(0, 0, 1)$ |
| | $\pi c_8$ | $[2 \times 1 \times 1]$ | $(2, 0, 1)$ | $(2, 0, 1)$ |
| | $\pi c_9$ | $[2 \times 1 \times 1]$ | $(0, 1, 1)$ | $(0, 1, 1)$ |
| | $\pi c_{10}$ | $[2 \times 1 \times 1]$ | $(2, 1, 1)$ | $(2, 1, 1)$ |
| | $\pi c_{11}$ | $[2 \times 1 \times 1]$ | $(0, 2, 1)$ | $(0, 2, 1)$ |
| | $\pi c_{12}$ | $[2 \times 1 \times 1]$ | $(2, 2, 1)$ | $(2, 2, 1)$ |
| | $\pi c_{13}$ | $[2 \times 1 \times 1]$ | $(0, 0, 2)$ | $(0, 0, 2)$ |
| | $\pi c_{14}$ | $[2 \times 1 \times 1]$ | $(2, 0, 2)$ | $(2, 0, 2)$ |
| | $\pi c_{15}$ | $[2 \times 1 \times 1]$ | $(0, 1, 2)$ | $(0, 1, 2)$ |
| | $\pi c_{16}$ | $[2 \times 1 \times 1]$ | $(2, 1, 2)$ | $(2, 1, 2)$ |
| | $\pi c_{17}$ | $[2 \times 1 \times 1]$ | $(0, 2, 2)$ | $(0, 2, 2)$ |
| | $\pi c_{18}$ | $[2 \times 1 \times 1]$ | $(2, 2, 2)$ | $(2, 2, 2)$ |

Table 4.1: Predefined Configuration of $\pi$-containers in the three scenarios: Oriented Dimensions, FLB Coordinates and Coordinates of sensor nodes

defined by the IEEE standard 802.15.4 (2006) [117]. While NS-3 does not contain a default graphical animation tool, there are currently two ways to provide animation, namely using the PyViz method or the NetAnim method. NetAnim is a standalone, Qt4-based software executable that uses a trace file generated during an NS-3 simulation to display the topology and animate the packet flow between nodes. In order to view the performance of network during simulating process in NetAnim, two steps are implemented:

1. Step 1: Generate the animation XML trace file during simulation using an animation interface named as"*ns3::AnimationInterface*" in the NS-3 code base.

2. Step 2: Load the XML trace file generated in Step 1 with the offline Qt4-based animator named NetAnim.

Fig.4.3 shows a captured screen describing the deployment of nodes in the network of scenario 1 before simulation launching.


Figure 4.3: Topology of network of scenario 1 is displayed in NetAnim animator before simulating the counting algorithm. Two additional nodes are deployed in the network to examine the algorithm in recognizing nodes of different networks

Since NetAnim does not support deployment of nodes in three dimensional space, the networks in three scenarios can be deployed in a two dimensional manner such that physical distances among nodes are respected to. By this way, all communication conditions are respected such as the communication range, wireless interference. Consequently the network performances are not inferred by the two different spaces of network deployment.

### CSP Solver

In our model, the variables include nonnegative integers. In addition, the finite domain is quite narrow (medium size of H-container). Therefore, we use the backtracking algorithm that is based on assigning possible values for the variables and checking the satisfaction of constraints. The performance of the algorithm is verified in the simulation processes in term of running time. To program the CSP mathematical model, we use MATLAB software running on a quad-core Intel 2.4 GHz processor with 8GB of RAM. Fig.4.4 shows the development environment for programming the CSP.

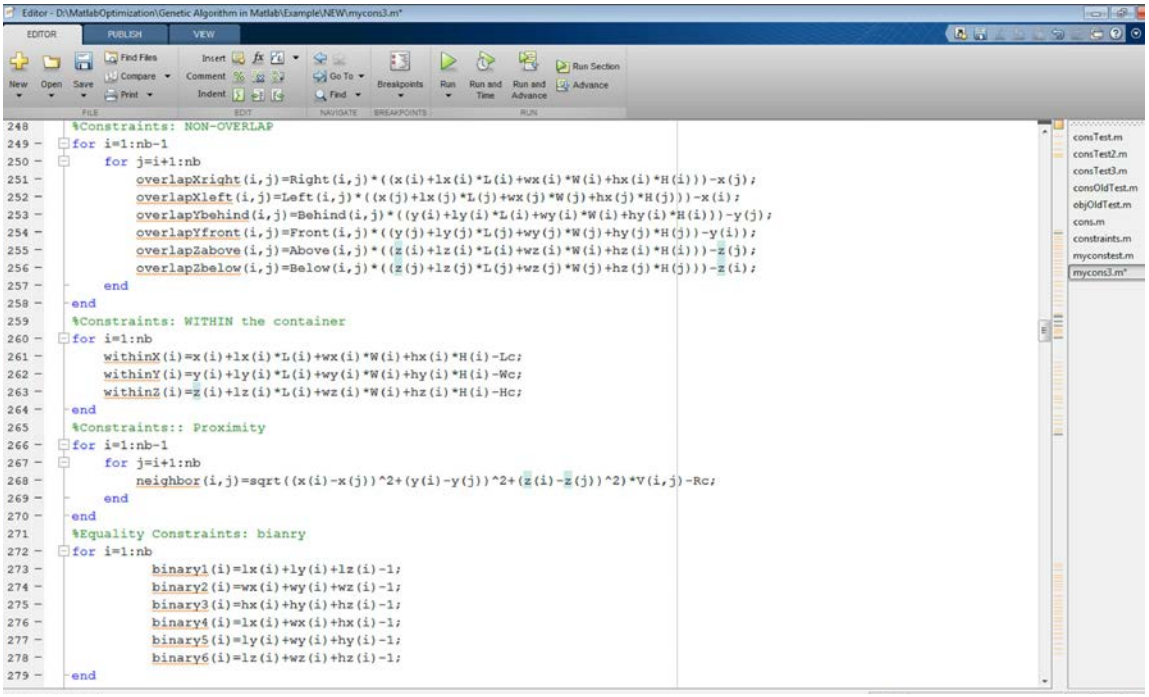


Figure 4.4: The constraints of the CSP are programmed in the script of Matlab Simulator

The solutions of the CSP in combination with the data collected at the GW are used to constructs the 3D layouts. Fig.4.5 illustrates an example of constructing a 3D layout from a solution of the CSP.

## 4.1.3 Network Configuration

### Network Topology

By deploying the MAC and Physical layer as defined by IEEE 802.15.4 standard, the topology of network can be one of two main types: star, peer-to-peer network as Fig. 4.6.

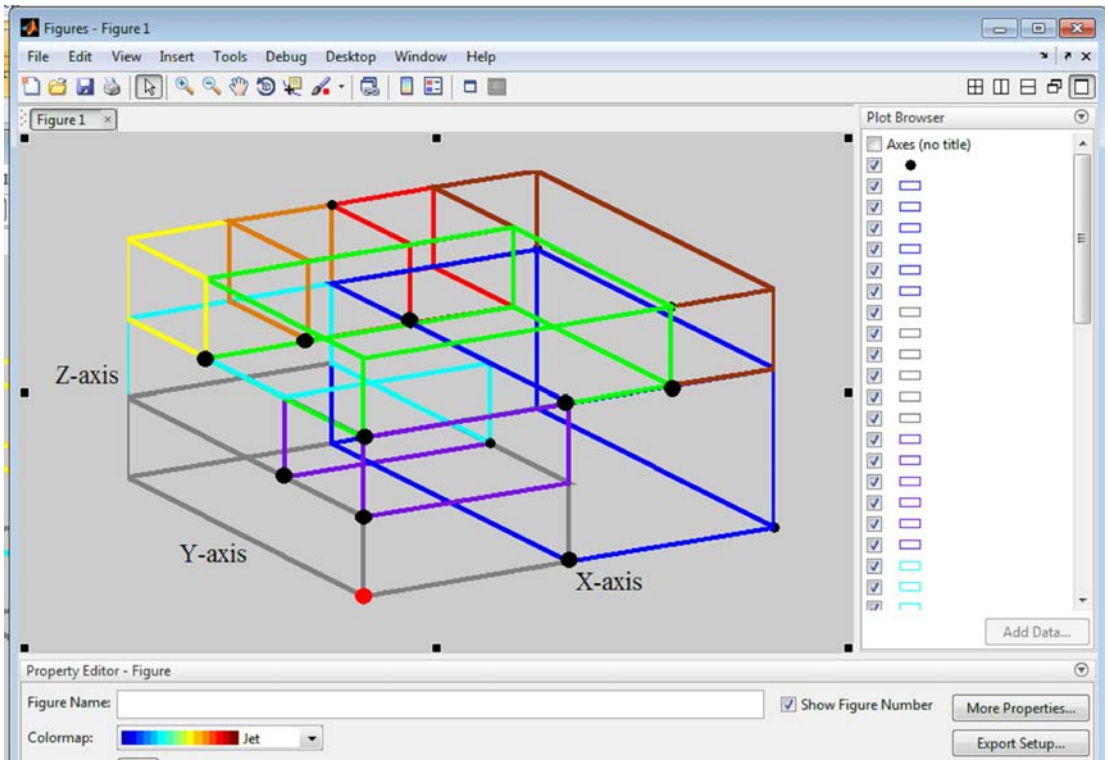


Figure 4.5: A 3D layout virtualized from a solution of the CSP in Matlab Simulator

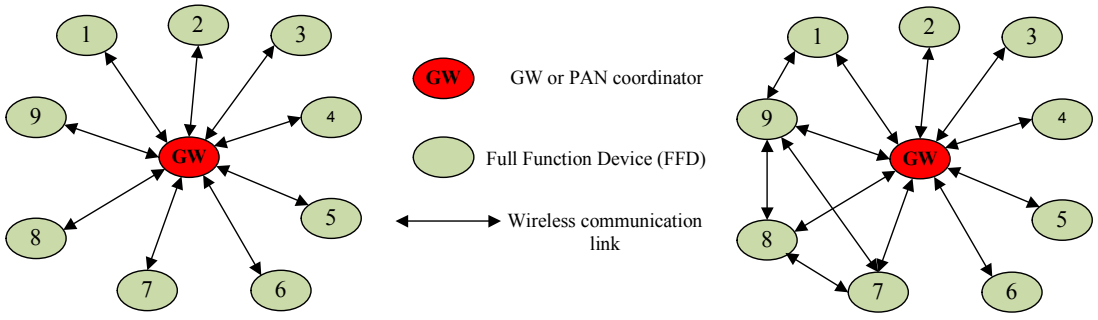


(a) Star Topology

(b) Peer-to-Peer Topology

Figure 4.6: Two topologies of networks deployed in our algorithms

Depending on the type of nodes (Full Function Device - FFD or Reduced Function Device - RFD), the network is operated following the corresponding topology. Accordingly, FFD can communicate with FFDs or RFD, meanwhile, RFD can only communicate with FFDs but other RFDs. In addition, FFD can be selected to be a coordinator that coordinates the communication between nodes in the network. In our algorithms, since all nodes have capability to communicate with each other, thus they are all FFDs. Therefore, the operation topology of the network is decided by the GW according to the applications. In our cases, in the counting algorithm, the topology is star form, meanwhile in the joint neighbor discovery and neighbor table forwarding algorithm, the topology is peer-to-peer form since all node are required to exchange the necessary packets according to the proposed algorithm. For all the nodes used in our simulation modes, their physical layer and media access control layer are based on IEEE 802.15.4 standard, which supports a low data rate and power consumption.

Fig. 4.7 shows a typical stack architecture of nodes.

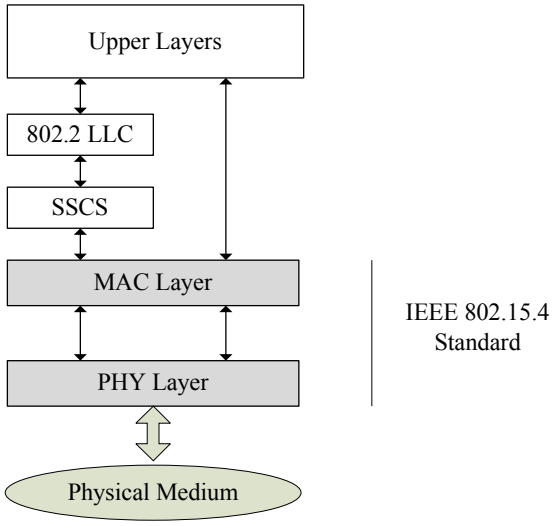


Figure 4.7: Stack architecture of devices in the network

The simulation model is built by modifying the model of LR-WPAN [45] based on NS-3 simulator [118].

An LR-WPAN device comprises a physical layer (PHY), which contains the radio frequency (RF) transceiver along with its low-level control mechanism, an a MAC sublayer that provides access to the physical channel for all types of transfer. In addition, the upper layers consist of a network layer, which provides network configuration, manipulation, and message routing, and an application layer, which provides intended function of the device.

[45] LR-WPAN module in NS-3, https://www.nsnam.org/docs/models/html/lr-wpan.html

In the next Section, these layers are described in more detail.

Simulations are configured for the performance evaluation of the proposed algorithms with the metrics like counted number of nodes, average end-to-end delay, packet loss ratio (PLR) and average energy consumption of nodes.

### Physical Layer

The original IEEE 802.15.4 standard released in 2003 adopted a wideband physical layer using Direct Sequence Spread Spectrum technique (DSSS). It provided physical layer operations in three frequency bands: the 868 MHz band available in Europe, the 915 MHz band available in US, and the 2.4 GHz ISM ban, which is the unlicensed band available worldwide.

The physical layer is responsible for controlling the output power of radio transceiver by which the communication range ($Rc$) of node is adjusted accordingly. In fact, the range is dependent on various factors including the environment, positions of nodes, directions of antenna, etc. In the Chapter A, we implement a series of experiment testbeds measuring the communication range of Micaz motes. Different scenarios including with/without interference of other nodes, with or without obstacles between two motes are demonstrated to examine the nature of wireless communication.

### MAC layer

The main function of MAC layer is to control medium access to transmit the data packets. The IEEE 802.15.4 LR-WPAN employs various mechanisms to improve the probability of successful data transmission. These mechanisms include the CSMA-CA (Carrier sense multiple access with collision avoidance) mechanism, frame acknowledgment, and data verification. In all the scenario simulations, we implement the network algorithms using the CSMA-CA mechanism. The standard IEEE 802.15.4 supports two operational modes. They are: (a) Beacon-enabled mode: in this mode, beacons are periodically sent by the PAN or Coordinator to synchronize nodes that are associated with it. This mode uses superframe, as shown in Fig. 4.8 which has contention access and contention free period divided into different guaranteed time slots (GTS); (b) Non beacon-enabled mode: in this mode, PAN coordinator does not transmit beacons. It does not support GTS and uses un-slotted CSMA/CA MAC protocol. The IEEE 802.15.4 allows the operational use of superframe structure defined by the coordinator.

The beacon packets are transmitted periodically by the coordinator to describe the superframe structure. Beacon Interval (BI) defines the superframe length, which includes an active period and an inactive period. BI and the length of active portion are determined

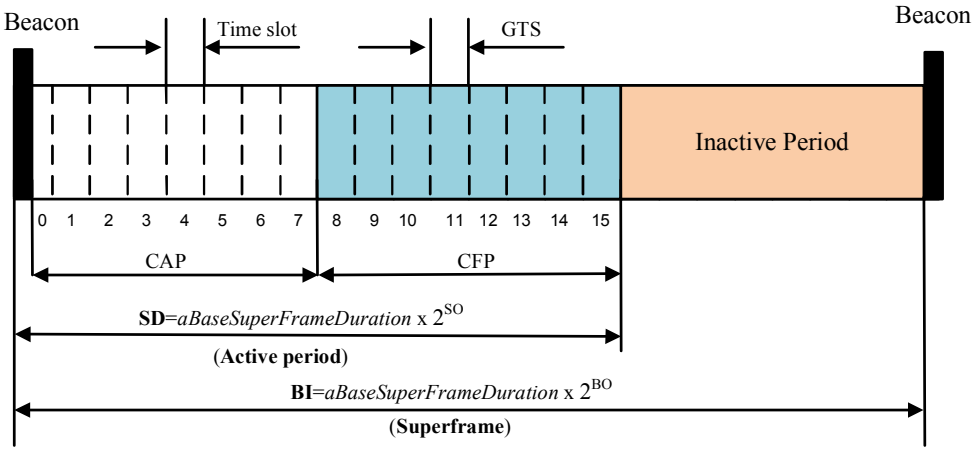


Figure 4.8: The IEEE 802.15.4 superframe structure

by two parameters: Beacon Order (BO) and Superframe Order (SO). The minimum length of a superframe (*aBaseSuperframeDuration*) is fixed to 960 symbols corresponding to 15.36 ms, assuming 250 kbps in the 2.4 GHz frequency band (as equation 4.1.

$$aBaseSuperframeDuration = \frac{960 \times 4}{250000} = 0.01536(s). \tag{4.1}$$

The active portion may consist of two periods: contention access period (CAP) and contention free period (CFP). During CAP, nodes use the slotted CSMA-CA algorithm to access the channel to transmit their data packets. By this way, when nodes in the network receive the beacon message, they randomly chose their own time slots to transmit packets requested by the coordinator. Meanwhile, during CAP, nodes are assigned their own time slots to transmit their data reliably.

BO and SO are set up by the coordinators in the beacon frames as shown in Fig. 4.9.

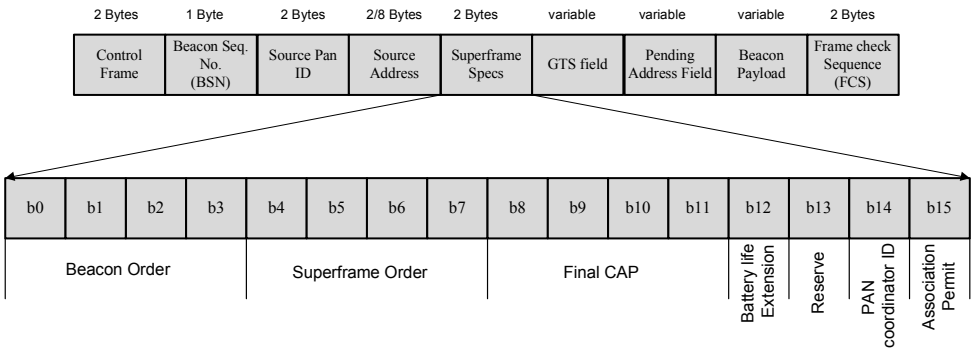


Figure 4.9: Beacon frame with Superframe specification field description

In the next section, we implement the simulation on the network that configures

the values of SO and BO to examine the performance of networks under the proposed algorithms deployed.

## 4.2 Simulation Results and Analysis for WSN Performances

In this Section, we present the simulation results when WSNs deploy the counting algorithm and the joint algorithm.

### 4.2.1 Counting Algorithm

With the objective of detecting all the nodes in the network, we conduct different simulation cases to examine under what conditions the algorithm ensures to reach the target. As described in the counting algorithm, the simulation process will stop when the **list_nodes** storing the number of detected nodes is unchangeable in the first stable period. This interval is varied to be a number of consecutive BIs, for example {2, 3, 4, 5, 6 or 7}BI to verify these stable number in these intervals. During the stable periods, no ACK_CNT packets are received at the GW. One reason may be that all the ACK_CNT packets are collided when they are sent at the same time slot. In another case, nodes defer these messages to send due to carrier sensing of CSMA/CA mechanism. To examine these cases in our simulation scenarios, the values of SO are varied in order to analyze the transmissions of packets under impact of packet collision and packet loss. To investigate the confidence of algorithm performance, each simulation case is implemented in 100 samples with the same simulation condition (i.e., interference, noise models of wireless channel) and parameter configurations (i.e., $\Delta T_{CNT\_stable}$, SO, etc.). For ease of demonstration, Table 4.2 summaries key parameters used to simulate the counting algorithms.

| Symbol | Definition |
|---|---|
| SO, BO | Superframe Order and Beacon Order, SO=BO={0, 1, 2} |
| SD, BI | Superframe Duration and Beacon Interval, SD=BI |
| TS | Time Slot |
| TSD | Time Slot Duration |
| $\Delta T_{CNT\_packet}$ | Beacon generation interval, $\Delta T_{CNT\_packet} = BI$ |
| $\Delta T_{CNT\_stable}$ | Stable duration of counter, $\Delta T_{CNT\_stable} = \{2, 3, 4, 5, 6, ...\}BI$ |
| $N_{sample}$ | Number of sample tests for each simulation scenario (Set to 100) |

Table 4.2: Symbols used in the counting algorithm demonstration

After the simulation stops, we examine the simulation results that includes number of nodes detected, corresponding running time (delay) and energy consumed by a certain node.

### Number of detected nodes versus $\Delta T_{CNT\_stable}$ and SO

In the first simulations, we examine the number of nodes detected by the GW under impact of two factos: the duration of the first stable period ($\Delta T_{CNT\_stable}$) during which this number is unchangeable and SO.

Fig. 4.10 depict the variation of node counter values for the two networks of scenarios 1, 2. These numbers are examined in impact of different values of SO, $\Delta T_{CNT\_stable}$ through 100 simulation samples.

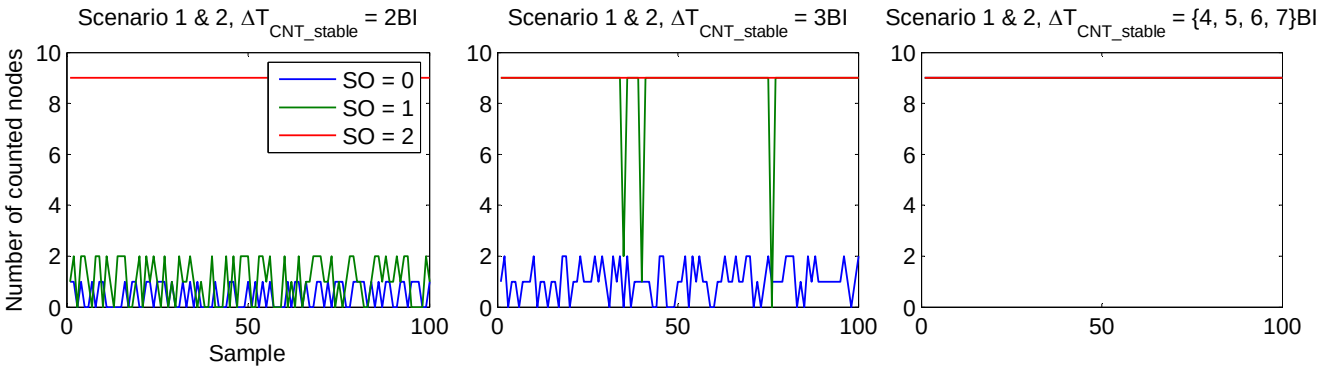


Figure 4.10: Impact of SO and $\Delta T_{CNT\_stable}$ on number of detected nodes in networks of scenarios 1 & 2

The simulation results show that when the SO values are small (0 and 1), short durations of stable (i.e., 2BI or 3BI) are insufficient for the algorithm to detect all the nodes in the network. For instance, only two nodes in maximum are detected by the GW in the network 1 if SO is equal to 1; and this number is just 1 in the case that SO is set to 0 if the length of stable duration just lasts in two consecutive BIs. When the length increases by 1BI ($\Delta T_{CNT\_stable}$ = 3BI), the algorithm still fails to detect all the nodes. Although in majority of simulation samples, the expected number of nodes (9 nodes) is detected when the SO is set to 1, the instability of the result prevents the algorithm from deploying in the practices. Meanwhile, when SO is equal to 2, the algorithm allows the GW to detect all the nodes in network if the **list_nodes** is stable in at least two continuous BIs.

For the best performance, if **list_nodes** is unchangeable in at least 4 consecutive BIs, the algorithm ensures that all the nodes of network are detected regardless different

values of SO. The simulation results are originated from networking performance in term of packet loss ratio (PLR) since the values of SO impact on competition of nodes in transmitting ACK_CNT packets. Fig. 4.11 shows the PLR for all the simulation samples of networks in the scenarios 1 & 2.

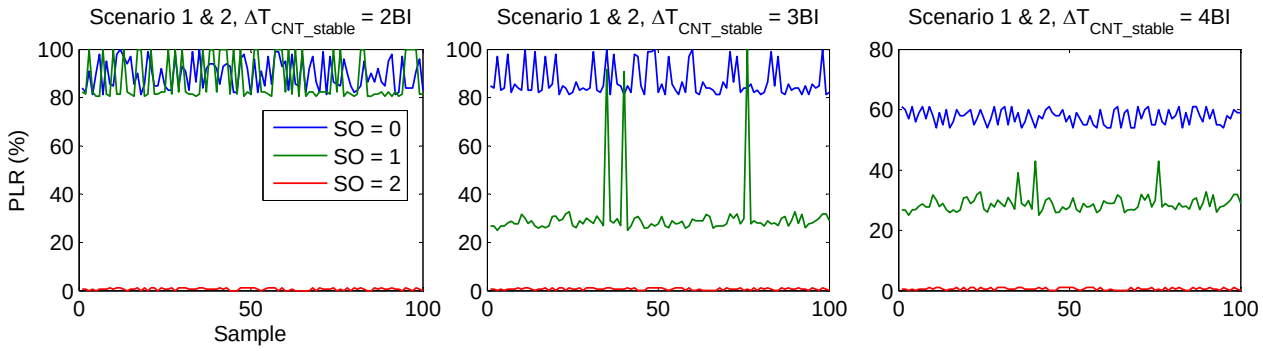


Figure 4.11: PLR for the networks of scenario 1 & 2

The first observation is that a lower SO values (i.e., SO=0 or SO=1) leads to a higher PLR (up to 80% when $\Delta T_{CNT\_stable} = 2BI$). This is because of the fact that when SO is small the narrow contention window can cause lots of packet collisions in the first several superframes. As a result, more nodes will delay sending ACK_CNT packets in some consecutive superframes, thus only some nodes can announce their existences successfully. Certainly, when SO is set to be 2, the PLR is reduced considerably since the nodes competing in a wider contention window allows them to avoid collision. Therefore, more nodes are detected within one BI since they have high probability of transmit ACK_CNT packet successfully. In addition, in the next BIs, only few undiscovered nodes compete to obtain channel access rights that in turn increases the success ratio of ACK_CNT packet transmissions.

The result is similar to the network of the scenario 3 under performance of the counting algorithm as shown in Fig. 4.12. Accordingly, with lower values of SO (SO is equal to 0 or 1) and shorter stable durations of counter ($\Delta T_{CNT\_stable}$ = 2BI or 3BI), only a few nodes (maximum number is 3 or 5) are detected by the GW.

Although, when SO is increased to up 2, the algorithm can detect all the nodes in majority of simulation samples, the result is unstable since in some samples, the a few number of nodes are detected. The exact counter of nodes (i.e., 9 and 18 nodes respectively) in the three networks can be reached if the stable duration is set to be at least 4 consecutive BIs regardless set values of SO. The best performance of algorithm can be obtained when SO is set to 2 at the MAC layer. In this case, the duration stable lasts only two consecutive BIs to detect all the nodes present in the network. When the **list_nodes**

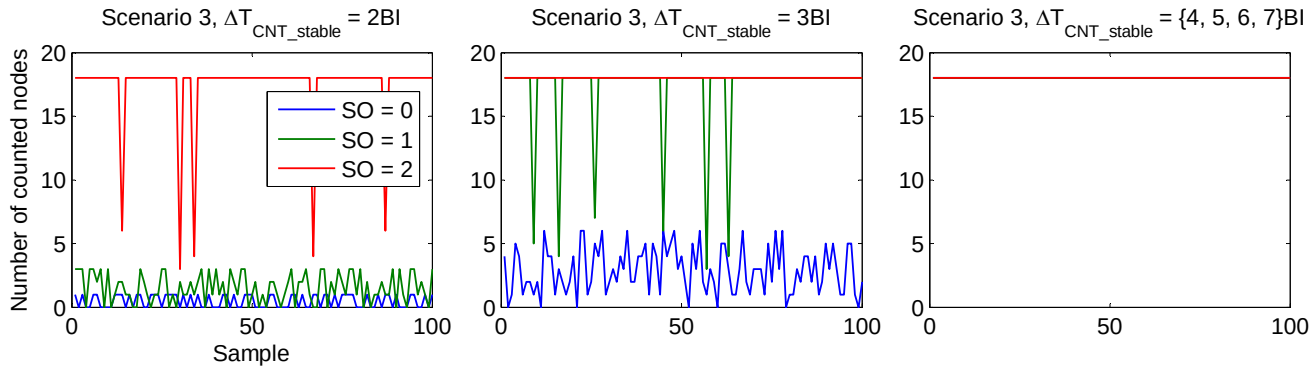


Figure 4.12: Impact of SO and $\Delta T_{CNT\_stable}$ on number of detected nodes in network of scenario 3

is stable during a period whose length is greater than three consecutive BIs, the algorithm obtains the exact number of nodes regardless the value of SO is selected.

With more nodes try to transmit their ACK_CNT packets, the PLR of the network is expected to be higher. Fig. 4.13 present the packet loss rates (PLR) for all the simulation samples of the network in the scenario 3.

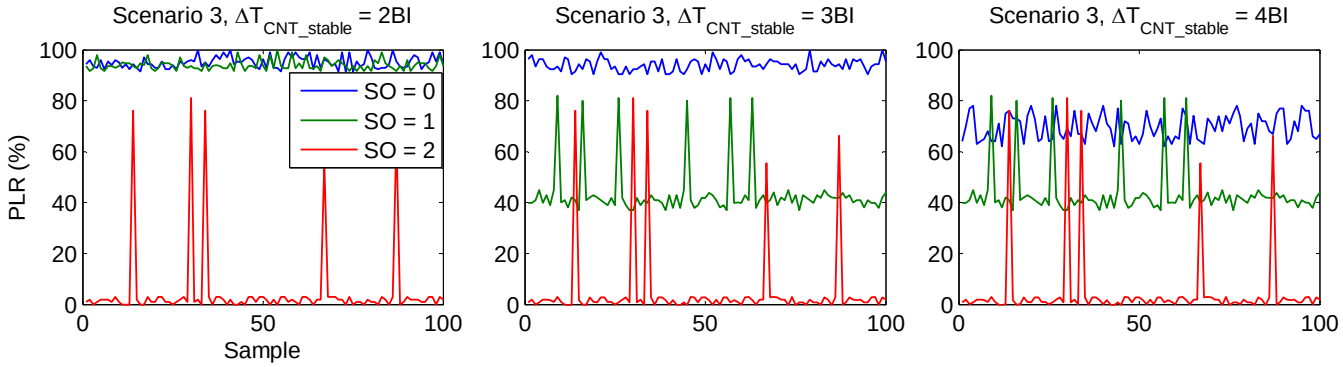


Figure 4.13: PLR for the network of scenario 3

The networking performance of scenario 3 in terms of PLR is similar to the networks of scenario 1 & 2. Accordingly, when SO is small (i.e., SO=0 or 1) narrow contention windows contribute to high ratio of packet loss due to collisions. Furthermore, having a double number of nodes the PLR of network of scenario 3 is higher than that of network 1 & 2. In addition, even SO is set to be 2, wider contention window can reduce packet collisions, the PLR of network 3 is still higher than that of network 1 & 2. These facts impact significantly on the relation between the number of detected nodes and $\Delta T_{CNT\_stable}$ as seen in Fig. 4.12.

Examined over different simulation scenarios and each run repeatedly 100 times, the following Table 4.3 summarizes the optimal conditions by which the algorithm allows the GW detect all the nodes in the network.

| Scenario | Optimal Conditions | |
|---|---|---|
| Scenario 1 & 2 | SO={0, 1} & $\Delta T_{CNT\_stable} = 4BI$ | SO=2 & $\Delta T_{CNT\_stable} = 2BI$ |
| Scenario 3 | SO={0, 1} & $\Delta T_{CNT\_stable} = 4BI$ | SO=2 & $\Delta T_{CNT\_stable} = 3BI$ |

Table 4.3: Optimal conditions based on that the GW is able to determine the exact number of nodes in the network

Fig.4.14 shows a screen capture illustrating the simulation environment after finishing the counting algorithm of the networks of scenario 1 &2. The all detected nodes are listed on the right hand side of NetAnim animator along with their identifiers and dimensions.

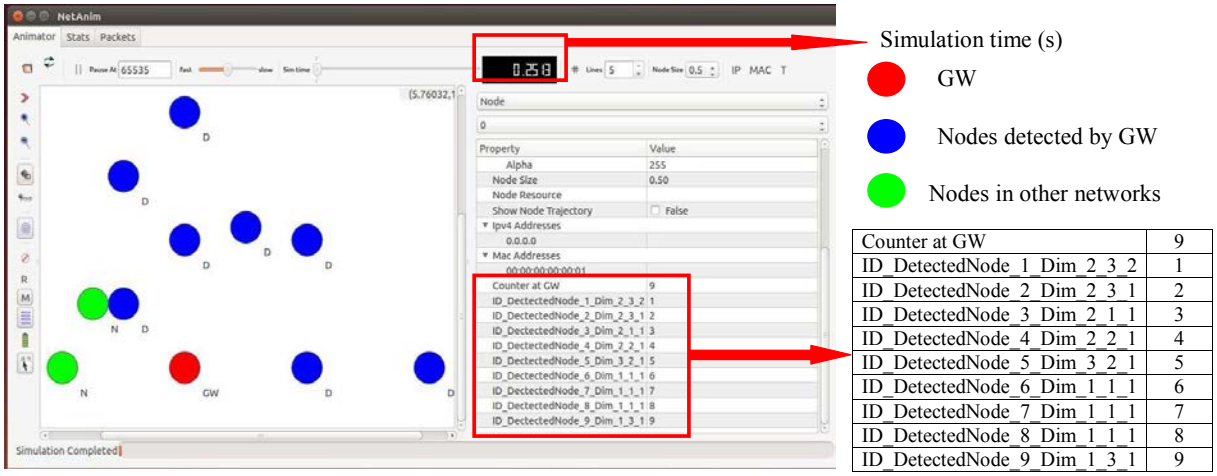


Figure 4.14: Screen Capture of network 1 and 2 after simulating the counting algorithm

### Delay

As mentioned in the Algorithm 1 and 2, the delay for the simulation calculated from the start of simulation until the stable counter can be retrieved from the two factors: $\Delta T_{CNT\_packet}$ and $\Delta T_{CNT\_stable}$. In this Section, the delay needed for obtaining the precise counter of nodes is examined in the networks in respect to different values of stable durations set up in the simulation configuration.

For the scenarios 1 & 2, Fig. 4.15 depicts the needed number of superframes that the GW used in the simulation samples.

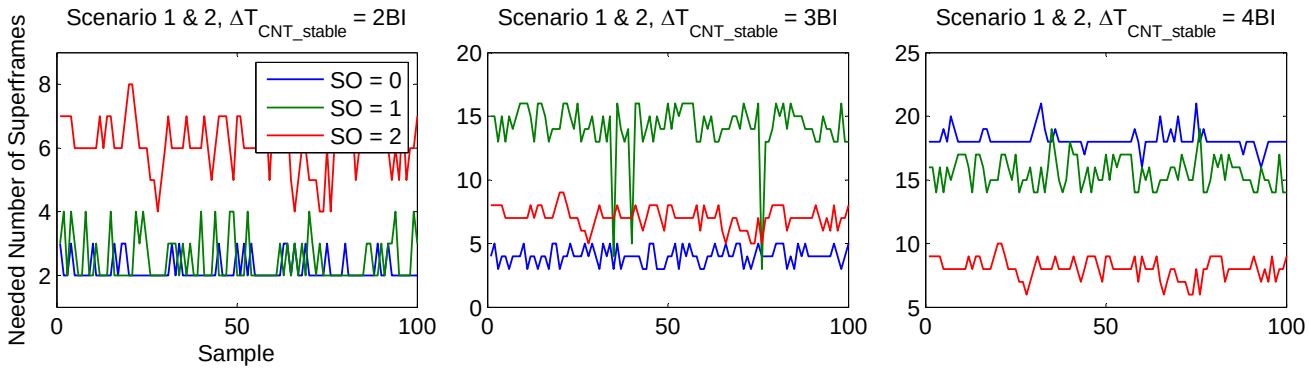


Figure 4.15: Running time of the counting algorithm measured in a number of superframes for the networks of scenarios 1 & 2 under impact of SO & $\Delta T_{CNT\_stable}$

For cases of fail in counting, for example, when SO ={0, 1} & $\Delta T_{CNT\_stable}$=2BI, a small number of superframes is used. As seen in Fig. 4.10, in majority of simulation samples, no nodes are detected in the first two superframes. In addition, in some samples, only one node is detected and this number is kept unchanging in the next two superframes. Considering the successful cases of counting with the optimal conditions, the simulation results show that the needed number of superframes significantly increase with the corresponding decrease of SO. For instance, the $\Delta T_{CNT\_stable}$ set to be 4 consecutive BIs guarantees the exact number of detected nodes regardless values of SO. However, among simulation cases with three values of SO (i.e., 0, 1, 2), the GW used the least number of superframes to complete the counting task when SO is set to be 2. The maximum number of superframes over the 100 simulation samples in this case is 10. Meanwhile, the minimum numbers of superframes used are 14 and 16 when SO is 1 and 0 respectively. In the best performance, the GW only requires in minimum 4 superframes and in maximum 8 superframes to determine 9 nodes in the network when the SO is configured to be 2. More nodes results in having more collisions of their data packets in the beginning of algorithms due to high probability that nodes choose the same time lots to transmit their packets. That in turns, leads to more backoff delays in the next superframes since there are still more nodes to compete the channel to send their packets. In addition, low value of *SO* causes high probability of collisions since 1 packet requires more time slots to complete its transmission. Table 4.4 and Fig. 4.16 supports this statement by comparing the time interval to transmit the 100-byte ACK_CNT packet with duration of a time slot in different values of SO.

With the average size of 100 bytes for each packet, it requires at least 4, 2 and 1 time slots corresponding to the 3 values (0, 1, 2) of *SO* to accomplish it transmission.

| SO | Time Duration (ms) | |
|---|---|---|
| | $SD = BI$ | TSD=SD/16 |
| SO=0 | 15.36 | 0.96 |
| SO=1 | 30.72 | 1.92 |
| SO=2 | 61.44 | 3.84 |

Table 4.4: SD, BI and TSD of 3 superframes

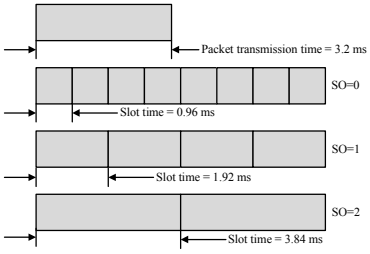


Figure 4.16: Packet transmission delay verse TSD of 3 superframes

Therefore, within contention widows of three supperframes (i.e., SO={0, 1, 2}), there is the maximum number 4, 8, 16 nodes that can transmit their ACK_CNT packets successfully if their selected time slots are uncollided.

Fig. 4.17 illustrates the number of supperframes for the network of scenario 3 required in the simulation cases.

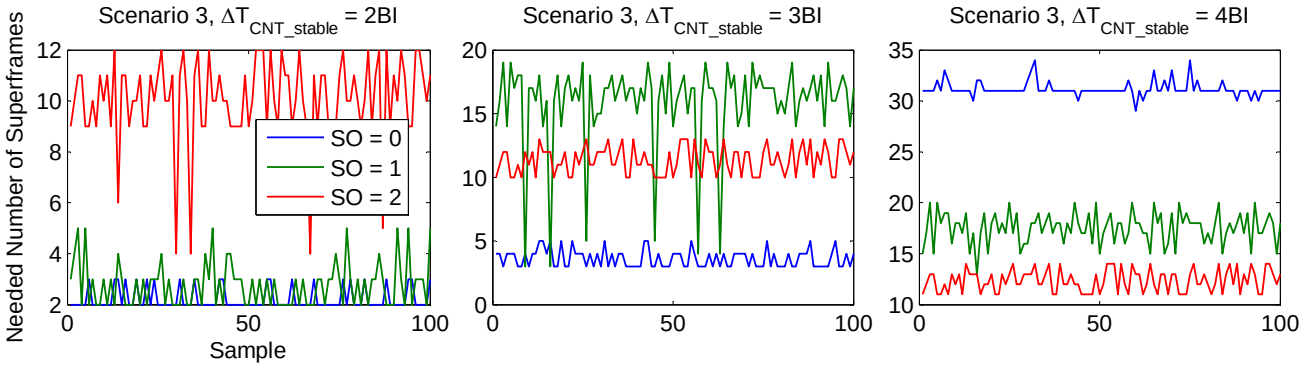


Figure 4.17: Impact of SO on number of superframes in network of scenario 3

For the both cases: fail counting and success counting, the number of superframes that the GW used in this network is similar to the network 1 & 2. Certainly, since the number of nodes is greater (18 nodes), the corresponding number of superframes is required to be much more.

Table 4.5 summaries the number of superframes in maximum, minimum and mean values needed for the GW to successfully detect all the nodes in the networks.

Above all, short duration of time required for the GW to determine exactly number of nodes in the network allows the algorithm to be suitable for the very high dynamic environment of the PI.

| Scenario | Optimal Conditions | Delay measured in number of superframes (sf)/in seconds (s) | | |
|---|---|---|---|---|
| | | Max | Min | Mean |
| Scenario 1 & 2 | $SO = 0$ & $\Delta T_{CNT\_stable} = 4BI$ | 21(sf)/0.32(s) | 16(sf)/0.25(s) | 18(sf)/0.28(s) |
| | $SO = 1$ & $\Delta T_{CNT\_stable} = 4BI$ | 19(sf)/0.58(s) | 14(sf)/0.43(s) | 16(sf)/0.49(s) |
| | $SO = 2$ & $\Delta T_{CNT\_stable} = 2BI$ | 8(sf)/0.49(s) | 4(sf)/0.25(s) | 6(sf)/0.37(s) |
| Scenario 3 | $SO = 0$ & $\Delta T_{CNT\_stable} = 4BI$ | 34(sf)/0.52(s) | 29(sf)/0.45(s) | 31(sf)/0.48(s) |
| | $SO = 1$ & $\Delta T_{CNT\_stable} = 4BI$ | 20(sf)/0.61(s) | 13(sf)/0.40(s) | 18(sf)/0.55(s) |
| | $SO = 2$ & $\Delta T_{CNT\_stable} = 3BI$ | 13(sf)/0.80(s) | 10(sf)/0.61(s) | 12(sf)/0.74(s) |

Table 4.5: Impact of SO values on required number of superframes broadcasted by the GW for three different networks

### Energy Consumption

The wireless motes are powered by two AA sized batteries [46]. Since, the batteries is non-rechargeable, the expected lifetime of a node can vary from days to months, depending on applications and duty cycle deployed for it. Traditionally, the Micaz mote can be interfaced to a number of sensors such as photoresistors, thermistors, passive infrared, magnetometers, and accelerometers to support environment sensing and monitoring. In our scenarios, the sensing application is neglected, thus the energy consumption used for the service is ignored. In addition, since the duty cycle mechanism is not deployed in the nodes (e.g., SO=BO), the consumption energy depends mostly on the two factors: retransmission of ACK_CNT packets and the delay of counting that in turn are impacted by SO.

Fig. 4.18, Fig. 4.19 plot the percentage of average energy consumed by a node to implement the counting algorithm for the three networks respectively. The energy is tracked and averaged with 100 simulation samples.

Considering the cases with the optimal conditions of counting, the simulation results show that the energy consumption lowers fast as SO increases. This is due to that too many beacon frames generated by too small value of SO can intensify the channel contention and the collision. The intensive channel contention results in significant carrier-sensing overhead for devices, and thus increases energy consumption. In addition, the longer delays resulted in cause nodes to consume more energy since they must maintain their listening mode. By this way, more nodes the networks have, more energy each node of networks consume.

Above all, less energy consumed by a node to finish its task in the counting algorithm is acceptable in practices.

[46] Energizer AA Battery Data sheet 2010. Available http://data.energizer.com/pdfs/191.pdf

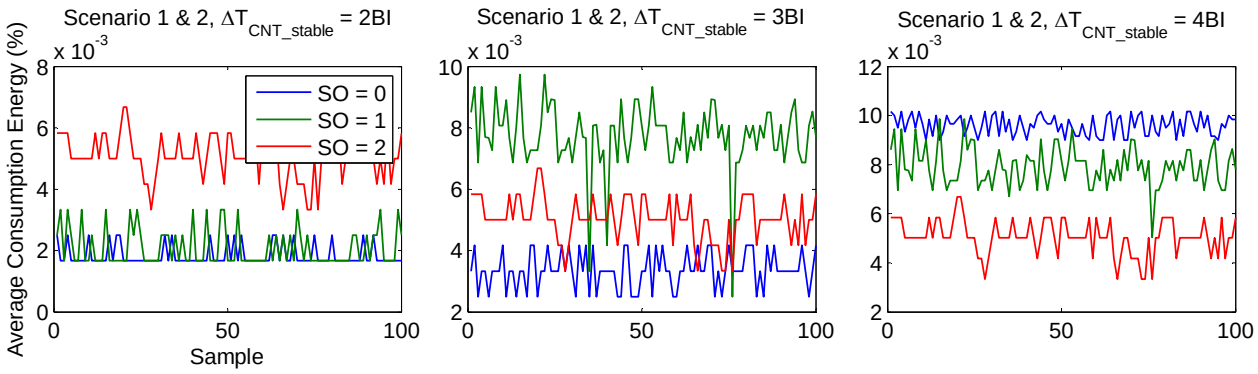


Figure 4.18: Average consumption energy of nodes in the counting algorithm in the networks of scenarios 1 & 2

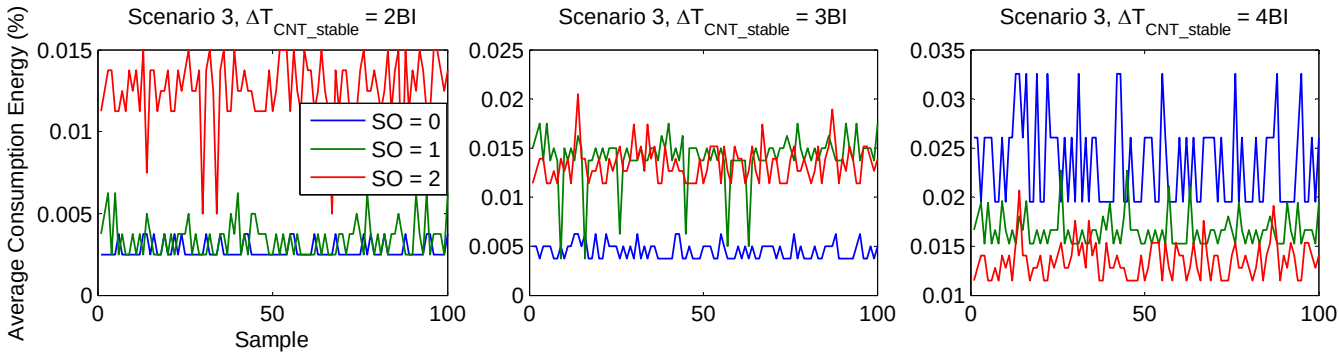


Figure 4.19: Average consumption energy of nodes in the counting algorithm in the network of scenario 3

### 4.2.2 Joint Neighbor Discovery and Neighbor Table Forwarding Algorithm

As observed from the simulation results of counting algorithm, the best performance of network is obtained when the SO is equal to 2. Although the BI is longer, the less collision of packets results in less packet errors, shorter latency and less overhead, thus energy consumption is reduced. For simulation of the joint algorithm, we examine the network performance when SO is set to 2. In addition, under the optimal conditions of counting, the GW can discover all the nodes in the network within $D_{max}$. Therefore, since using the same mechanism to discover neighbors, all the nodes in the network are expected to find all their own neighbors within their smaller communication ranges (e.g., $Rc \leq D_{max}$) when they deploy the joint algorithm using the optimal conditions of counting. Exploiting this result observation, we use the optimal conditions obtained from the counting algorithm to apply and examine the performance of the joint algorithm. Base on that, Table 4.6 describes the parameters set up in the scenarios to simulate the joint algorithm.

| Scenario | Rc | SO | $\Delta T_{NBR\_packet}$ | $\Delta T_{NBR\_stable}$ |
|---|---|---|---|---|
| Scenario 1 | 1.0, 1.5, 2.0, 2.25, 2.5, 3.0 | 2 | BI | 2BI |
| Scenario 2 | 1.0, 1.5, 2.0, 2.25, 2.5, 3.0 | 2 | BI | 2BI |
| Scenario 3 | 1.0, 1.5, 2.0, 2.25, 2.5, 3.0 | 2 | BI | 3BI |

Table 4.6: Parameters used in the simulation scenarios for the joint algorithm

#### Accuracy of global neighbor lists

Fig.4.20 shows a screen capture illustrating the simulation results of the joint algorithm implemented in the network of scenario 1. The right hand side shows the global neighbor list collected at the GW when Rc is 1.0.

The simulation result shows that the global neighbor list obtained from simulation is absolutely in conformity with the real neighborhood relationship among the nodes in the network represented by the connectivity graph as Fig. 4.21.

Consequently, the optimal conditions resulted from the counting algorithm allow the joint algorithm obtain the accurate global neighbor list for each value of chosen Rc. Based on this result, we continued to conduct the simulation implementation for three scenarios that use the optimal conditions of counting to investigate other performance terms of the network such as the required delay, consumed energy of sensor nodes.

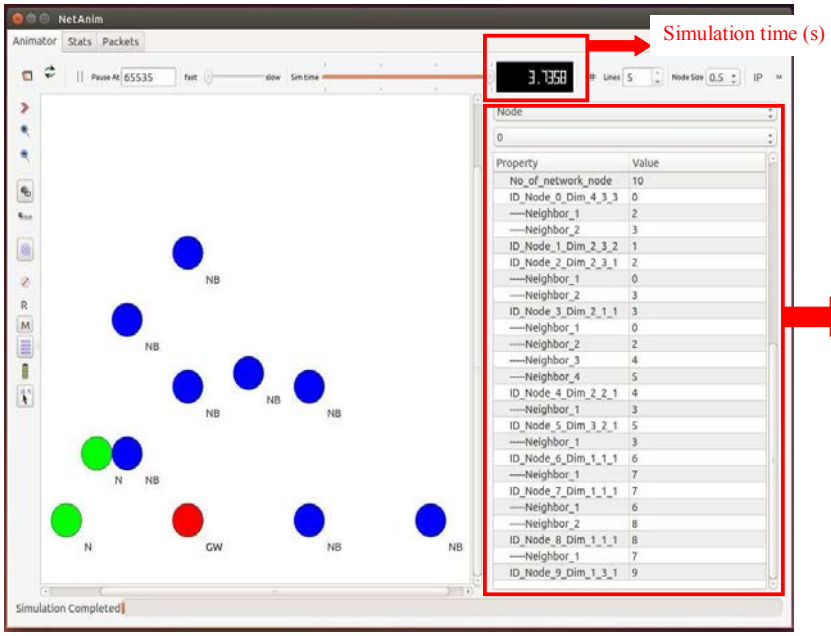


| No_of_network_node | 10 |
|---|---|
| ID_Node_0_Dim_4_3_3 | 0 |
| ---Neighbor_1 | 2 |
| ---Neighbor_2 | 3 |
| ID_Node_1_Dim_2_3_2 | 1 |
| ID_Node_2_Dim_2_3_1 | 2 |
| ---Neighbor_1 | 0 |
| ---Neighbor_2 | 3 |
| ID_Node_3_Dim_2_1_1 | 3 |
| ---Neighbor_1 | 0 |
| ---Neighbor_2 | 2 |
| ---Neighbor_3 | 4 |
| ---Neighbor_4 | 5 |
| ID_DetectedNode_4_Dim_2_2_1 | 4 |
| ---Neighbor_1 | 3 |
| ID_DetectedNode_5_Dim_3_2_1 | 5 |
| ---Neighbor_1 | 3 |
| ID_DetectedNode_6_Dim_1_1_1 | 6 |
| ---Neighbor_1 | 7 |
| ID_DetectedNode_7_Dim_1_1_1 | 7 |
| ---Neighbor_1 | 6 |
| ---Neighbor_2 | 8 |
| ID_DetectedNode_8_Dim_1_1_1 | 8 |
| ---Neighbor_1 | 6 |
| ID_DetectedNode_9_Dim_1_3_1 | 9 |

Figure 4.20: The network 1 is displayed in NetAnim animator after finishing the joint algorithm. The global neighbor table stored in the GW is shown in the right side corresponding to case that Rc is 1.0

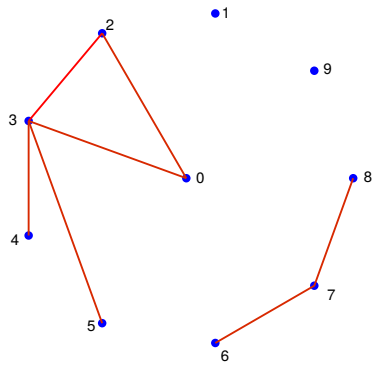


Figure 4.21: The connectivity graph illustrates the real neighbor relationship among nodes in network of scenario 1 when Rc is 1.0

### Delay

Fig.4.22 summarizes the results in term of delay for the three networks deploying the joint algorithm.

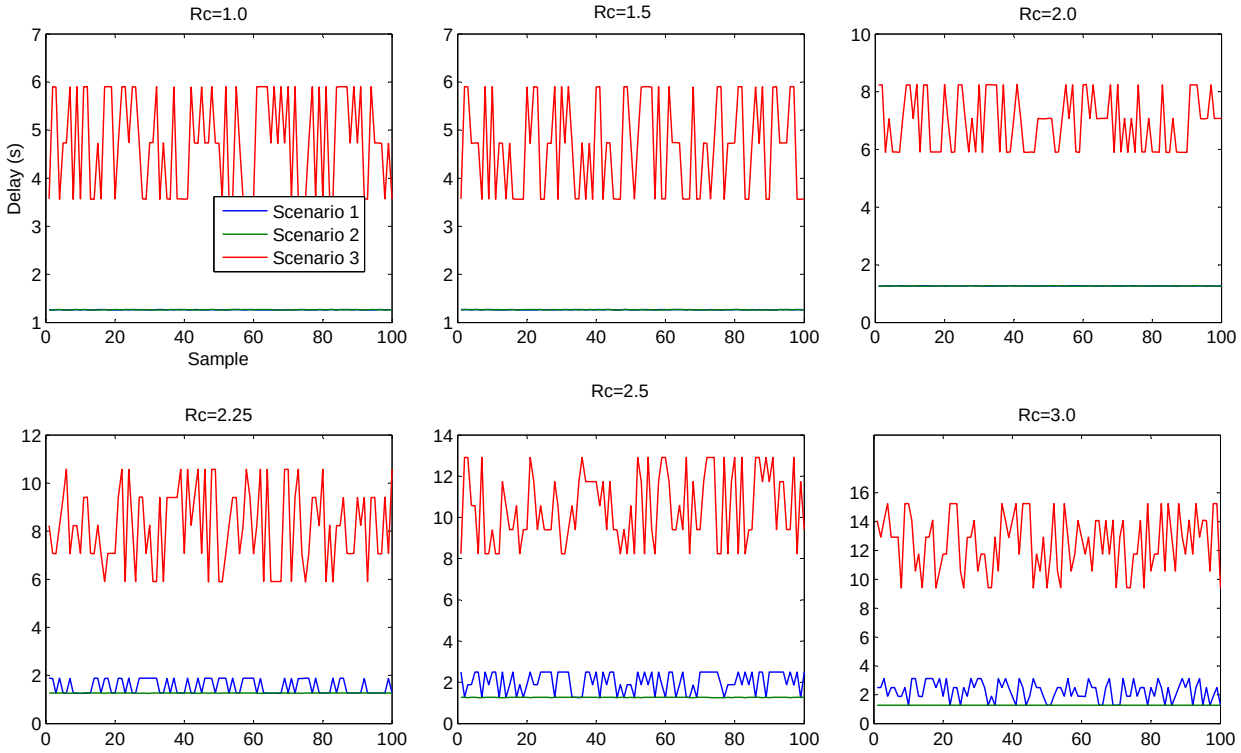


Figure 4.22: Delay for the three networks with different values of Rc in the joint algorithm

Since the joint algorithm is based on token based mechanism, the number of nodes in the network impacts directly on the delay. Accordingly, the network of scenario 3 requires much more time to finish the algorithm than the network 1 and network 2. In addition, higher value of Rc causes the delay prolong because each node requires more time to discover a larger number of neighbors in comparing to lower value of Rc with smaller number of neighbors.

Although, the MAC layer sets value of SO to be 2, random selection of same time slots to transmit ACK_NBR packets may cause collision. This in turn, influences on the delay since they need backoff delay to retransmit the packets successfully. Fig.4.23 shows the PLR for three networks performing the joint algorithm with different values of Rc. The simulation results indicate that higher value of Rc cause higher PLR.

Because within a higher communication range, a node can have more neighbors that in turn increase the packet collision during competition of ACK_NBR packet transmis-

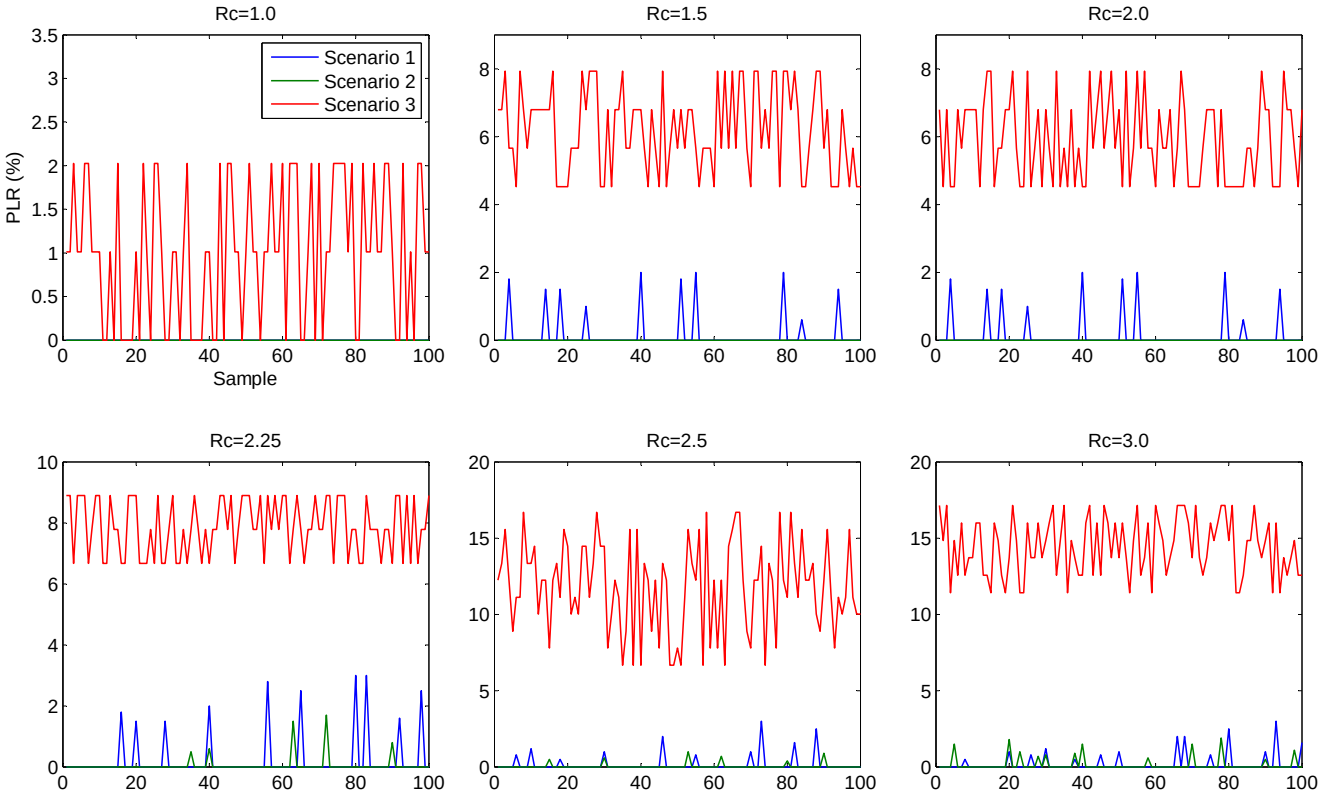


Figure 4.23: Corresponding PLR values for the 3 networks in the joint algorithm

sion. However, in overall, the PLR is quite low for all the simulation scenarios. This result can take advantage of networks in energy consumption since retransmission ratio of ACK_NBR packets is reduced significantly. Fig.4.24 depicts the simulation results in term of energy consumed by a specific node to run the joint algorithm. The energy is computed in percentage of the residual energy of the node. The simulation results lead to two main conclusions.

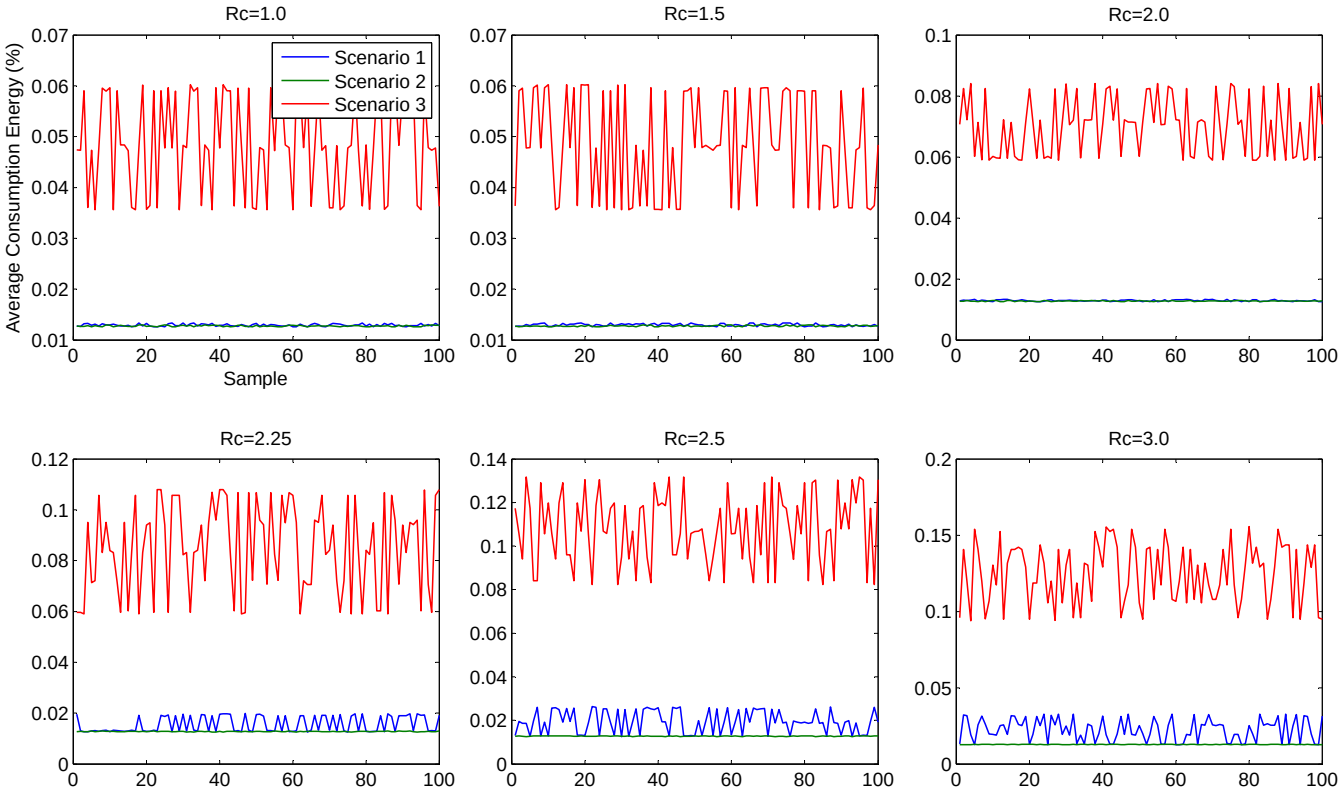


Figure 4.24: Consumption energy of a node in the three networks deploying the joint algorithm

Firstly, in the network having a larger number of nodes, the consumption energy of the node is higher. Accordingly, with the double number of nodes in the network, the consumption energy of nodes in the network 3 is much higher than that in the network 1, 2. The result is originated from following facts:

- In the network with larger number of nodes, one node may transmit or retransmit the ACK_NBR packets in many times since it can be more neighbors to request the packet transmission.

- Without deploying the duty cycle mechanism, the node consumes a higher energy since they must be maintain the listening mode for a longer time.

Secondly, using longer communication range, the consumption energy is higher. That is because it firstly configures a higher power level of transmission. In addition, it may have more neighbors that, in turns, leads to more transmission and/or retransmission of ACK_NBR packets. Longer delay required to discovery more neighbors cause the node to consume more energy during listening mode.

However, in general, only very small percentage of energy used to complete the joint algorithm is acceptable in the practical deployments.

### 4.2.3 Discussion

Despite a small number of nodes in the network, the good performance of the two proposed algorithms allows them to be deployed effectively in practical applications. The accurate data (number of $\pi$-containers, global neighbor lists, dimensions of $\pi$-containers) collected at the GW within a short duration and at low cost (low energy consumption) proves the statement. To verify the effectiveness of the algorithms, we conducted additional simulations as followings.

For the algorithms to count the number of $\pi$-containers, there is a case that the number is the maximum number of $\pi$-containers possibly placed in the H-container. Thanks to the modularity of containers, the GW can deduce a maximum number of nodes in the network which is equivalent to the maximum number of $\pi$-containers with the smallest size ($[1 \times 1 \times 1]$) filled fully inside the composite $\pi$-containers with the size ($[L_c \times W_c \times H_c]$). By mathematical calculation, the number ($N_{max}$) can be obtained by following equation:

$$N_{max} = L_c \times W_c \times H_c. \tag{4.2}$$

In our scenarios with the H-container size $[4 \times 3 \times 3]$, $N_{max}$ is equal to 36. Thus, the counting algorithm can stop if **list_nodes** reaches this number instead of waiting a stable duration. For examine the upper bound of the algorithm performances, the network consisting of $N_{max}$ nodes is simulated. Fig. 4.25 presents the performance of the algorithm for the GW to detect the $N_{max}$ nodes.

Due to a larger number of nodes in the network, the task of detecting all 36 nodes requires longer delay, thus higher consumption energy. Higher PLR is obvious since there are more nodes competing to reply ACK_CNT packets.

With the joint algorithm, in the case that the GW requires the global neighbor list for all values of Rc, the joint algorithm is implemented repeatedly. Fig.4.26 shows the simulation results in terms of delay, PLR and consumption energy. Certainly, when the

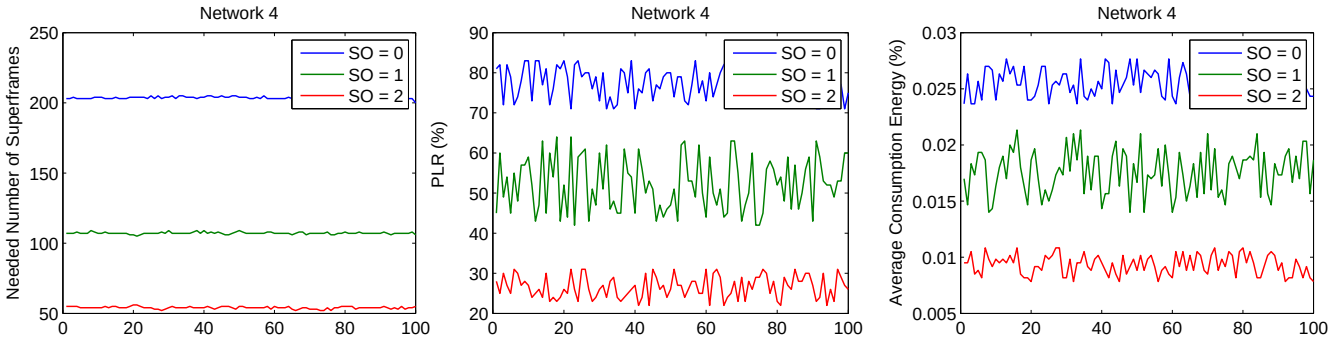


Figure 4.25: Performance of network 4 in counting algorithms

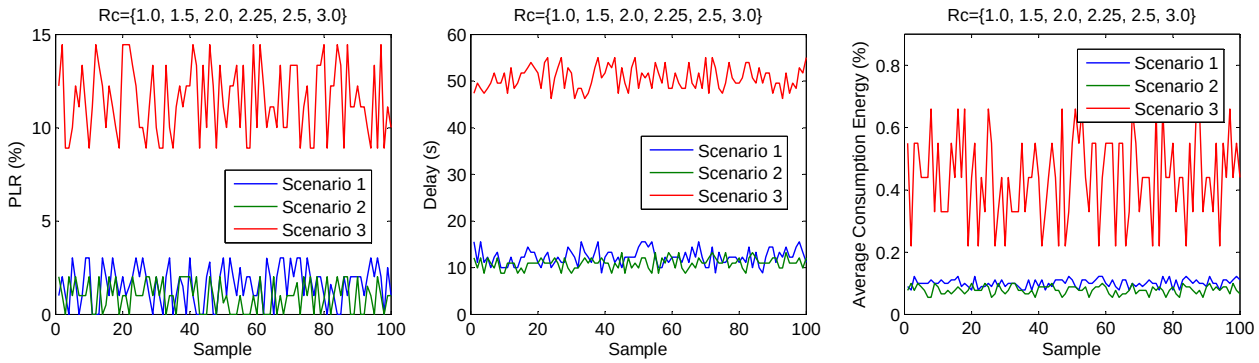


Figure 4.26: PLR, Delay and Average Consumption Energy for the three networks

neighbor discovery and neighbor table forwarding tasks are implemented continuously, the PLR is getting higher, the delay is longer and energy is consumed much more. However, in overall, the all task can be finished in acceptable cost (quite low delay, small percentage of consumption energy) that is adaptable to the logistic environment.

## 4.3 Simulation Results and Discussion for CSP performances

In the stage of CSP solving, the results are presented to analyze the conformity of the 3D layout with the real layout of $\pi$-container spatial arrangement predefined as Fig. 4.2.

### 4.3.1 Simulation Results

The corresponding 3D layouts are virtualized from the solutions of the CSP which distinguished into match solution and feasible solution (Fig. 4.27). The former indicates that the values of variables after solving the CSP are identical to that of the predefined layout. Meanwhile the latter represents other possible ways for arranging the unitary $\pi$-containers so that they satisfy all the stated constraints.

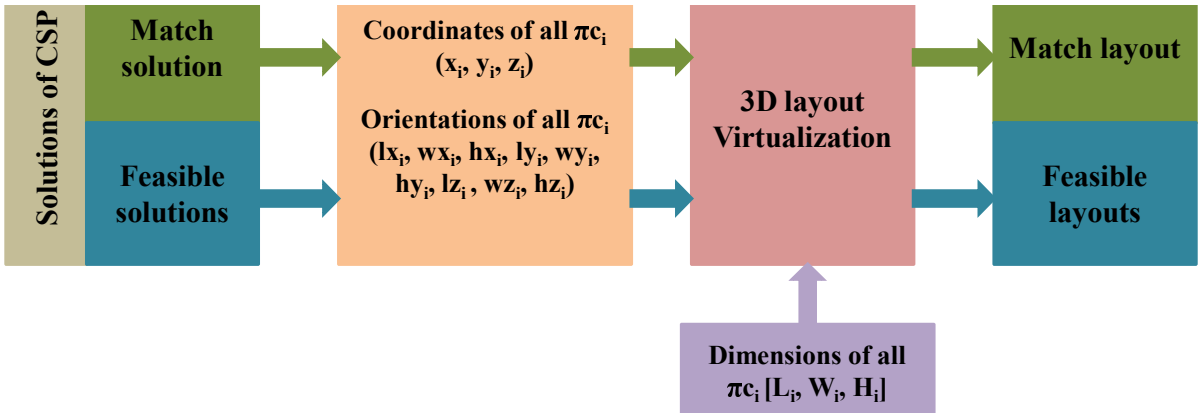


Figure 4.27: Virtualizing 3D layouts from solutions of the CSP

Table 4.7 summaries the simulation results of solving the CSP taken in three scenarios with a set of different values Rc (Rc=1, 1.5, 2, 2.25, 2.5, 3).

The results show number of solutions to the CSP and corresponding time durations of simulation. In majority of simulations cases, there are many solutions obtained for each value of Rc. However, unique solutions can be found for the scenarios with specific value of Rc. For example, when Rc is equal to 2.25 and 2.5 in the scenario 1 and 2 respectively,

| Normalized Rc | Scenario 1 | | Scenario 2 | | Scenario 3 | |
|---|---|---|---|---|---|---|
| | Number of Solutions | Simulation Time (Seconds) | Number of Solutions | Simulation Time (Seconds) | Number of Solutions | Simulation Time (Seconds) |
| 1 | 492 | 236 | 2776 | 575 | 720 | 5894 |
| 1.5 | 24 | 37 | 720 | 288 | 248 | 1985 |
| 2 | 2 | 0.8 | 12 | 8.6 | 2 | 15.5 |
| 2.25 | **1** | 0.5 | 5 | 7.1 | 2 | 2953 |
| 2.5 | 4 | 2.9 | **1** | 4.9 | 5688 | 18232 |
| 3 | 180 | 75.8 | 322 | 187 | 5688 | 18232 |

Table 4.7: The number of solutions and corresponding simulation time periods of algorithms for three scenarios with different values of normalized Rc

the 3D layouts virtualized are representative to the real ones as shown in Fig.4.28a and Fig.4.28b). In addition, a running time inferior to 5 seconds shows that our proposed method yields quick and satisfactory results.

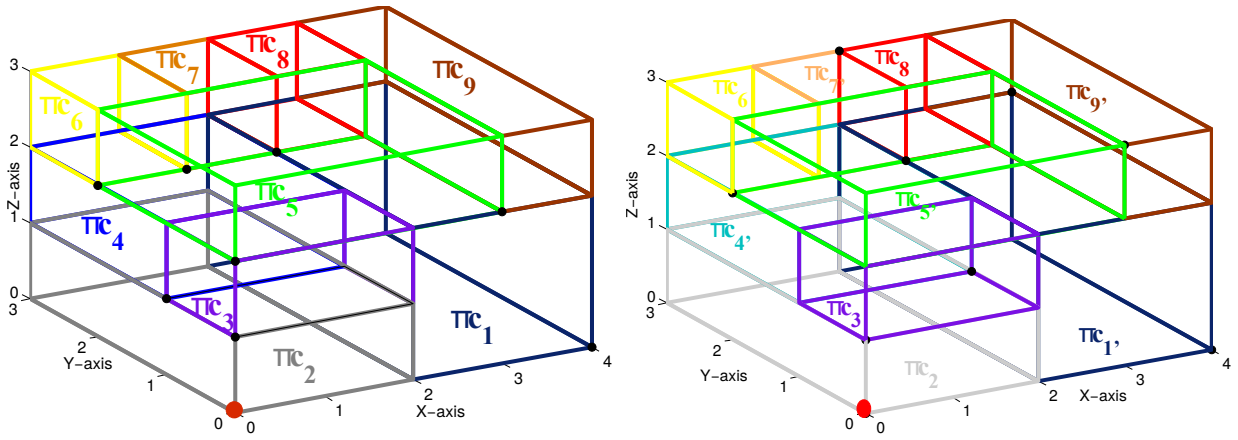


(a) Solution of model 1 when Rc=2.25 (b) Solution of model 2 when Rc=2.5

Figure 4.28: The match 3D layouts are constructed from the corresponding unique solutions to the CSP in the scenarios 1 and 2 respectively

For all the 6 values of Rc used for the scenario 3, we obtained a minimum number including two solutions (Fig.4.29a and Fig.4.29b) when Rc is equal to 2 and a corresponding running time inferior to 15 seconds.

The time is satisfactory but the neighborhood information is not sufficient to determine the unique layout. Although Fig.4.29a shows the real composition of the composite $\pi$-container, the same set of constraints is being respected with the obtained stacking

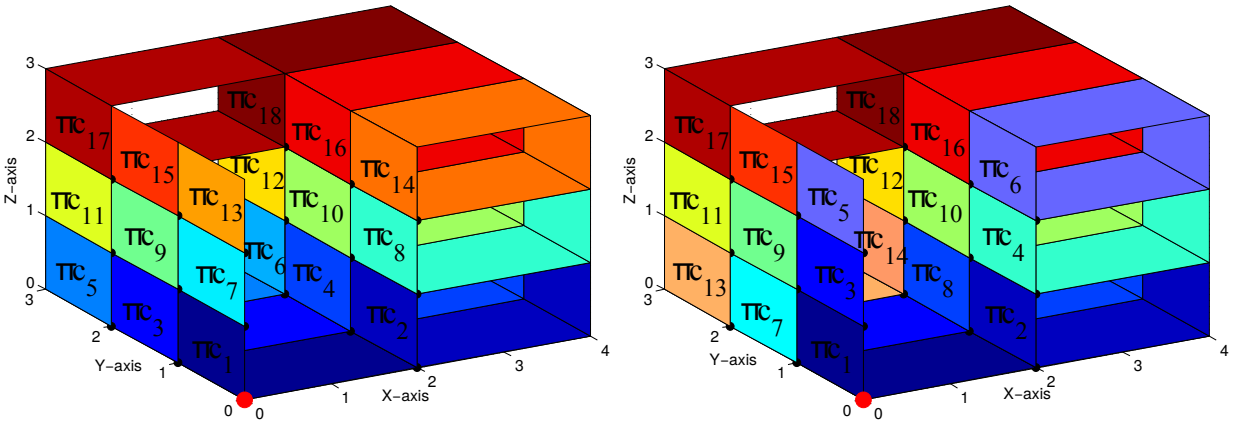


(a) Solution 1 of model 3

(b) Solution 2 of model 3

Figure 4.29: Solution of model 1 and 2 when Rc=2

Fig.4.29b. This can be explained by the homogeneity set of $\pi$-containers and the orientation constraints which leads to a distribution of the sensor nodes as a regular grid. Thus, positions of some $\pi$-containers can be displaced without violating the constraints of the CSP. For example, in the second solution (Fig.4.29b), position of $\pi c_3$ and position of $\pi c_7$ are displaced in comparing with the real layout shown in Fig.4.29a.

### 4.3.2 Discussion

#### Impact of Rc on number of solutions of CSP

In order to investigate the simulation results effectively, a connectivity graph replacing the neighbor relations between the sensors in the network is used. According to the graph theory introduced in [119], the graph $(G = V, E)$ includes two components: a set of vertices $(V = v_i, \forall i = 1 \ldots n)$ and a set of edges $(E = e_{ij}, \forall i, j = 1..n \& i \neq j)$ connecting the vertices. The two components represent a set of sensors and a set of wireless communication links between sensors respectively. The graph indicates connectivity level of sensors in network representing by number of edges and number of isolated vertices. The graph is connected when there is a path between every pair of vertices. In contrast, when there is a vertex isolated from the other vertices, the graph is disconnected. In addition, if two or more vertices are isolated, the graph is called an edgeless graph. From Table 4.7, the computational time and the number of solutions increase with Rc close to 1 or 3. This can be explained when we observe the neighbor graphs corresponding to communication ranges, as depicted in Fig. 4.30, Fig. 4.31, Fig. 4.32, Fig. 4.33, Fig. 4.34, Fig. 4.35.

In the first case (Rc=1), the neighbor graphs are disconnected. A lot of vertices are isolated (with no edges connected) in the scenario 1 and 2. The scenario 3 shows a

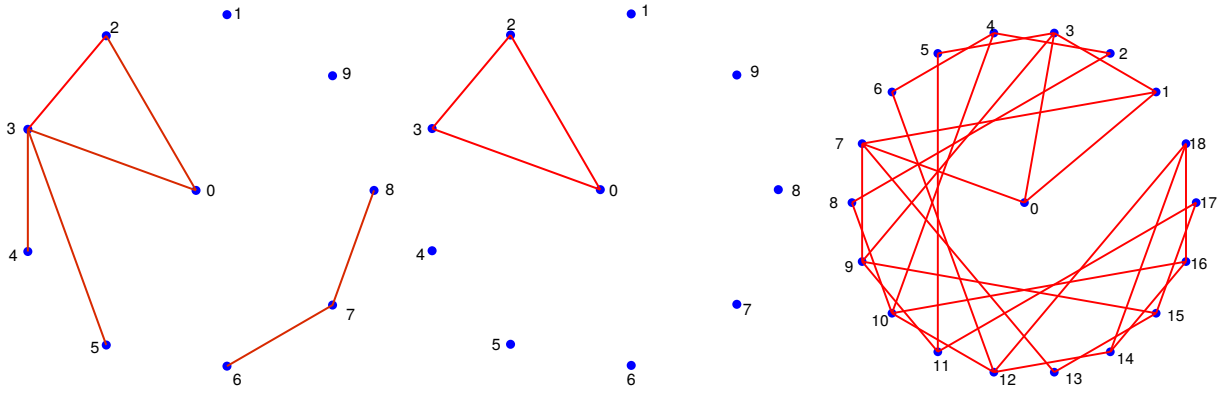

(a) Scenario 1 (b) Scenario 2 (c) Scenario 3

Figure 4.30: Connectivity Graph for 3 scenarios with $Rc = 1.0$

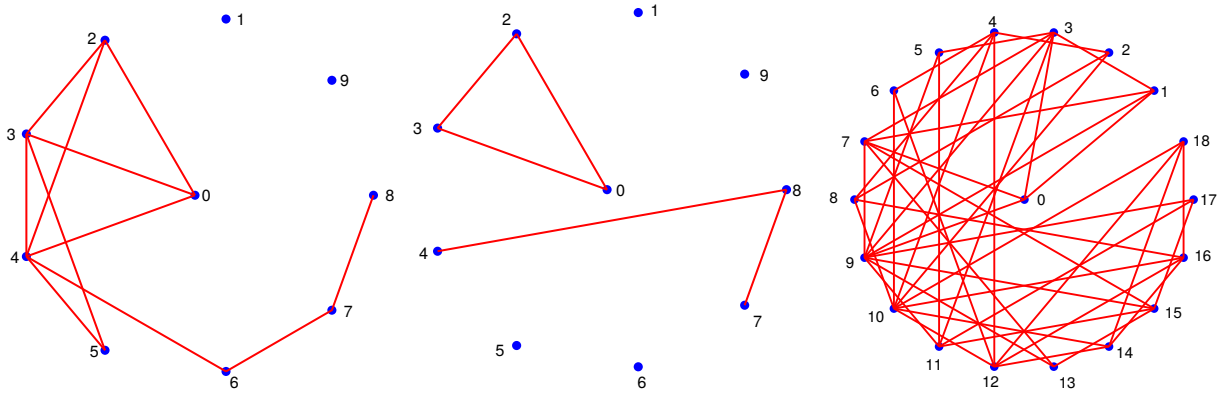

(a) Scenario 1 (b) Scenario 2 (c) Scenario 3

Figure 4.31: Connectivity Graph for 3 scenarios with $Rc = 1.5$

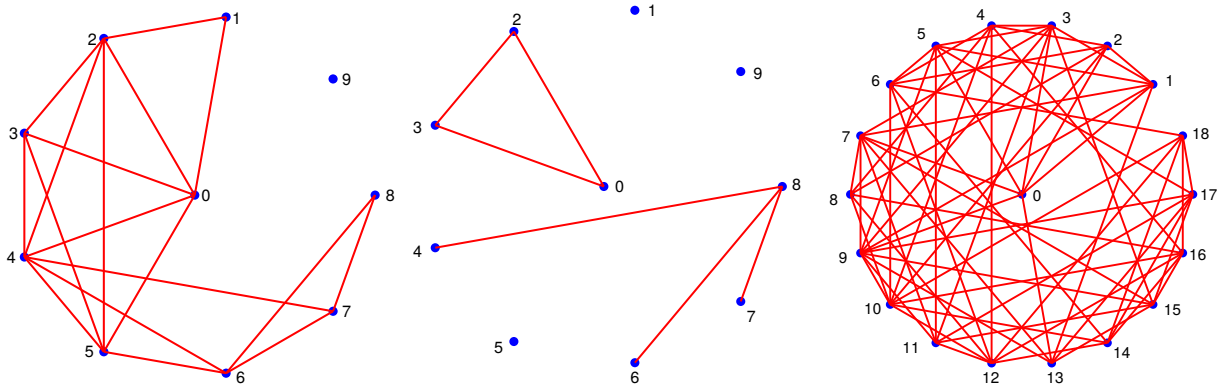

(a) Scenario 1 (b) Scenario 2 (c) Scenario 3

Figure 4.32: Connectivity Graph for 3 scenarios with $Rc = 2.0$

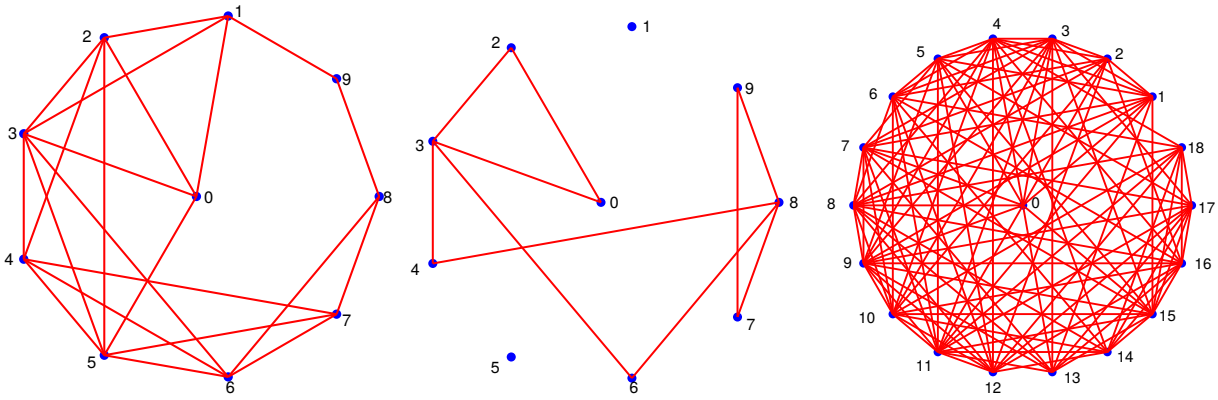

(a) Scenario 1 (b) Scenario 2 (c) Scenario 3

Figure 4.33: Connectivity Graph for 3 scenarios with $Rc = 2.25$

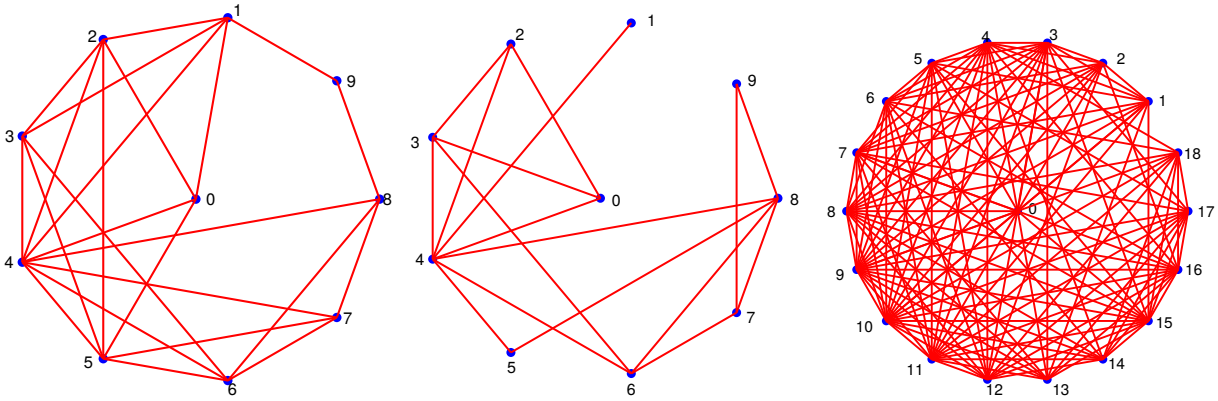

(a) Scenario 1 (b) Scenario 2 (c) Scenario 3

Figure 4.34: Connectivity Graph for 3 scenarios with $Rc = 2.5$

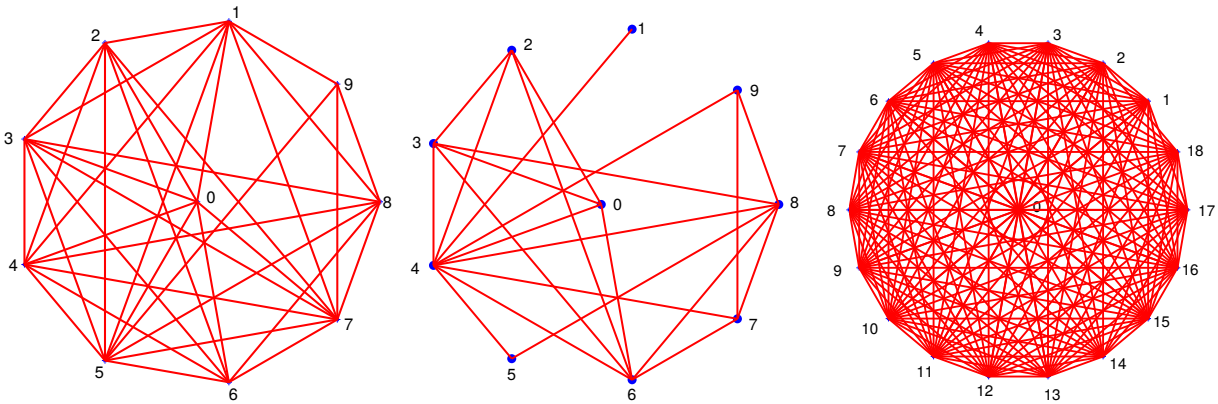

(a) Scenario 1 (b) Scenario 2 (c) Scenario 3

Figure 4.35: Connectivity Graph for 3 scenarios with $Rc = 3.0$

disconnected graph with 2 connected components. Conversely, all vertices are strongly connected with a value of Rc=3. For these values of Rc, the neighborhood graphs are not relevant to reduce the research space, thereby increasing the number of solutions and the running time.

Obviously, for different values of Rc leads to different neighbor tables for each sensor, and then different connectivity graph of network. Fig.4.36 illustrates the curve showing the impact of Rc on number of solutions of the CSP.

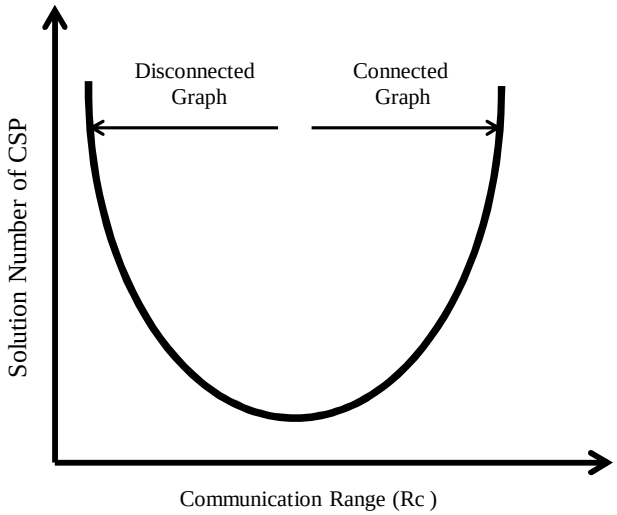


Figure 4.36: Impact of Rc on number of solutions to the CSP

The curve represents the above statement that the connectivity of the neighbor graph influences the solving of the CSP problem. Fig.4.37 illustrates the scaled connectivity and the connectivity properties (i.e. connected or disconnected) of the neighborhood graphs for different communication ranges.

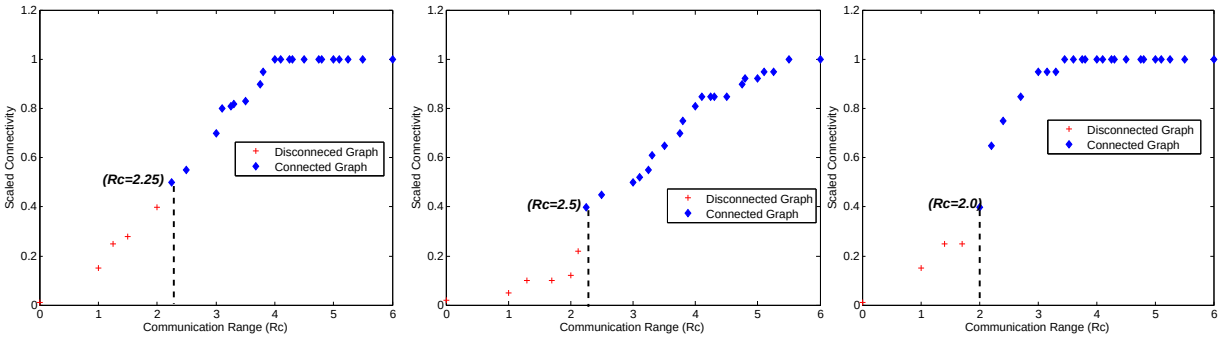


(a) Network 1 (b) Network 2 (c) Network 3

Figure 4.37: Scaled connectivity of networks versus different values of *Rc*

We can observe that the best results (minimum solutions found) for each scenario are obtained with a minimum connected graph. This interesting result could be exploited in our approach to create pertinent and sufficient neighborhood constraints, and deduce the virtual 3D layout of the composite $\pi$-container. Before to execute the CSP, the gateway could validate the relevance of the global neighbor graph and select an appropriate (Rc) so that unique solutions or a little number of solutions can be obtained.

## 4.4 Conclusion

In order to examine the performance of our proposed methodology, we conducted several simulations for three scenarios. The simulation results show that low delay for aggregation of WSN algorithms and CSP resolution demonstrates that it is feasible to obtain 3D layout in a reasonable time and with a unique solution in lot of case. In addition, different networking performances such as PLR and energy consumption indicates that the proposed algorithm can be effectively applied in real scenarios with proper conditions set up for networks.

One of expectations of the proposed methodology is to obtain the unique solution to the CSP which then leads to retrieve the match layout. Although there exists optimal values of Rc by which the unique solution is obtained, in majority of cases there are multiple solutions to the CSP. In other words, the constraints about relative positions between the unitary $\pi$-containers are not a sufficient condition to reach only one solution to the CSP. Thus, in order to obtain the real layout, two solution directions can be developed as followings: (1) develop more constraints to increase the tightness of the CSP; (2) Develop way to extract the real layouts from all the layouts constructed after solving the CSP. These solutions are discussed more in Chapter 5 on the pespectives.

# Chapter 5

# Conclusions and Perspectives

## Contents



In this chapter, we conclude our dissertation by firstly highlighting the main contributions and then discussing perspectives relating on the applications of the proposed methodology for the Physical Internet realization.

## 5.1 Conclusions

Despite the huge contributions to development of areas (i.e, economy, education, transportation, etc.), the current logistics operations still face the grand challenge termed as the unsustainability in all three perspectives: environment, economy and society. In order to deal with the issue, many logistics paradigms are proposed such as intelligent logistics, green logistics, reverse logistics and physical internet. Among them, the Physical Internet is potentially expected to replace the current logistics since it, by proof-of-concept, allows the physical objects to be transported, handled, stored, realized, supplied and used through the world efficiently and effectively. Based on this vision, we focus on realizing the Physical Internet defined as an open global logistics system in the future via modular container, standardized interfaces and protocols.

One of the key enablers of the PI is $\pi$-containers characterized by modularity, smartness, being green and world standard. Replacement of modular $\pi$-containers with the tra-

ditional boxes benefits in easily creating efficient unit loads (composite $\pi$-containers). The universal interconnection causes the Physical Internet become a highly dynamic transport and logistic system in which composite $\pi$-containers can be quickly set up and/or modify in order to increase the sustainability and efficiency of the global logistics chain. However, the dynamic nature of logistics activities requires composing/decomposing/loading/unloading processes to be fast. That, in turn, are prone to error in arranging $\pi$-containers ruled by predefined layouts. Consequently, such a system requires a perfect synchronization between the physical and informational flows. We consider this requirement as a challenge to meet in the Physical Internet operations.

In general, the identification and localization of stacked $\pi$-containers in a composite $\pi$-container can help to maintain the traceability information, and thus contribute to the control of the Physical Internet in real-time manner. Many advanced technologies can be used to provide the services such as RFID, positioning systems with both indoor and outdoor environment based on wireless networks. We surveyed in this dissertation all the position systems based on wireless technologies (i.e., light, RF, ultrasound) that aim at determining the position of objects in traditional applications. Depending on the way to use the wireless signal, two classes of positioning techniques: range-based and range-free are deployed in the systems. The range-based method translates the wireless signal into the absolute distances between the target and the reference points and uses them to compute the position of target. Meanwhile, the range-free method exploits the proximity information extracted from the wireless signals for positioning the target. On the performance, the first method obtains the more accurate position but it requires professional hardwares for ranging.

In the Physical Internet, since $\pi$-containers are proposed to be equipped with wireless sensors to provide the intelligence, they can be exploited in wireless communication signals to deploy the positioning services. However, the signals can be impacted negatively by obstacles (i.e., cover of $\pi$-containers) or high interferences caused by a huge number of sensors, the proximity information is suitable to be exploited in this manner to position the $\pi$-containers. Based on this, in this thesis, we described our work on the design of an auto-managed system for localizing $\pi$-containers inside composite $\pi$-containers by dynamically generating and maintaining a virtual 3D layouts of the composite $\pi$-containers. The layouts are retrieved from the solutions of a CSP composed of the traditional geometrical constraints from the container loading problems and the relative position constraints of $\pi$-containers resulted from the corresponding proximity information. In order to formulate the relative position constraints, we proposed two algorithms applying for the network of sensor nodes: (1) The counting algorithm is to count the number of $\pi$-containers inside the composite container; (2) The joint algorithm is to obtain the local neighbor lists of nodes

within a communication range Rc and forwards all the lists to the GW. The function of the GW is to generate the global neighbor list showing all the relationships among nodes or relative positions among $\pi$-containers.

To examine the performance of our proposed methodology, we conducted a series of simulations on both the networking perspective and CSP resolution. The three different scenarios representing the predefined layouts and deployment of sensor nodes are described in all the simulation cases. In the networking performances, the simulation results show that the two algorithms can be adapted to the Physical Internet environment since they can obtain the accurate data (i.e., number of $\pi$-containers and the global neighbor list) in a short duration of time and at acceptable cost (i.e., low energy consumption). Meanwhile, results from the CSP solving show that number of solutions is influenced by value of Rc. One conclusion can be found that our CSP can only one solution if a suitable value of Rc is chosen. This value is intended to be a future perspective. The unique solution means that the corresponding layout is in conformity with the real layout. Thus when we retrieve the layout it provides the visual view of arrangement of $\pi$-containers inside compact $\pi$-containers or composite $\pi$-containers. Thank to this layout, the location and information of unitary $\pi$-containers and thus corresponding products are provided when requested. As a proof-of-concept, the proposed approach and model have been validate through computational experiments. The experiment results show that the virtual 3D layout reflecting the spatial distribution can be obtained within a reasonable amount of time. Particularly, under the optimal conditions, our system requires a few seconds to generate a 3D layout. Notably, this delay includes the delay for execution of the two algorithms to derive the neighborhood information and the running time to solve the CSP. This approach can be applied to provide up-to-date information (permanent inventory), as well as detect any error during the encapsulation process, which might have a negative impact on the overall effectiveness and efficiency of the Physical Internet. Furthermore, new value-added services such as guidance information for loading/unloading systems can be developed.

## 5.2 Perspectives

The proposed methodology is modeled and developed under exploitation of wireless sensor network. The aim of the methodology finally is to retrieve the 3D layouts reflecting the real arrangement of $\pi$-containers inside H-containers for solutions of CSP model. In this section, we discuss some perspectives relating to performance of WSN algorithms, CSP. Furthermore, potential applications of 3D layouts can indicated as future work development.

### 5.2.1 WSN Algorithms and Perspectives

Although the proposed algorithms deployed for WSNs obtained the good results in terms of delay, energy efficiency, they can be improved in order to adapt efficiently in the very dynamic environment of the PI network. For example, the delay can be reduced if we use the consensus algorithm for counting [120]. However, the complexity of algorithm causes the sensor network increase the processing cost. The future perspective can be to apply and verify this alternative to examine its performance when the size of networks (i.e., number of nodes) can be increased.

In the joint algorithm combining the neighbor discovery and neighbor table forwarding, we proposed to deploy the token mechanism aiming for the GW to obtain the accurate global list of neighbors with a communication range Rc. This scheme can be applied effectively in the small-scale network since it requires low delay to obtain the target. However, in large-scale network with a large number of sensor nodes corresponding to a large number of $\pi$-containers distributed in a T-container, the algorithm can be prevented from applying because it can take a long time to finish the task (see Section 5.2.3). In this case, distributed algorithms should be developed and applied to allow sensor nodes perform the task simultaneously. One of perspective is to consider and develop these algorithms as well as examine their performance.

In our two proposed algorithms, the sensor nodes execute their tasks without deployment of duty cycle mechanism at MAC layer, that in turn, leads to the sensor nodes to consume more energy. This limitation can prevent the algorithms from deploying in the practical applications since the all sensor nodes are powered by un-rechargeable batteries. Therefore, one of the most important perspectives is to improve the performance of proposed algorithms in term of energy efficiency. Deployment of duty cycle mechanism allows sensor nodes to save their energy during their sleeping modes. Depending on the applications, the cycles can be adjusted properly, however, a synchronization scheme for waking-up sensor nodes properly is required to be developed simultaneously. That, in turn can prolong the delay of the algorithm execution since the nodes require their own time duration to transform among states (i.e., sleeping, active).

The good performance of the proposed algorithms in terms of delay, energy efficiency potentially enables them to be implemented in real case. In this scenario, the sensor motes (i.e., Micaz, TelosB) can be attached to the real $\pi$-containers designed by MODULUSHCA. Thus, the real performance of WSN with the proposed algorithm can be examined under the impact of real conditions (i.e., interference, noise and obstacles). As a future work, We are planning to develop real testbed aiming for obtaining the 3D layout to support automated depalletization (see Section 5.2.3).

### 5.2.2 CSP Performance and Perspectives

One of expectation of our methodology is to obtain the unique layout matching with the real layout. For the most of simulation cases conducted in Chapter 4, the CSP have multiple solutions. In these cases, recognizing the real layout becomes a challenge, especially in the cases a lot of feasible solutions are found. To overcome this problem, we propose here potential solutions

#### Matching Verification

Usually, multiple solutions of the CSP come from the two possibilities: the rotation ability and position changes of the unitary $\pi$-containers. The both commonly lead to change of sensor coordinates. In other word, the connectivity graphs before/after simulation can be changed with different values of $Rc$. The observation motivates to the way to find out layouts among the obtained layouts by using the connectivity graphs. Fig.5.1 illustrates an example which creating the connectivity graph by two ways: before and after simulation with $Rc = Rc_1$. Obviously, the two created graphs are identical since the graphs are built from the solutions of the CSP.

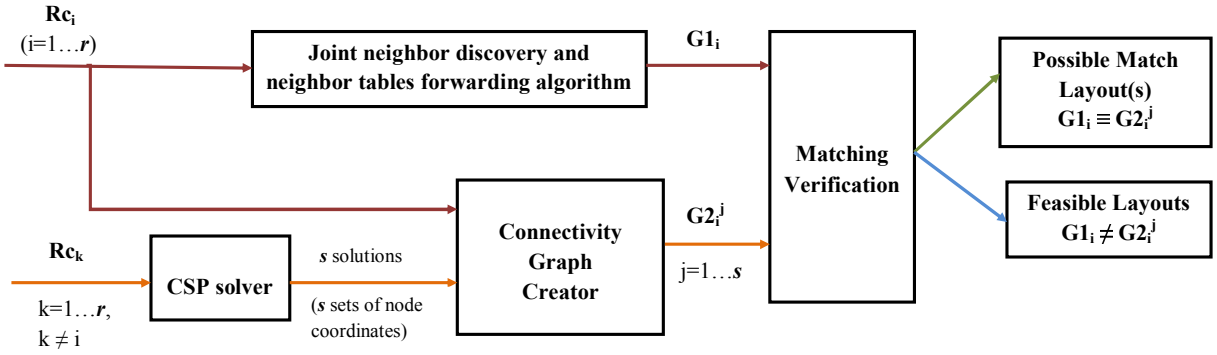


Figure 5.1: The matching verification process using different values of $Rc$ to recognize possible match and feasible layouts obtained from $\boldsymbol{s}$ solutions of the CSP when $Rc = Rc_k(k \neq i)$

For illustration of the matching verification algorithms, the scenario 3 which has 2 found solutions when Rc is equal to 2 is analyzed. Table 5.1 presents the two solutions.

Fig.5.2 and Fig.5.3 show the connectivity graphs in the matching process to differentiate the match and feasible layouts.

The matching process described above can be used effectively to extract the match layout from the all constructed layouts. However, it can face a challenge when it may

| $\pi c_i$ | Oriented Dimensions $[L_i \times W_1 \times H_i]$ | Solution 1 Coordinates $(x_i, y_i, z_i) = (x_{ni}, y_{ni}, z_{ni})$ | Solution 2 Coordinates $(x_i, y_i, z_i) = (x_{ni}, y_{ni}, z_{ni})$ |
|---|---|---|---|
| $\pi c_1$ | $[2 \times 1 \times 1]$ | $(0, 0, 0)$ | $(0, 0, 0)$ |
| $\pi c_2$ | $[2 \times 1 \times 1]$ | $(2, 0, 0)$ | $(2, 0, 0)$ |
| $\pi c_3$ | $[2 \times 1 \times 1]$ | $(0, 1, 0)$ | $(0, 0, 1)$ |
| $\pi c_4$ | $[2 \times 1 \times 1]$ | $(2, 1, 0)$ | $(2, 0, 1)$ |
| $\pi c_5$ | $[2 \times 1 \times 1]$ | $(0, 2, 0)$ | $(0, 0, 2)$ |
| $\pi c_6$ | $[2 \times 1 \times 1]$ | $(2, 2, 0)$ | $(2, 0, 2)$ |
| $\pi c_7$ | $[2 \times 1 \times 1]$ | $(0, 0, 1)$ | $(0, 1, 0)$ |
| $\pi c_8$ | $[2 \times 1 \times 1]$ | $(2, 0, 1)$ | $(2, 1, 0)$ |
| $\pi c_9$ | $[2 \times 1 \times 1]$ | $(0, 1, 1)$ | $(0, 1, 1)$ |
| $\pi c_{10}$ | $[2 \times 1 \times 1]$ | $(2, 1, 1)$ | $(2, 1, 1)$ |
| $\pi c_{11}$ | $[2 \times 1 \times 1]$ | $(0, 2, 1)$ | $(0, 1, 2)$ |
| $\pi c_{12}$ | $[2 \times 1 \times 1]$ | $(2, 2, 1)$ | $(2, 1, 2)$ |
| $\pi c_{13}$ | $[2 \times 1 \times 1]$ | $(0, 0, 2)$ | $(0, 2, 0)$ |
| $\pi c_{14}$ | $[2 \times 1 \times 1]$ | $(2, 0, 2)$ | $(2, 2, 0)$ |
| $\pi c_{15}$ | $[2 \times 1 \times 1]$ | $(0, 1, 2)$ | $(0, 2, 1)$ |
| $\pi c_{16}$ | $[2 \times 1 \times 1]$ | $(2, 1, 2)$ | $(2, 2, 1)$ |
| $\pi c_{17}$ | $[2 \times 1 \times 1]$ | $(0, 2, 2)$ | $(0, 2, 2)$ |
| $\pi c_{18}$ | $[2 \times 1 \times 1]$ | $(2, 2, 2)$ | $(2, 2, 2)$ |

Table 5.1: Coordinates of $\pi$-containers and associated sensors for the scenario 1

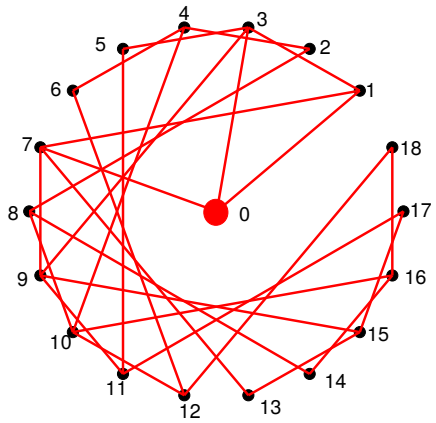


(a) The connectivity graph of scenario 3 obtained from the joint algorithm

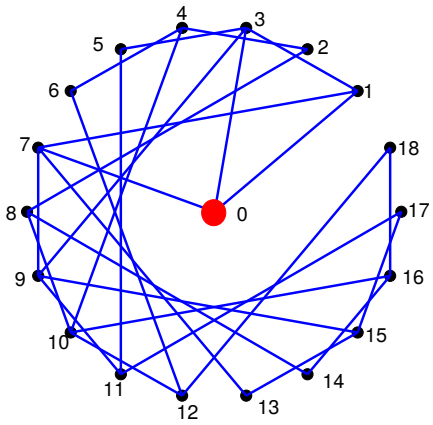


(b) Solution 1 of scenario 3

Figure 5.2: The matching verification scheme proves that solution 1 is the match one since the two connectivity graphs with Rc=1 are identical

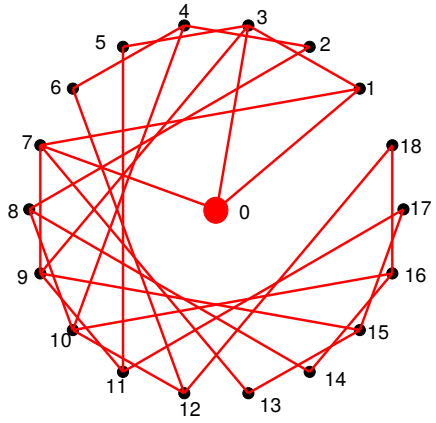


(a) The connectivity graph of scenario 3 obtained from the joint algorithm

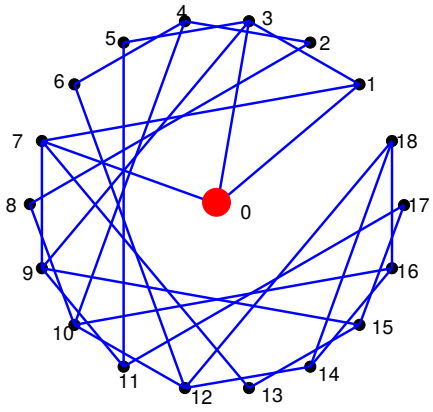


(b) Solution 2 of model 3

Figure 5.3: The matching verification scheme proves that solution 2 is a feasible one since the two connectivity graphs with Rc=1 are different (node 14 and 18 is connected in the graph of solution 2, meanwhile they are disconnected in reality

require to use more additional values of Rc. In other words, the WSN executes the algorithms more times to obtain different proximity constraints. To deal with the issues, we present followings two solutions that can be developed in the future.

#### Domain Filtering

For the scenario 3, we obtained a minimum of two layouts (Fig.4.29a and Fig.4.29b) with R=2 and a computational time inferior to 15 seconds. The time is satisfactory but the neighborhood information is not sufficient to determine the unique layout. Although the Fig.4.29a shows the real composition of the composite $\pi$-container, the same set of constraints is being respected with the obtained stacking Fig.4.29b. This can be explained by the homogeneity set of $\pi$-containers and the orientation constraints which leads to a distribution of the sensor nodes as a regular grid. To overcome this problem, a domain filtering was developed to identify a unique layout. The successive operations (described in Section 3.3) are executed twice to obtain a new neighborhood graph. This can be achieved from the gateway node with a different transmission range, or by using a second gateway fixed to the composite $\pi$-container. The information is used to filter the space of possible solutions where each solution must fit with the two neighborhood graphs. For instance, a second gateway at the front-left top corner of the composite $\pi$-container (scenario 3) can be used to generate new neighbor constraints between the gateway and the $\pi$-container 13. Hence the solution 2 (Fig.4.29b) would be eliminate and the unique layout will be obtained without increasing the computational time. Consequently, the CSP is expected to have less number of solutions or the unique solution in the best performance. However, more cost of network (i.e., delay, energy consumption) is resulted in since they have to to execution of the two proposed algorithm for different values of Rc.

### 5.2.3 Applications and Developed Services of Layouts

Utilization of feasible layouts for other applications is other aim of the proposed methodology. Our future perspectives can be based on 3D layouts to develop added-value services that can improve the performance of the PI network.

#### Permanent checking and management of inventory

Due to the 3D layouts can be obtained automatically or on-demand ubiquitously, these can be used as effective tools to check the inventory at different time in the logistics supply chain, for example, input inventory before storing in the warehouses, output inventory during handling and transportation.

### Security

Whenever wrong $\pi$-containers are composed and placed inside a H-container, they can cause inefficiency of the logistics operations since it requires additional costs (i.e., time, labor cost, logistics costs) to correct the mistake $\pi$-containers. To avoid this issues, the accurate 3D layouts can be used effectively to check validations of $\pi$-containers before their composite $\pi$-containers are moved, stored, handled or transported.

In addition, deploying the sensor with capability of sensing environment conditions, the 3D layouts can provide the map illustrating the distributions of environment parameters such as temperature, humidity level inside the H-containers. This information allows the conditions inside the containers to be monitored in real time and the contents of $\pi$-containers are kept under the best conditions.

### Automated Depalletization

In another applications, the 3D layouts can used to guide the robots or human operators in partially unloading, picking, decomposing. Fig.5.4 illustrates an example to use the 3D layouts to guide the operators in unloading partial $\pi$-containers efficiently.

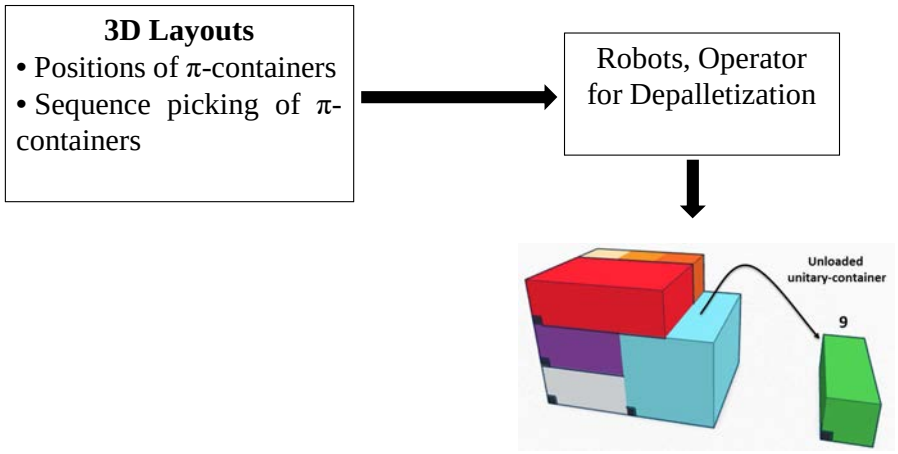


Figure 5.4: The outermost $\pi$-container 9 will be loaded first during depalletization process thanks to the 3D layout

### Extension of methodology in other levels of encapsulation

We can extend our proposed methodology to retrieve the 3D layouts for different levels of encapsulation. Fig.5.5 illustrates the ability of our model in application with $\pi$-pallet (Fig.5.5(a)) and T-container encapsulation (Fig.5.5(b)).

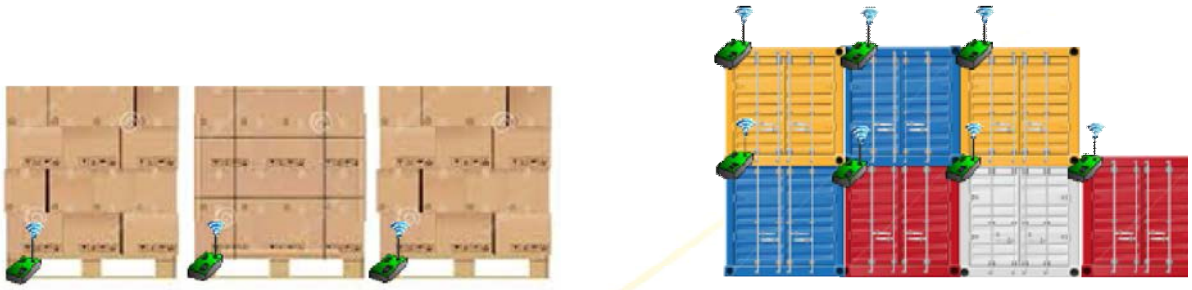

(a) π-Pallet Level (b) T-container Level

Figure 5.5: The methodology can be extended and developed in different levels of encapsulation

In fact, the $\pi$-pallets are equivalent to the H-containers, however, their heights are standardized differently depending on their ability of stackability. Therefore, given the acceptable heights, the 3D layouts illustrating the spatial stacking of P-containers on the $\pi$-pallets can be retrieved. that are composed of sets of H-containers. However, the performance of methodology should be examined under some challenges. Firstly, H-containers can be made by metallic material that prevents communication between sensor nodes, thus the proximity information can be impacted negatively. To deal with this problem, deployment of sensor nodes must consider the line of sight of RF antenna. This design, therefore, involves the physical size of sensor nodes as well as the structure of $\pi$-containers. Nowadays, the advanced technologies, particularly advanced material can make sensor motes with small size, or event at nano scale, micro scale (i.e., nano-sensors, micro-sensors) but their capacity is improved (i.e., communication, storage, processing, etc). The tiny sensors can be embedded physically into the material making the cover of $\pi$-containers. However, performance of this kind of sensor networks in term of networking must be verified [121], [122].

# Appendix A

# Communication Range Controlled by Transmission Power

## Contents



## A.1 Testbed: Communication Range Control by Transmission Power

The communication range (Rc) of sensors depends on the output power of RF. We use Micaz platform [47] to perform experiment testbeds. The mote supports 31 levels of transmission power, then 31 corresponding ranges of Rc. The experiments are conducted related to spatial distance of two sensor motes, saying mote $\boldsymbol{i}$ and mote $\boldsymbol{j}$ in all experiment scenarios, (corresponding to the real case of spatial distribution of sensors of $\pi$–containers) in indoor computer laboratory environment. The two motes are configured as follows: mote $\boldsymbol{j}$ fixed by connecting to a PC functions as a recipient, while mote i varies the transmission power levels and transmits the signal periodically. Then mote $\boldsymbol{i}$ is mobile to measure the maximum range that it can communicate mote $\boldsymbol{j}$ for each power level. Whenever mote $\boldsymbol{j}$ receives messages from mote $\boldsymbol{i}$, its red LED is toggled and the PC displays parameters relating to the received signals such as RSSI (Received Signal Strength Indicator) and LQI (Link Quality Indicator).

Depending on the environment between the two motes, the communication range,

[47] MicaZ mote, http://www.memsic.com/userfiles/files/Datasheets/WSN/micaz_datasheet-t.pdf

hence the parameters are impacted. To investigate the influences, we implement a series including 8 experimental tests for 4 testbeds (two similar tests for each testbed to verify the stability of wireless signal). Fig.A.1 and Fig. A.2 show the deployment of Micaz motes for experiment.

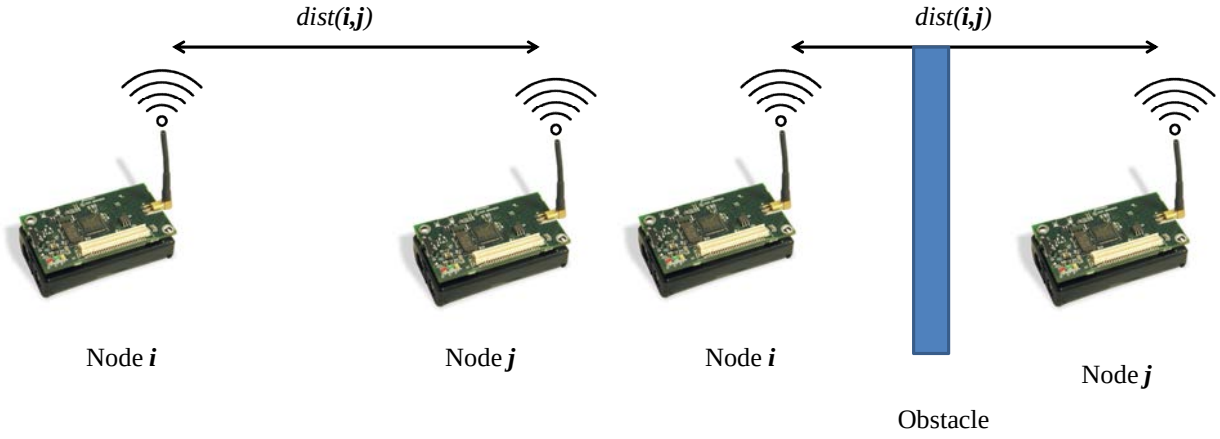


(a) Testbed 1 (b) Testbed2

Figure A.1: Testbed models of model 1 and 2

Fig.A.1(a) describes the device setup of the testbed 1 in which the wireless signal of two motes is propagated in the environment with Line-of-Sight (LOS) characteristics and no interference caused by other sensor motes around. Meanwhile, as shown in Fig.A.1(b), the two modes are separated by an obstable which causes Non Line-of-Sight (NLOS) for the radio propagation. In addition, no interference is assumed to be available in this testbed model.

In the testbed 3 illustrated as Fig.A.2(a), the radio propagation between two radio antenna of the two motes is LOS, but it is interfered by two other motes (i.e., mote $m$, mote $k$) transmitting signals periodically. The model of testbed 4 as depicted in Fig.A.2(b) is similar to the practical case of sensor nodes deployed in the composite $\pi$-container. In this case, NLOS and interference are available and cause major impact on the performance of radio propagation.

Table A.1 presents experiment results showing varying of communication range according to the transmission power in all scenarios. In the four testbeds, the environment of the forth testbed for the networking performance of WSN is similar to that of the practical scenario that we describes in the previous Section. Accordingly, the propagation model used in our experiments is log normal shadowing which is studied to be best fit with the wireless sensor networks [123]. The results obtained from the experiments provide some significant conclusions.

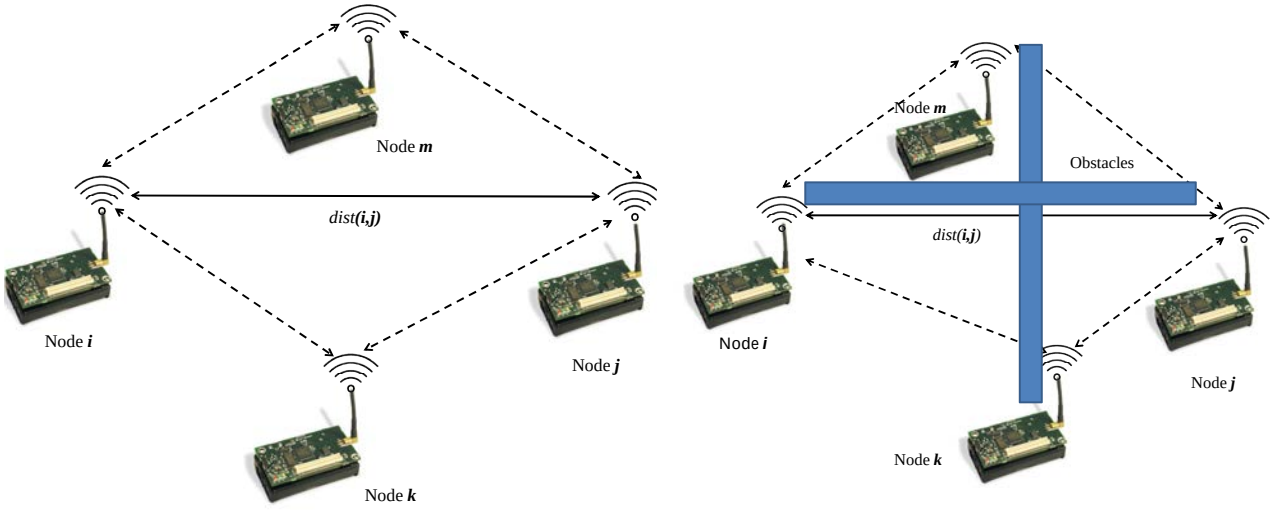


(a) Testbed 3 (b) Testbed 4

Figure A.2: Testbed models of model 3 and 4

First of all, the experiment results of the two similar tests of each testbed (e.g., test 4.1 and test 4.2) reveal that the communication link between the two motes is quite stable. The conclusion ensures the high confidences and accuracy of simulation results of the proposed algorithms. For example, as the stability of LQI values guarantees that all available motes are detected by the Gateway, hence the number of motes is obtained exactly in the algorithm of counting sensor nodes. After that, each mote can discover all other motes positioned in its communication range in the algorithm of neighbor discovery. Secondly, the adjustment of transmission power levels fine-tunes communication ranges between two consecutive levels. For instance, the difference range of communication between the two first levels is juts 6 cm which is half of minimum size of the unitary $\pi$-containers (12 cm). The result can allow choosing the optimal value of Rc by which the tightness of relative position constraints is maximized, thus the algorithm solving the CSP results in the unique and exact solution. Lastly, as the transmission power is set at maximum value, the maximum communication range (6.5 m) can support the communication between two farthest motes inside an H-container whose maximum size is assumed to be equal to 1.2 m. The conclusion allows the proposed algorithms to operate in one-hop scenario when needed (e.g., the algorithm of counting number of sensor nodes). However, the level 31 is not recommended for sensors to operate since it consumes more and fast residual energy. In simulation models, the communication range is normalized in order to fit with the normalized dimensions of $\pi$-containers. For instance, Rc (12cm) can be normalized to be 1 in simulation processes as the unit size used to normalize the

dimensions of $\pi$-containers is 12 cm.

| Level of Tx power | Power (dBm) | Maximum Communication Range (cm) | | | | | | | |
|---|---|---|---|---|---|---|---|---|---|
| | | Testbed 1 | | Testbed 2 | | Testbed 3 | | Testbed 4 | |
| | | Test 1.1 | Test 1.2 | Test 2.1 | Test 2.2 | Test 3.1 | Test 3.2 | Test 4.1 | Test 4.2 |
| 1 | -25 | 14 | 14 | 6 | 8 | 12 | 12 | 6 | 6 |
| 2 | -24 | 16 | 18 | 6 | 10 | 15 | 15 | 12 | 12 |
| 3 | -23 | 70 | 60 | 50 | 45 | 70 | 70 | 45 | 40 |
| 4 | -22 | 120 | 140 | 80 | 100 | 120 | 120 | 80 | 84 |
| 5 | -19 | 140 | 150 | 90 | 100 | 130 | 130 | 80 | 82 |
| 6 | -17 | 160 | 160 | 100 | 120 | 140 | 140 | 90 | 92 |
| 7 | -15 | 180 | 180 | 130 | 125 | 150 | 150 | 100 | 98 |
| 8 | -13 | 200 | 200 | 150 | 150 | 190 | 190 | 130 | 130 |
| 9 | -12 | 220 | 210 | 160 | 150 | 210 | 210 | 150 | 154 |
| 10 | -11 | 230 | 210 | 180 | 160 | 220 | 220 | 180 | 176 |
| 11 | -10 | 260 | 240 | 200 | 180 | 250 | 250 | 210 | 200 |
| 12 | -9 | 300 | 270 | 250 | 210 | 300 | 300 | 250 | 260 |
| 13 | -8 | 350 | 330 | 300 | 240 | 350 | 350 | 300 | 310 |
| 14 | -7.6 | 380 | 400 | 330 | 300 | 380 | 380 | 330 | 330 |
| 15 | -7 | 400 | 420 | 350 | 330 | 400 | 400 | 350 | 330 |
| 16 | -6.4 | 415 | 420 | 350 | 330 | 420 | 420 | 360 | 360 |
| 17 | -6 | 420 | 450 | 360 | 350 | 420 | 420 | 370 | 360 |
| 18 | -5.5 | 430 | 450 | 360 | 355 | 435 | 435 | 375 | 380 |
| 19 | -5 | 435 | 460 | 380 | 360 | 440 | 440 | 370 | 380 |
| 20 | -4.5 | 440 | 450 | 390 | 380 | 440 | 440 | 370 | 380 |
| 21 | -4 | 460 | 460 | 400 | 380 | 460 | 460 | 400 | 410 |
| 22 | -3.5 | 470 | 470 | 430 | 410 | 470 | 470 | 420 | 420 |
| 23 | -3 | 500 | 500 | 450 | 440 | 510 | 510 | 450 | 450 |
| 24 | -2.5 | 530 | 530 | 460 | 450 | 530 | 530 | 460 | 460 |
| 25 | -2 | 550 | 550 | 480 | 460 | 550 | 550 | 460 | 460 |
| 26 | -1.5 | 560 | 560 | 500 | 476 | 560 | 560 | 470 | 470 |
| 27 | -1 | 580 | 570 | 500 | 480 | 580 | 580 | 500 | 500 |
| 28 | -0.6 | 600 | 600 | 500 | 500 | 600 | 600 | 530 | 530 |
| 29 | -0.3 | 650 | 650 | 530 | 540 | 640 | 640 | 570 | 570 |
| 30 | -0.1 | 680 | 680 | 530 | 580 | 660 | 660 | 600 | 600 |
| 31 | 0 | 800 | 800 | 600 | 620 | 800 | 800 | 650 | 650 |

Table A.1: Maximum communication ranges of sensor corresponding to the levels of transmission power in 4 experiment testbeds

# Bibliography


[1] Sunil Chopra and Peter Meindl. *Supply Chain Management: Strategy, Planning, and Operation (6th Edition)*. Pearson, 6 edition, 1 2015.

[2] B. Tilanus, Tilanus, and Bernhard Tilanus. *Information Systems in Logistics and Transportation*. Emerald Group Publishing Limited, 2 edition, 6 1997.

[3] Kent Gourdin. *Global Logistics Management: A Competitive Advantage for the 21st Century*. Wiley-Blackwell, 2 edition, 2 2006.

[4] Valentinas Navickas, Leila Sujeta, and Sergej Vojtovich. Logistics systems as a factor of country's competitiveness. *Economics & Management*, 16, 2011.

[5] Hugh F. Durrant-Whyte. *An autonomous guided vehicle for cargo handling applications*, pages 372–379. Springer Berlin Heidelberg, Berlin, Heidelberg, 1997.

[6] Mohammad M. Aref, Reza Ghabcheloo, Antti Kolu, and Jouni Mattila. *Vision-Guided Autonomous Forklift*, pages 338–346. Springer International Publishing, Cham, 2017.

[7] Eleonora Morganti, Laetitia Dablanc, and François Fortin. Final deliveries for online shopping: The deployment of pickup point networks in urban and suburban areas. *Research in Transportation Business & Management*, 11:23 – 31, 2014. Managing Freight in Urban Areas.

[8] Donald J Bowersox, David J Closs, and Omar K Helferich. *Logistical management*, volume 6. McGraw-Hill New York, NY, 1996.

[9] Brian Wixted. *Logistics Clusters: Delivering Value and Driving Growth*. 2015.

[10] R. D. Meller Montreuil, B. and E. Ballot. Towards a physical internet: the impact on logistics facilities and material handling systems design and innovation. In *Progress in Material Handling Research, Edited by K. Gue et al., Material Handling Industry of America*, page 23 p., 2010.

[11] Christian BOISSIEU. Division par quatre des emissions de gaz à effet de serre de la france à l'horizon 2050. Technical report, Ministère de l'Ecologie et du développement durable, 2006.

[12] CITEPA. Substances relatives à l'accroisement de l'effet de serre. emissions dans l'air en france. Technical report, Centre Interprofessionnel Techniques d'Etudes de la Pollution Atmosphérique, France, 2009.

[13] Luciano de Angelis. A fall in average vehicle loads. *Average loads, distances and empty mnning in road freight transport-2010," Statistics in Focus*, (63), 2011.

[14] Alan MCKINNON. Performance measurement in freight transport. 2015.

[15] James F. Robeson. *Logistics Handbook*. Free Press, 7 1994.

[16] Teodor Gabriel Crainic, Michel Gendreau, and Jean-Yves Potvin. Intelligent freight-transportation systems: Assessment and the contribution of operations research. *Transportation Research Part C: Emerging Technologies*, 17(6):541–557, 2009.

[17] Gerben G. Meyer, Kary Främling, and Jan Holmström. Intelligent products: A survey. *Computers in Industry*, 60(3):137 – 148, 2009. {INTELLIGENT} {PRODUCTS}.

[18] L. Zhou and C. X. Lou. Intelligent cargo tracking system based on the internet of things. In *2012 15th International Conference on Network-Based Information Systems*, pages 489–493, Sept 2012.

[19] Jens Schumacher, Mathias Rieder, Manfred Gschweidl, and Philip Masser. *Intelligent Cargo - Using Internet of Things Concepts to Provide High Interoperability for Logistics Systems*, pages 317–347. Springer Berlin Heidelberg, Berlin, Heidelberg, 2011.

[20] M. Forcolin, E. Fracasso, F. Tumanischvili, and P. Lupieri. Euridice-iot applied to logistics using the intelligent cargo concept. In *2011 17th International Conference on Concurrent Enterprising*, pages 1–9, June 2011.

[21] Silvia Cosimato and Orlando Troisi. Green supply chain management: Practices and tools for logistics competitiveness and sustainability. the dhl case study. *The TQM Journal*, 27(2):256–276, 2015.

[22] Rommert Dekker, Jacqueline Bloemhof, and Ioannis Mallidis. Operations research for green logistics - an overview of aspects, issues, contributions and challenges. *European Journal of Operational Research*, 219(3):671 – 679, 2012. Feature Clusters.

[23] Alan Rushton, Phil Croucher, and Peter Baker, editors. *The Handbook of Logistics and Distribution Management*. Kogan Page, fourth edition edition, 7 2010.

[24] Benoit Montreuil. Toward a physical internet: meeting the global logistics sustainability grand challenge. *Logistics Research*, 3(2):71–87, 2011.

[25] Rochdi Sarraj, Eric Ballot, Shenle Pan, and Benoit Montreuil. Analogies between internet network and logistics service networks: challenges involved in the interconnection. *Journal of Intelligent Manufacturing*, 25(6):1207–1219, 2014.

[26] Russell D. Meller, Yen-Hung Lin, and Kimberly P. Ellis. The impact of standardized metric physical internet containers on the shipping volume of manufacturers. *IFAC Proceedings Volumes*, 45(6):364 – 371, 2012.

[27] Meller RD, Lin YH, Ellis KP, and Thomas LM. Standardizing container sizes saves space in the trailer. Technical report, Center for Excellence in Logistics and Distribution (CELDi), University of Arkansas., 2012.

[28] Christian Landschützer, Florian Ehrentraut, and Dirk Jodin. Containers for the physical internet: requirements and engineering design related to fmcg logistics. *Logistics Research*, 8(1):8, 2015.

[29] E. Ballot, B. Montreuil, and R.D. Meller. *The Physical Internet: The Network of Logistics Networks*. 2014.

[30] R. D. Meller and K.P. Ellis. Establishing the logistics system gain potential of the physical internet. Technical report, U.S. National Science Foundation and Physical Internet Thought Leaders, 2012.

[31] R. D. Meller and K. P. Ellis. An investigation into the physical internet: Establishing the logistics system gain potential. In *The International Conference on Industrial Engineering and Systems Management*, pages 575–584, Metz - France, 2011.

[32] Yves Sallez, Benoit Montreuil, and Eric Ballot. *On the Activeness of Physical Internet Containers*, pages 259–269. Springer International Publishing, Cham, 2015.

[33] Faranak Nekoogar and Farid Dowla. *Ultra-wideband radio frequency identification systems*. Springer Science & Business Media, 2011.

[34] Isaac Amundson and Xenofon D. Koutsoukos. A survey on localization for mobile wireless sensor networks. In *Proceedings of the 2Nd International Conference on Mobile Entity Localization and Tracking in GPS-less Environments*, MELT'09, pages 235–254, Berlin, Heidelberg, 2009. Springer-Verlag.

[35] Hui Liu, H. Darabi, P. Banerjee, and Jing Liu. Survey of wireless indoor positioning techniques and systems. *Trans. Sys. Man Cyber Part C*, 37(6):1067–1080, November 2007.

[36] Yunhao Liu and Zheng Yang. *Location, Localization, and Localizability: Location-awareness Technology for Wireless Networks*. Springer Publishing Company, Incorporated, 2014.

[37] Sinan Gezici. A survey on wireless position estimation. *Wirel. Pers. Commun.*, 44(3):263–282, February 2008.

[38] C. Fritsche and A. Klein. On the performance of hybrid gps/gsm mobile terminal tracking. In *2009 IEEE International Conference on Communications Workshops*, pages 1–5, June 2009.

[39] Holger Linde. *On Aspects of Indoor Localization*. PhD thesis, University of Dortmund, August 2006.

[40] Yanying Gu, A. Lo, and I. Niemegeers. A survey of indoor positioning systems for wireless personal networks. *Commun. Surveys Tuts.*, 11(1):13–32, January 2009.

[41] Kegen Yu and I. Oppermann. Performance of uwb position estimation based on time-of-arrival measurements. In *Ultra Wideband Systems, 2004. Joint with Conference on Ultrawideband Systems and Technologies. Joint UWBST IWUWBS. 2004 International Workshop on*, pages 400–404, May 2004.

[42] M. Z. Win and R. A. Scholtz. Characterization of ultra-wide bandwidth wireless indoor channels: a communication-theoretic view. *IEEE Journal on Selected Areas in Communications*, 20(9):1613–1627, Dec 2002.

[43] V. Lottici, A. D'Andrea, and U. Mengali. Channel estimation for ultra-wideband communications. *IEEE Journal on Selected Areas in Communications*, 20(9):1638–1645, Dec 2002.

[44] Chiara Falsi, Davide Dardari, Lorenzo Mucchi, and Moe Z. Win. Time of arrival estimation for uwb localizers in realistic environments. *EURASIP J. Appl. Signal Process.*, 2006:152–152, January 2006.

[45] I. Guvenc and C. C. Chong. A survey on toa based wireless localization and nlos mitigation techniques. *IEEE Communications Surveys Tutorials*, 11(3):107–124, rd 2009.

[46] Y. Takabayashi, T. Matsuzaki, H. Kameda, and M. Ito. Target tracking using tdoa/fdoa measurements in the distributed sensor network. In *2008 SICE Annual Conference*, pages 3441–3446, Aug 2008.

[47] S. Bartelmaos, K. Abed-Meraim, and R. Leyman. General selection criteria to mitigate the impact of nlos errors in rtt measurements for mobile positioning. In *2007 IEEE International Conference on Communications*, pages 4674–4679, June 2007.

[48] A. Zeitoun, Zhiheng Wang, and S. Jamin. Rttometer: measuring path minimum rtt with confidence. In *Proceedings of the 3rd IEEE Workshop on IP Operations Management (IPOM 2003) (IEEE Cat. No.03EX764)*, pages 127–134, Oct 2003.

[49] D. Niculescu and Badri Nath. Ad hoc positioning system (aps) using aoa. In *IEEE INFOCOM 2003. Twenty-second Annual Joint Conference of the IEEE Computer and Communications Societies (IEEE Cat. No.03CH37428)*, volume 3, pages 1734–1743 vol.3, March 2003.

[50] K. E. Bekris, A. A. Argyros, and L. E. Kavraki. Angle-based methods for mobile robot navigation: reaching the entire plane. In *Robotics and Automation, 2004. Proceedings. ICRA '04. 2004 IEEE International Conference on*, volume 3, pages 2373–2378 Vol.3, April 2004.

[51] J. Friedman, Z. Charbiwala, T. Schmid, Y. Cho, and M. Srivastava. Angle-of-arrival assisted radio interferometry (ari) target localization. In *MILCOM 2008 - 2008 IEEE Military Communications Conference*, pages 1–7, Nov 2008.

[52] Saw Mon Yee Aung and Myo Myint Maw. Poster: 2.4 ghz indoor path loss prediction model for multifloored building. In *Proceedings of the 14th Annual International Conference on Mobile Systems, Applications, and Services Companion*, MobiSys '16 Companion, pages 11–11, New York, NY, USA, 2016. ACM.

[53] Jun Zhao. Zero-configuration indoor positioning system based on rf signal strength. Master's thesis, Zhejiang University, 2007.

[54] Qingjiu Zhang and Shiliang Sun. A centroid k-nearest neighbor method. In *Proceedings of the 6th International Conference on Advanced Data Mining and Applications: Part I*, ADMA'10, pages 278–285, Berlin, Heidelberg, 2010. Springer-Verlag.

[55] G. Han, D. Choi, and W. Lim. A novel reference node selection algorithm based on trilateration for indoor sensor networks. In *7th IEEE International Conference on Computer and Information Technology (CIT 2007)*, pages 1003–1008, Oct 2007.

[56] Lin Min, Hui Li, and Zhengwei Guo. *Placement and Selection Algorithm of Reference Nodes in WSN Localization*, pages 357–362. Springer Berlin Heidelberg, Berlin, Heidelberg, 2013.

[57] Z. Yang and Y. Liu. Quality of trilateration: Confidence-based iterative localization. *IEEE Transactions on Parallel and Distributed Systems*, 21(5):631–640, May 2010.

[58] N. Patwari, A.O. Hero, III, M. Perkins, N.S. Correal, and R.J. O'Dea. Relative location estimation in wireless sensor networks. *Trans. Sig. Proc.*, 51(8):2137–2148, August 2003.

[59] In Jae Myung. Tutorial on maximum likelihood estimation. *Journal of Mathematical Psychology*, 47(1):90 – 100, 2003.

[60] N. Bulusu, J. Heidemann, and D. Estrin. Gps-less low-cost outdoor localization for very small devices. *IEEE Personal Communications*, 7(5):28–34, Oct 2000.

[61] J. Wang, P. Urriza, Y. Han, and D. Cabric. Weighted centroid localization algorithm: Theoretical analysis and distributed implementation. *IEEE Transactions on Wireless Communications*, 10(10):3403–3413, October 2011.

[62] Tian He, Chengdu Huang, Brian M. Blum, John A. Stankovic, and Tarek Abdelzaher. Range-free localization schemes for large scale sensor networks. In *Proceedings of the 9th Annual International Conference on Mobile Computing and Networking*, MobiCom '03, pages 81–95, New York, NY, USA, 2003. ACM.

[63] D. Niculescu and B. Nath. Ad hoc positioning system (aps). In *Global Telecommunications Conference, 2001. GLOBECOM '01. IEEE*, volume 5, pages 2926–2931 vol.5, 2001.

[64] Yu Hu and Xuemei Li. An improvement of dv-hop localization algorithm for wireless sensor networks. *Telecommunication Systems*, 53(1):13–18, 2013.

[65] Roy Want, Andy Hopper, Veronica Falcão, and Jonathan Gibbons. The active badge location system. *ACM Trans. Inf. Syst.*, 10(1):91–102, January 1992.

[66] E. Aitenbichler and M. Muhlhauser. An ir local positioning system for smart items and devices. In *23rd International Conference on Distributed Computing Systems Workshops, 2003. Proceedings.*, pages 334–339, May 2003.

[67] T. Komine and M. Nakagawa. Fundamental analysis for visible-light communication system using led lights. *IEEE Trans. on Consum. Electron.*, 50(1):100–107, February 2004.

[68] M. Akanegawa, Y. Tanaka, and M. Nakagawa. Basic study on traffic information system using led traffic lights. *Trans. Intell. Transport. Sys.*, 2(4):197–203, December 2001.

[69] Jeffrey Hightower and Gaetano Borriello. Location systems for ubiquitous computing. *Computer*, 34(8):57–66, August 2001.

[70] Naveed Ul Hassan, Aqsa Naeem, Muhammad Adeel Pasha, Tariq Jadoon, and Chau Yuen. Indoor positioning using visible led lights: A survey. *ACM Comput. Surv.*, 48(2):20:1–20:32, November 2015.

[71] Ye-Sheng Kuo, Pat Pannuto, Ko-Jen Hsiao, and Prabal Dutta. Luxapose: Indoor positioning with mobile phones and visible light. In *Proceedings of the 20th Annual International Conference on Mobile Computing and Networking*, MobiCom '14, pages 447–458, New York, NY, USA, 2014. ACM.

[72] Markus Funk, Robin Boldt, Bastian Pfleging, Max Pfeiffer, Niels Henze, and Albrecht Schmidt. Representing indoor location of objects on wearable computers with head-mounted displays. In *Proceedings of the 5th Augmented Human International Conference*, AH '14, pages 18:1–18:4, New York, NY, USA, 2014. ACM.

[73] Liqun Li, Pan Hu, Chunyi Peng, Guobin Shen, and Feng Zhao. Epsilon: A visible light based positioning system. In *Proceedings of the 11th USENIX Conference on Networked Systems Design and Implementation*, NSDI'14, pages 331–343, Berkeley, CA, USA, 2014. USENIX Association.

[74] U. Nadeem, N. U. Hassan, M. A. Pasha, and C. Yuen. Highly accurate 3d wireless indoor positioning system using white led lights. *Electronics Letters*, 50(11):828–830, May 2014.

[75] S. H. Yang, H. S. Kim, Y. H. Son, and S. K. Han. Three-dimensional visible light indoor localization using aoa and rss with multiple optical receivers. *Journal of Lightwave Technology*, 32(14):2480–2485, July 2014.

[76] H. S. Kim, D. R. Kim, S. H. Yang, Y. H. Son, and S. K. Han. An indoor visible light communication positioning system using a rf carrier allocation technique. *Journal of Lightwave Technology*, 31(1):134–144, Jan 2013.

[77] P. Bahl and V. N. Padmanabhan. Radar: an in-building rf-based user location and tracking system. In *Proceedings IEEE INFOCOM 2000. Conference on Computer Communications. Nineteenth Annual Joint Conference of the IEEE Computer and*

*Communications Societies (Cat. No.00CH37064)*, volume 2, pages 775–784 vol.2, 2000.

[78] Nissanka B. Priyantha, Anit Chakraborty, and Hari Balakrishnan. The cricket location-support system. In *Proceedings of the 6th Annual International Conference on Mobile Computing and Networking*, MobiCom '00, pages 32–43, New York, NY, USA, 2000. ACM.

[79] J. Maneesilp, C. Wang, H. Wu, and N. F. Tzeng. Rfid support for accurate 3d localization. *IEEE Transactions on Computers*, 62(7):1447–1459, July 2013.

[80] Moustafa Youssef and Ashok Agrawala. The horus location determination system. *Wirel. Netw.*, 14(3):357–374, June 2008.

[81] W. G. Griswold, P. Shanahan, S. W. Brown, R. Boyer, M. Ratto, R. B. Shapiro, and T. M. Truong. Activecampus: experiments in community-oriented ubiquitous computing. *Computer*, 37(10):73–81, Oct 2004.

[82] Anthony LaMarca, Yatin Chawathe, Sunny Consolvo, Jeffrey Hightower, Ian Smith, James Scott, Timothy Sohn, James Howard, Jeff Hughes, Fred Potter, Jason Tabert, Pauline Powledge, Gaetano Borriello, and Bill Schilit. Place lab: Device positioning using radio beacons in the wild. In *Proceedings of the Third International Conference on Pervasive Computing*, PERVASIVE'05, pages 116–133, Berlin, Heidelberg, 2005. Springer-Verlag.

[83] Jun-geun Park, Ben Charrow, Dorothy Curtis, Jonathan Battat, Einat Minkov, Jamey Hicks, Seth Teller, and Jonathan Ledlie. Growing an organic indoor location system. In *Proceedings of the 8th International Conference on Mobile Systems, Applications, and Services*, MobiSys '10, pages 271–284, New York, NY, USA, 2010. ACM.

[84] Xueli An, Jing Wang, R. Venkatesha Prasad, and I. G. M. M. Niemegeers. Opt: Online person tracking system for context-awareness in wireless personal network. In *Proceedings of the 2Nd International Workshop on Multi-hop Ad Hoc Networks: From Theory to Reality*, REALMAN '06, pages 119–121, New York, NY, USA, 2006. ACM.

[85] J. Larranaga, L. Muguira, J. M. Lopez-Garde, and J. I. Vazquez. An environment adaptive zigbee-based indoor positioning algorithm. In *2010 International Conference on Indoor Positioning and Indoor Navigation*, pages 1–8, Sept 2010.

[86] S. Tadakamadla. Indoor local positioning system for zigbee based on rssi. Master's thesis, Mid Sweden University, 2006.

[87] Mortaza S. Bargh and Robert de Groote. Indoor localization based on response rate of bluetooth inquiries. In *Proceedings of the First ACM International Workshop on Mobile Entity Localization and Tracking in GPS-less Environments*, MELT '08, pages 49–54, New York, NY, USA, 2008. ACM.

[88] Xinwei Wang, Ole Bischoff, Rainer Laur, and Steffen Paul. Localization in wireless ad-hoc sensor networks using multilateration with rssi for logistic applications. *Procedia Chemistry*, 1(1):461 – 464, 2009.

[89] Xinwei Wang, Shaoping Yuan, Rainer Laur, and Walter Lang. Dynamic localization based on spatial reasoning with {RSSI} in wireless sensor networks for transport logistics. *Sensors and Actuators A: Physical*, 171(2):421 – 428, 2011.

[90] Alexander Wessels, Xinwei Wang, Rainer Laur, and Walter Lang. Dynamic indoor localization using multilateration with rssi in wireless sensor networks for transport logistics. *Procedia Engineering*, 5:220 – 223, 2010.

[91] W. Lang, R. Jedermann, D. Mrugala, A. Jabbari, B. Krieg-Brückner, and K. Schill. The intelligent container: A cognitive sensor network for transport management. *IEEE Sensors Journal*, 11(3):688–698, March 2011.

[92] S. Byun and M. Kim. Real-time positioning and orienting of pallets based on monocular vision. In *2008 20th IEEE International Conference on Tools with Artificial Intelligence*, volume 2, pages 505–508, Nov 2008.

[93] S. Spieker and C. Rohrig. Localization of pallets in warehouses using wireless sensor networks. In *Control and Automation, 2008 16th Mediterranean Conference on*, pages 1833–1838, June 2008.

[94] Frederic Thiesse, Markus Dierkes, and Elgar Fleisch. Lottrack: Rfid-based process control in the semiconductor industry. *IEEE Pervasive Computing*, 5(1):47–53, January 2006.

[95] S. Abbate, M. Avvenuti, P. Corsini, and A. Vecchio. Localization of shipping containers in ports and terminals using wireless sensor networks. In *Computational Science and Engineering, 2009. CSE '09. International Conference on*, volume 2, pages 587–592, Aug 2009.

[96] S. Abbate, M. Avvenuti, P. Corsini, B. Panicucci, M. Passacantando, and A. Vecchio. An integer linear programming approach for radio-based localization of shipping containers in the presence of incomplete proximity information. *IEEE Transactions on Intelligent Transportation Systems*, 13(3):1404–1419, Sept 2012.

[97] M. Fogel, N. Burkhart, H. Ren, J. Schiff, M. Meng, and K. Goldberg. Automated tracking of pallets in warehouses: Beacon layout and asymmetric ultrasound observation models. pages 678–685, Sept 2007.

[98] Andreas Bortfeldt and Gerhard Wäscher. Constraints in container loading: A state-of-the-art review. *European Journal of Operational Research*, 229(1):1 – 20, 2013.

[99] H. Gehring and A. ortfeldt. A genetic algorithm for solving the container loading problem. *International Transactions in Operational Research*, 4(5):401 – 418, 1997.

[100] E.E. Bischoff and M.S.W. Ratcliff. Issues in the development of approaches to container loading. *Omega*, 23(4):377 – 390, 1995.

[101] Eberhard E. Bischoff and Michael D. Marriott. A comparative evaluation of heuristics for container loading. *European Journal of Operational Research*, 44(2):267 – 276, 1990.

[102] WILLIAM B. DOWSLAND. Three-dimensional packing: solution approaches and heuristic development. *International Journal of Production Research*, 29(8):1673–1685, 1991.

[103] C.S. Chen, S.M. Lee, and Q.S. Shen. An analytical model for the container loading problem. *European Journal of Operational Research*, 80(1):68 – 76, 1995.

[104] Shan Lin, Jingbin Zhang, Gang Zhou, Lin Gu, John A. Stankovic, and Tian He. Atpc: Adaptive transmission power control for wireless sensor networks. In *Proceedings of the 4th International Conference on Embedded Networked Sensor Systems*, SenSys '06, pages 223–236, New York, NY, USA, 2006. ACM.

[105] E. Le Merrer, A. M. Kermarrec, and L. Massoulie. Peer to peer size estimation in large and dynamic networks: A comparative study. pages 7–17, 2006.

[106] D. Kostoulas, D. Psaltoulis, I. Gupta, K. Birman, and A. Demers. Decentralized schemes for size estimation in large and dynamic groups. In *Fourth IEEE International Symposium on Network Computing and Applications*, pages 41–48, July 2005.

[107] Laurent Massoulié, Erwan Le Merrer, Anne-Marie Kermarrec, and Ayalvadi Ganesh. Peer counting and sampling in overlay networks: Random walk methods. In *Proceedings of the Twenty-fifth Annual ACM Symposium on Principles of Distributed Computing*, PODC '06, pages 123–132, New York, NY, USA, 2006. ACM.

[108] A. Montresor and A. Ghodsi. Towards robust peer counting. In *2009 IEEE Ninth International Conference on Peer-to-Peer Computing*, pages 143–146, Sept 2009.

[109] M. Jelasity and A. Montresor. Epidemic-style proactive aggregation in large overlay networks. In *Distributed Computing Systems, 2004. Proceedings. 24th International Conference on*, pages 102–109, 2004.

[110] S. S. Kunniyur and S. S. Venkatesh. Threshold functions, node isolation, and emergent lacunae in sensor networks. *IEEE Transactions on Information Theory*, 52(12):5352–5372, Dec 2006.

[111] Z. Khalid, S. Durrani, and J. Guo. A tractable framework for exact probability of node isolation and minimum node degree distribution in finite multihop networks. *IEEE Transactions on Vehicular Technology*, 63(6):2836–2847, July 2014.

[112] R. Cohen and B. Kapchits. Continuous neighbor discovery in asynchronous sensor networks. *IEEE/ACM Transactions on Networking*, 19(1):69–79, Feb 2011.

[113] M. Jamalabdollahi and S. A. R. Zekavat. Joint neighbor discovery and time of arrival estimation in wireless sensor networks via ofdma. *IEEE Sensors Journal*, 15(10):5821–5833, Oct 2015.

[114] L. Wei, B. Zhou, X. Ma, D. Chen, J. Zhang, J. Peng, Q. Luo, L. Sun, D. Li, and L. Chen. Lightning: A high-efficient neighbor discovery protocol for low duty cycle wsns. *IEEE Communications Letters*, 20(5):966–969, May 2016.

[115] L. Chen, Y. Shu, Y. Gu, S. Guo, T. He, F. Zhang, and J. Chen. Group-based neighbor discovery in low-duty-cycle mobile sensor networks. *IEEE Transactions on Mobile Computing*, 15(8):1996–2009, Aug 2016.

[116] Vipin Kumar. Algorithms for constraint-satisfaction problems: A survey. *AI Mag.*, 13(1):32–44, April 1992.

[117] K El Ghomali, Najib Elkamoun, Kun Mean Hou, Yibo Chen, Jean-Pierre Chanet, and JJ Li. A new wpan model for ns-3 simulator. In *NICST'2103 New Information Communication Science and Technology for Sustainable Development: France-China International Workshop*, pages 8–p, 2013.

[118] K. El Ghomali, N. Elkamoun, K. M. Hou, Y. Chen, J.P. Chanet, and J.J. Li. A new wpan model for ns-3 simulator. In *NICST'2103 New Information Communication Science and Technology for Sustainable Development: France-China International Workshop*, page 8 p., Clermont-Ferrand, France, September 2013.

[119] Jonathan L Gross and Jay Yellen. *Handbook of graph theory*. CRC press, 2004.

[120] Christoph Koch Oliver Kennedy, Al Demers. Dynamic approaches to in-network aggregation. *2009 IEEE 25th International Conference on Data Engineering, ICDE 2009*, 00:1331–1334, 2009.

[121] H. Tran-Dang, N. Krommenacker, and P. Charpentier. Localization algorithms based on hop counting for wireless nano-sensor networks. In *2014 International Conference on Indoor Positioning and Indoor Navigation (IPIN)*, pages 300–306, Oct 2014.

[122] K. Mekki, W. Derigent, A. Zouinkhi, E. Rondeau, A. Thomas, and M. Naceur Abdelkrim. Rawpg: A data retrieval protocol in micro-sensor networks based on random walk and pull gossip for communicating materials. *IEEE Internet of Things Journal*, 4(2):414–426, April 2017.

[123] Marco Zúñiga Zamalloa and Bhaskar Krishnamachari. An analysis of unreliability and asymmetry in low-power wireless links. *ACM Trans. Sen. Netw.*, 3(2), June 2007.

# Résumé

Le paradigme de l'Internet Physique (PI ou $\pi$) a été introduit il y a quelques années pour transformer globalement la manière dont les objets physiques seront manipulés, entreposés et transportés dans le cadre d'une logistique durable. L'une des caractéristiques importante de l'Internet Physique est liée à l'encapsulation des marchandises dans des conteneurs modulaires standardisés. Le modèle de fonctionnement proposé de l'Internet Physique, s'il rationnalise les transports, engendre des manutentions plus nombreuses, en particulier au sein des $\pi$-hubs, où les opérations de routage, de déchargement et (re)chargement des conteneurs nécessitent une organisation et une gestion rationnelle. La multiplicité et la diversité des opérations (automatisées ou non) à mettre en œuvre simultanément ne peut être conduite de manière efficiente qu'en cas de parfaite synchronisation entre la réalité du système physique et de celle du système informationnel.

Les propositions de cette thèse adressent cette problématique applicative et constituent à ce titre une contribution au concept de l'Internet Physique. Elles visent à l'obtention, en temps réel, d'une image ou d'un modèle spatial des $\pi$-conteneurs, qui disposent chacun d'un nœud WSN. L'assemblage de ces différents conteneurs au sein d'un conteneur de plus haut niveau (ou conteneur composite) permet de constituer alors un réseau de capteurs ad-hoc. Ces conteneurs deviennent ainsi des éléments actifs de l'automatisation de la chaine logistique. A partir des seules informations de proximité issues de cette instrumentation, nous montrons dans cette thèse qu'il est possible de construire le modèle spatial des $\pi$-conteneurs.



**Mots-clés:** Internet Physique, Conteneur modulaire, Réseaux de capteur sans fil, Contraintes de proximité, Problème de satisfaction de contraintes, modèle 3D.



# Abstract

The Physical Internet (PI or $\pi$ in short) paradigm was introduced few years ago to transform globally how physical objects will be handled, stored and transported as part of a sustainable logistics. One of the important characteristics of the Physical Internet is the encapsulation of goods in standardized modular containers. Although the Physical Internet rationalizes transport, it generates more frequent handling, particularly within $\pi$-hubs, where the operations of routing, unloading and (re) loading containers require an efficient organization and management. The multiplicity and the diversity of operations (automated or not) to be implemented simultaneously can only be carried out efficiently in the case of perfect synchronization between the reality of the physical system and that of the information system.

The proposals of this thesis address this problem and constitute a contribution to the concept of the Physical Internet. They aim to obtain in real time, the spatial distribution (or 3D layout) of the $\pi$-containers when they are stacked in a higher-level container, so called composite container. To do this, we propose to exploit the intelligence and the activeness concepts of each $\pi$-container which is equipped with wireless sensor node. Hence, the composition of a composite $\pi$-containers constitutes an adhoc network of sensor nodes. From neighborhood relationships between these nodes, we show in this thesis that it is possible to construct the spatial 3D layout of the $\pi$-containers and control at any time and at any place the effective compliance between the real composition and the data stored in the information system.

**Keywords:** Physical Internet, Modular Container, Wireless Sensor Network, Proximity Constraints, Constraints Satisfaction Problem (CSP), 3D Layout